REACTION RATES IN FISSILE MATERIAL

A Thesis submitted for the award of

the Doctor of Philosophy Degree of

the University of London

by

ALI PAZIRANDEH, B.Sc., M.Sc.

Nuclear Power Section

Department of Mechanical Engineering

Imperial College

London

December 1969

ABSTRACT

Fission rate ratios of U_{238} relative to U_{235} have been measured in reactor fuel elements by detecting the fission product gamma activity from irradiated uranium foils. The true fission ratio has been determined from the time-dependent calibration factor. This factor has been determined in a series of auxiliary experiments which utilises either a double fission chamber or the detection of the gamma activity from the decay of La-140 in irradiated foils.

Systematic errors in the technique have been investigated in detail and the most serious source of error has been found to be in the determination of the calibration factor. The neutron spectrum dependence of the calibration factor has been examined and it is found to decrease by about 10% as the spectrum is varied from a thermal spectrum to that of a typical fast reactor. The total systematic error in the whole technique has been reduced to 1.1%.

Fission ratio measurements have been made in the University of London Reactor. The U_{238} and U_{235} fission rate fine structure and U_{238}/U_{235} fission ratios are compared to theoretical predictions using the transport theory code GMS-I incorporating the latest UKAEA nuclear data file.

ACKNOWLEDGEMENTS

The author wishes to express his sincere gratitude to his Supervisor, Professor P. J. Grant, for his guidance and encouragement during the course of this work. Special thanks are due to Dr. C. B. Besant for his constant assistance and his interest in this work.

Many thanks are due to the technical staff of the Nuclear Power Section, especially G. Slater.

The author is grateful to Mr. M. Kerridge and his supporting staff of the London University Reactor for being cooperative and helpful. Special thanks are due to Mr. E. A. Y. Caesar for his valuable assistance and skilful help during the part of the work carried out at the Reactor.

Many thanks to the staff at the Neutron Physics Research Section at AWRE (Aldermaston) for their assistance in carrying out some experiments with the Van de Graaff. Also thanks are due to Professor C. O. Cogburn.

The author acknowledges the support of the Central Treary Organization (CENTO) under the auspice of whom this work was performed.

I am grateful to the staff of the Tehran University Nuclear Centre for their support in the period of my absence from job.

Last, but not the least, the particular thanks to my wife, Shahla, for her sacrifices during this period.

CONTENTS

LIST OF NOTATIONS

t	decay time in minutes
CD(t)	depleted foil count rate or CD
CD	count rate of 1.60 Mev peak of La-140 from depleted foil.
CN(t)	natural foil count rate or CN
CN	count rate of 1.60 Mev peak of La-140 from natural foil
N5D	number density of U_{235} in depleted foil.
N5N	number density of U_{235} in natural foil
N8D	number density of U_{238} in depleted foil
N8N	number density of U_{238} in natural foil
$\gamma(t)$	ratio of depleted to natural count rate CD(t)/CN(t)
F8(t)	fission in U_{238} per atom (gamma activity)
F5(t)	fission in U_{235} per atom (gamma activity)
$(F8(t)/F5(t))_\gamma$ or $(F8/F5)_\gamma$	gamma activity fission ratio
$\frac{F8}{F5}$	true fission ratio
δ_{28}	fission ratio in natural uranium = $\frac{N8N}{N5N}\ \frac{F8}{F5}$
p(t)	calibration factor - true fission ratio to gamma activity fission ratio
D8(t)	normalized U_{238} fission rate to unity at 240 minutes after the end of irradiation
D5(t)	normalized U_{235} fission rate to unity at 240 minutes after the end of irradiation

FN8	same as D8(t) which is obtained from one irradiation
FN5	same as D5(t) which is obtained from one irradiation
σ	standard deviation
$f_8(t)$	gamma activity of U_{238} of depleted foil irradiated in a hard spectrum
$f_5(t)$	gamma activity of U_{235} of depleted foil irradiated in a thermal spectrum
C_8	fission counts of depleted deposit irradiated in a fast flux
C_5	fission counts of depleted deposit irradiated in a thermal flux.
c8,c5	are gamma counts above 1.28 Mev threshold of depleted foils irradiated in a fast flux and thermal flux respectively.
f	a correction factor for delay counting in La-140 technique and utilization factor.
Eth	neutron energy for fission threshold detectors, namely U_{238} fission threshold.

LIST OF FIGURES

LIST OF TABLES

CHAPTER 1

INTRODUCTION

The basic aim in Nuclear Reactor physics research is to improve the fundamental nuclear data by accurate measurements using the best techniques and checking the results with theoretically predicted values. There have always been some discrepancies between experimental results and theoretical predictions. The aim is to establish theoretical methods for physics calculation of Nuclear Reactors. The gap between experimental values and theoretical predictions was partly due to the lack of knowledge of basic nuclear cross section data and the means and techniques to solve the transport equation in complex geometries. The availability of fast digital computers with large storage capacity has enabled the Reactor Physicist to accurately calculate the neutron behaviour in Reactors and to perform detailed calculations of burnup for design purposes.

Nuclear power is becoming economically competitive with other forms of power and it is increasingly important to predict accurately the future performance of nuclear power plants. Use of differential cross section data and multigroup diffusion and transport theory codes have resulted in advances in more complex cell calculations. It has therefore become necessary to measure detailed reaction rates in reactor fuels in mockup zero energy facilities in order to obtain information on the neutron balance in the various systems and so check theoretical predictions at a more detailed level. The vast change in reactor design, core configuration and cell structure, whether in thermal or fast reactors, has resulted in large changes in neutron spectrum and flux distributions in different reactors. Since some reaction rates are very spectrum dependent, such as resonances and threshold reaction, accurate detailed measurements have become essential to the development of reactor behaviour.

The reactor physics calculations are concerned with the prediction of criticality conditions, reactivity and fuel burnup or refuelling. In thermal reactors, fuelled with natural or enriched uranium fuel, fissions occur in U_{235} and U_{238} nuclei. Since fission in U_{238} has a threshold at about 1 Mev it is spectrum dependent; see Figs 2A and 2B. In order to calculate the contribution of U_{238} fission neutrons to the neutron balance in a reactor core fission in U_{238} relative to that in U_{235} is determined. Also in a reactor with significant amount of plutonium fuel fission in Pu_{239} to that of U_{235} is measured in order to find the contribution on neutron population.

In thermal reactors with thick fuel rods such as Magnox (44) type fuel elements or closely packed fuel clusters such as the Advance Gas Cooled Reactors (AGR) type fuel elements the fission ratios are different as compared with the ordinary light water moderated reactors. In fast reactors fission ratios such as U_{238}/U_{235}, Pu_{239}/U_{235} are more important than in thermal reactors since in fast reactors the neutron spectrum is hard (typically 100Kev) and the majority of fissions occur with high energy neutrons both in U_{235} and U_{238}. Fission neutrons from fissions in Pu_{239}, Pu_{240} and Pu_{241} contribute to neutron balance. Therefore a knowledge of fission ratios is important to understanding the neutron balance in the core. In fast reactors because of poor knowledge on present differential cross section data these kinds of measurement are very valuable in predicting the neutron behaviour in a hard spectrum. In the blanket of fast reactors the concentration of U_{238} is high. Because the neutron spectrum in the blanket is softer than in the core, the capture rate is of prime importance. The blanket is usually designed for producing Pu_{239} which can be used as fuel.

The work reported in this dissertation was concerned with the measurement of fission rates in various isotopes in reactor fuels.

The main effort has been concentrated on the measurement of fission ratios between the various isotopes which may exist in a reactor fuel. Particular emphasis has been placed on systematic errors which were present in some techniques and efforts were made to reduce the possible errors to acceptable levels. The effects of making measurements in fast reactors as well as thermal systems were studied with the view to understanding the spectrum dependence of parameters involved in the analysis of the measurements. The use of activation detectors for measuring fission ratios has numerous advantages. Some of these advantages are that the foil size can be adjusted easily so that low perturbation effects can be achieved, and foils may be accurately positioned. Fission ratio measurements using fission chambers lack these advantages (46).

The method adopted of measuring fission ratios consists of irradiating fissile foils in reactor lattices. After irradiation the foils were counted for fission product gamma activity to yield gamma activity fission ratios. The gamma activity ratio was converted to the true fission ratio by means of a time dependent calibration factor p(t), which was determined in an auxiliary experiment using a double fission chamber.

The aims of this project may be summarized as follows:-

(1) The investigation of a number of techniques for measuring fission ratio with the view to reducing systematic errors in each technique.

(2) The measurement of fission ratios to a target accuracy of $\pm$1% in a reactor spectrum.

(3) To investigate the spectrum dependence of any parameters involved in the measurements.

(4) To compare the experimental results with theoretical predictions using the latest UKAEA differential cross section data.

1.1 REVIEW OF PREVIOUS WORK

The present method of measuring fission ratio was developed at Winfrith by Brown et al (1) from the technique originally proposed by Tunnicliffe (2) of Chalk River, Canada. The principles of the method are given in Ref. (2). Since that time detailed modifications have been made to the technique to improve accuracy and to cover fast reactors as well as thermal reactor requirements.

Carter et al (3) have measured fission ratios by using aluminium catcher foils and a beta counting technique. They determined a calibration factor, p(t), to relate beta activity ratios to true fission ratios using two fission chambers and aluminium strips as foil catchers. They quoted 3.2% error in the calibration factor measurement. It is worth mentioning that the calibration factor p(t) depends on many factors as well as decay time. This point is discussed in chapter 5. Therefore, the determined calibration factors in different laboratories cannot be compared unless they have been measured under the same conditions. What is important here is the experimental errors, particularly systematic errors in the measurements. Brown et al(1) determined p(t) using a double fission chamber loaded with 500 $\mu g/Cm^2$ uranium deposits. They placed six uranium foils between the deposits for irradiation while they were counting fission events. They determined a value for the calibration factor at 240 minutes after the end of irradiation which was $p(240) = 1.22 \pm 2\%$, not including systematic errors. They also determined p(240) based on detecting the 1.60 Mev gamma activity from the fission product La-140 and obtained $p(240) = 1.32 \pm 6\%$. Later Besant et al (4, 5) using the ZEBRA parallel plate fission chambers developed by Stevenson and Broomfield have quoted a 3% error in p(t). Barnett et al (7) using a double fission chamber and La-140 techniques have reported $p(t) = 1.33 \pm 3\%$ using fission chamber and $p(t) = 1.32 \pm 6\%$ using the La-140 method.

However, the p (240 minutes) values given by Brown et al and Barnett et al, who used the same equipment differ by more than 6% which is outside the individual errors in each result. This suggests that there might be a larger systematic error present in the technique used.

CHAPTER 2

2.1 NEUTRON TRANSPORT EQUATION

In neutron transport theory, the Boltzmann equation was introduced to study neutron performance in Nuclear Reactors. Because of the intrinsic complexity of the general solution to the neutron transport equation, approximate methods of solution to the equation have been found.

In this chapter the neutron transport equation is briefly discussed and the technique of computation adopted in the calculation, leading to the determination of the angular distribution of neutrons of different energies is described. The time dependent neutron transport equation is given by

$$\frac{1}{r}\frac{\partial N(E,r,\Omega,t)}{\partial t} + \Omega\cdot\nabla N(E,r,\Omega,t) + (\Sigma_s(E)+\Sigma_a(E))\, N(E,r,\Omega,t)$$

$$= \int_{\Omega'}\int_{E'} \Sigma_s(r,E'\rightarrow E,\Omega'\rightarrow \Omega)\, N(E',r,\Omega',t)\, d\Omega' dE'$$

$$+ S(E,r,\Omega,t) \qquad (2.1)$$

where $N(E,r,\Omega,t)$ is the neutron flux per unit energy interval per unit solid angle at position r at time t, $\Sigma(r,E' \rightarrow E,\Omega' \rightarrow \Omega)$ is the differential scattering cross section. $S(E,r,\Omega,t)$ is the source term including fission neutrons(if any). In the steady state problem the first term on the left hand side vanishes, therefore the equation is given by:

$$\Omega.\nabla N(E,r,\Omega) + \Sigma(E)\ N\ (E,r,\Omega)$$

$$= \int_{\Omega'}\int_{E'} \Sigma_s(r,E' \rightarrow E,\Omega' \rightarrow \Omega)\ N\ (E',r',\Omega')\ d\Omega'\ dE'$$

$$+ S(E,r,\Omega) \qquad (2.2)$$

where $\Sigma(E) = \Sigma_s(E) + \Sigma_a(E)$

2.2 DISCRETE S_n APPROXIMATION TO THE NEUTRON TRANSPORT EQUATION

One of the extensively used methods for solving the neutron transport equation is the Discrete Ordinal Method, DSN, which was proposed by Carlson (41) in 1953. The neutron transport equation is integrated over all angles by a numerical procedure. The Carlson method has been improved and to some extent simplified so that different types of neutron transport problems can be solved. The detailed description of the method is found in the references 11 - 14 and in this section only the fundamental points of the method are described.

A cylindrical geometry was considered in which ϕ is the angle between the projection of Ω onto the horizontal plane and the outward radius , and ω is the angle between Ω and the vertical axis of the cylinder. Consider the steady state Boltzmann equation for a particular energy group. Equation 2.2 in cylindrical coordinates is given by

$$\left[\eta\mu \frac{\partial}{\partial r} - \eta \frac{\sqrt{1-\mu^2}}{r} \frac{\partial}{\partial \phi} + \Sigma\right] N\ (r,\omega,\phi,R) = S \qquad (2.3a)$$

where $\eta = \sin\omega$

$\mu = \cos\phi$

Σ is total cross section

N the angular flux

S is the source term for a specified energy group

includes all scattered neutrons including self scatter term.

In order to solve equation 2.3aby means of the Carlson method a set of cells C_{ij} is introduced where i is an index shows the distance from the origin and j is an index represents direction. Assume an octant of a unit sphere as shown in Fig. 1A. The octant is divided into levels or divisions by horizontal lines (latitude). Each level has a thickness $d\gamma$ when $\gamma = \cos\omega$. Each level also has a direction indicated by μ_j. The levels are divided by longitudinal lines in such a way that one zone on the top and two in the next level, three in the next level and so on. If the degree of approximation is n, number of levels is $\frac{n}{2}$ and number of zones is $\frac{n}{4}\left(\frac{n}{2}+1\right)$. The levels and zones are so divided that they have equal areas $d\Omega = d\gamma \cdot d\phi$, see Fig. 1 (A,B). Equation 2.2 for the level j is given by

$$\eta_j \left(\mu \frac{\partial N_j}{\partial r} - \frac{\sqrt{1+\mu^2}}{r} \frac{\partial N_j}{\partial \phi}\right) + \Sigma N_j = S_j \qquad (2.3)$$

$j = 1, 2, \ldots \frac{n}{2}$ $\frac{n}{2}$ number of levels

$N = \Sigma N_j d\gamma_j$ $d\gamma_j$ thickness of level j

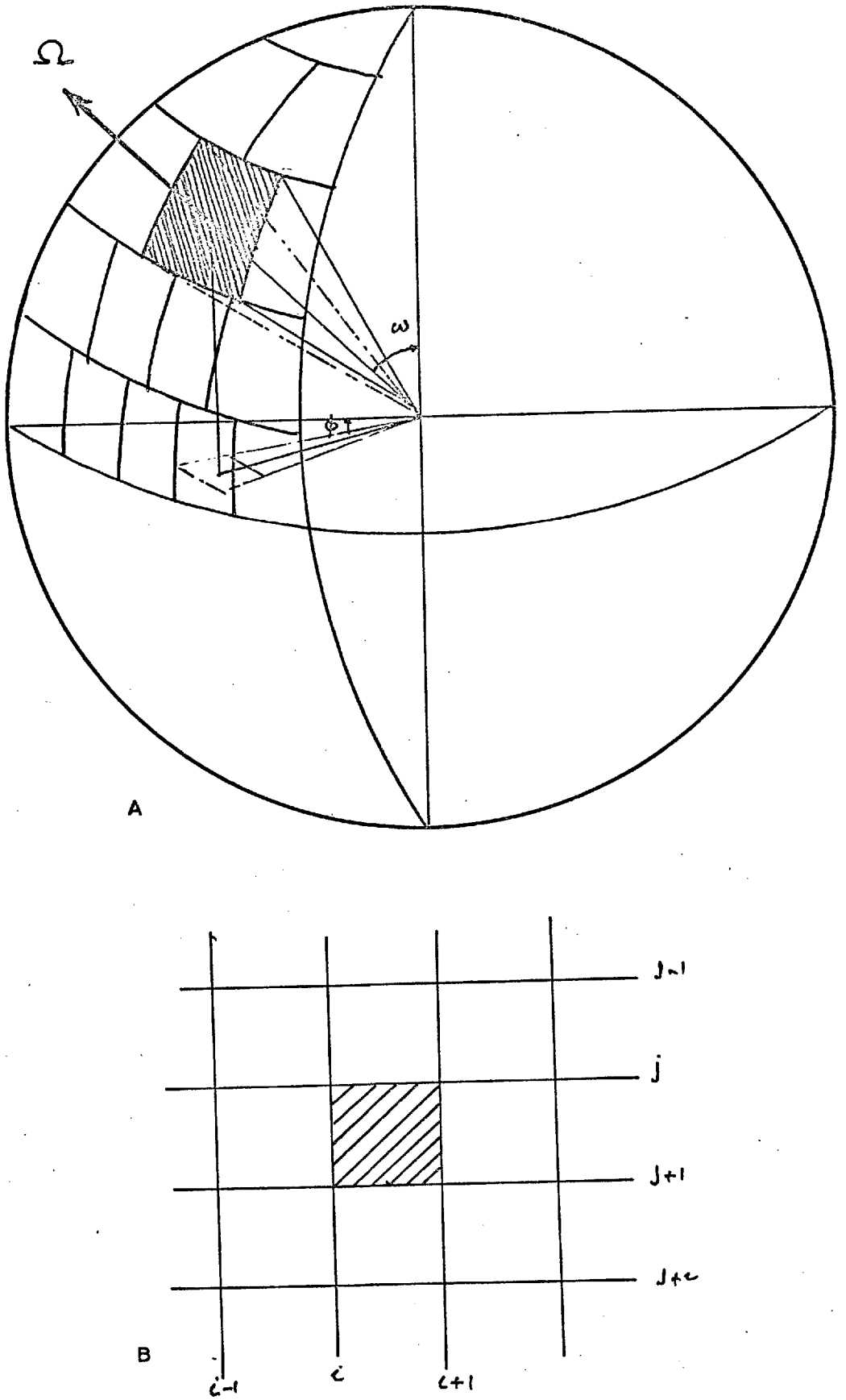

FIG. 1 Solid Angle and Zones Representation in Cylindrical Geometry

To find the angular flux in the zone, equation 2.3 is integrated over interval $\Delta\phi_{ji}$ we obtain

$$\eta_j \left(\frac{1}{r} + \frac{\partial}{r}\right) \int_{\Delta\phi_{ji}} N \cos\phi \, d\phi - \frac{\eta_j}{r} [N \sin\phi]_{\Delta\phi_{ji}}$$

$$+ \Sigma \int_{\Delta\phi_{ji}} N \, d\phi = S\Delta\phi_{ji} \qquad (2.4)$$

In order to solve equation 2.4 two terms indicated below must be calculated:-

$$\int_{\Delta\phi_{ji}} N \cos\phi \, d\phi \text{ and } \int_{\Delta\phi_{ji}} N \, d\phi \qquad (2.5)$$

In DSN method of calculation the two terms are given by

$$\int_{\Delta\phi_{ji}} N d\phi = \bar{N}_{ji} \Delta\phi_{ji}$$

$$\int_{\Delta\phi_{ji}} N \cos\phi \, d\phi = \bar{N}_{ji} \bar{\mu}_{ji} \Delta\phi_{ji} \qquad (2.6)$$

Where $\bar{N}$ is the mean value of N in a zone. By substituting 2.6 into 2.4 we obtain

$$\eta_j \left(\frac{\partial}{\partial r} + \frac{1}{r}\right) \bar{N}_{ji} \bar{\mu}_{ji} \Delta\phi_{ji} - \frac{\eta_j}{r} [N \sin\phi]_{\phi_{ji-1}}^{\phi_{ji}} + \Sigma N_{ji} \Delta\phi_{ji} = S\Delta\phi_{ji}$$

(2.7)

In equation 2.7 the term in the square brackets is to be determined. In order to calculate the term a linear variation of angular flux in each zone is assumed

$$N_{ji} = 2\,\bar{N}_{ji} - N_{ji-1} \tag{2.8}$$

Equation 2.7 is therefore given by

$$\eta\bar{\mu}\,\frac{\partial\bar{N}}{\partial r} + \frac{\eta}{r}\,(\mu\,\Delta\phi_{ji} - 2\sin\phi_{ji})\,\bar{N} + \frac{\eta}{r}\,(\sin\phi_{ji} + \sin\phi_{ji-1})N_{ji-1}$$

$$+ \Sigma\bar{N}\,\Delta\phi = S\Delta\phi \tag{2.9}$$

the indices were dropped for simplicity.

In equation (2.9) as $\Delta\phi \to 0$ two round brackets become equal. Therefore the equation is given as

$$\eta_j\,\bar{\mu}_{ji}\,\frac{\partial\bar{N}_{ji}}{\partial r} + \eta_i\,\frac{b_{ji}}{r}\,\bar{N}_{ji} - \eta_j\,\frac{b_{ji}}{r}\,N_{ji-1} + \Sigma\,\bar{N}_{ji} = S \tag{2.10}$$

where

$$b_{ji} = \bar{\mu}_{ji} - \frac{2}{\Delta\phi_{ji}}\sum_{k=1}^{k=i}\bar{\mu}_{ji}\,\Delta\phi_{jk} \tag{2.11}$$

The value of b_{ji} is calculated from a recurrence relation given below:-

$$(b_{ji} - b_{ji-1}) = -\,(\bar{\mu}_{ji} + \bar{\mu}_{ji-1}) \tag{2.12}$$

In order to derive the spatial form of the equation, equation 2.10 is integrated over Δr given as

$$(\eta_j \bar{\mu}_{ji} + \tfrac{1}{2}\eta_j b_{ji} \delta_r + h_r)\bar{N}_{jir} + (-\eta_{ji} \bar{\mu}_{ji} + \tfrac{1}{2}\eta_j b_{ji} \delta_r + h_r)\bar{N}_{ji-1}$$

$$- \eta_j b_{ji} \delta_r \tilde{N}_{ji-1} = \Delta S \qquad (2.13)$$

where

$$\tilde{N}_{ji-1\,r} = \left(\frac{N_{ji-1r} + N_{ji-1r-1}}{2}\right)$$

$$\delta_r = \frac{\Delta r}{\bar{r}}$$

$$h_r = \tfrac{1}{2}\Sigma_t \Delta r \qquad (2.14)$$

$$\bar{r} = \frac{R_r + R_{r-1}}{2}$$

R is the radial coordinates.

The difference equation 2.13 is solved by an iterative method starting from the first energy group (highest energy) for all the mesh points.

2.3 A GENERALIZED MULTIGROUP SYSTEM, GMS, OF CALCULATIONS

GMS is a generalized system of reactor physics calculations written in the FORTRAN programming language for IBM 7030 computer (14, 15, 43). The programme is also available in EGTRAN language for KDF9 computer at Winfrith (42). The programme will perform cell, super-cell and overall reactor physics problems within the limits of one dimension using either slab or cylindrical geometry. The Winfrith DSN (16) programme has been incorporated as a subroutine and all flux distribution calculations are performed using Transport Theory. The GMS programme is written in terms of 40 neutron energy groups. The programme solves the Boltzmann Transport Equation by means of Carlson discrete S_n approximation.

CHAPTER 3

TECHNIQUE OF FISSION RATIO MEASUREMENTS

3.1 INTRODUCTION

A Fission Ratio is usually referred to as the ratio of the fission rate in one fissile isotope relative to that of another isotope of the same material or different kind. Fissile materials are two classes as far as the fission cross section is concerned. Some fissile nuclei such as $_{92}U^{233}$, $_{92}U^{235}$, $_{94}Pu^{239}$ and $_{94}Pu^{241}$ can undergo fission with any neutrons whereas some nuclei such as $_{90}Th^{232}$, $_{92}U^{234}$, $_{94}Pu^{240}$ and $_{94}Pu^{242}$ have a potential for fission above a certain energy. Detectors utilising isotopes of the latter group are usually referred to as threshold detectors. The fission cross sections for the two types of fissile nuclei are shown (17) in Figs. 2A and 2B. The reason for the difference in the fission process mode can be described by the amount of binding energy per nucleon in the compound nucleus in the two types of fissile nuclei. It is found in nuclear physics that nuclei with an odd number of neutrons have lower fission thresholds than nuclei with even number of neutrons (18).

3.2 IMPORTANCE OF FAST FISSION

In the early days of Nuclear Reactor development the only fissile material well known and available in nature was uranium. From preliminary experiments it was found that U_{235} can be utilized as a fuel in Nuclear Reactors. After further developments of Nuclear Reactors and the theory of neutron transport attention was drawn to the fact that energy can be extracted from fissile materials for the purpose of power production. Critical assemblies were designed on the

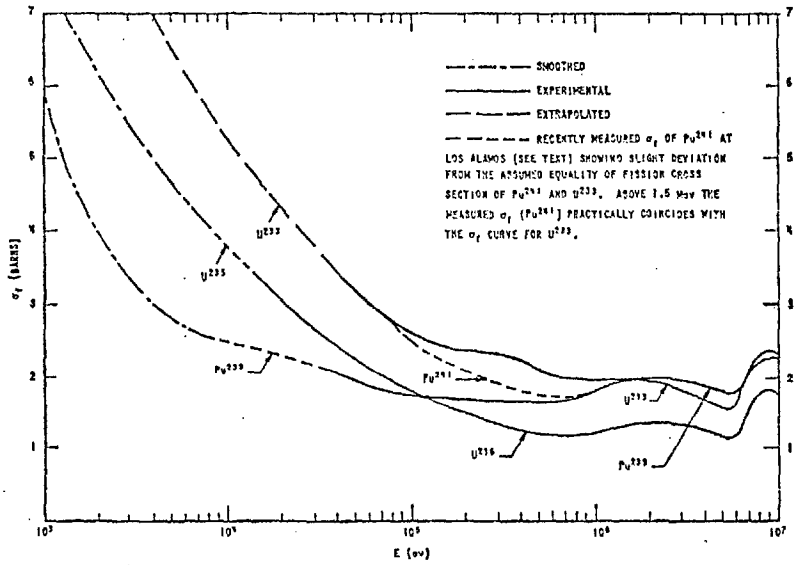

FIG. 2A Fission cross section of even-odd fissile nuclides U^{235}, U^{233}, Pu^{239} and Pu^{241} showing extrapolated gaps in Pu^{239} and U^{233}.

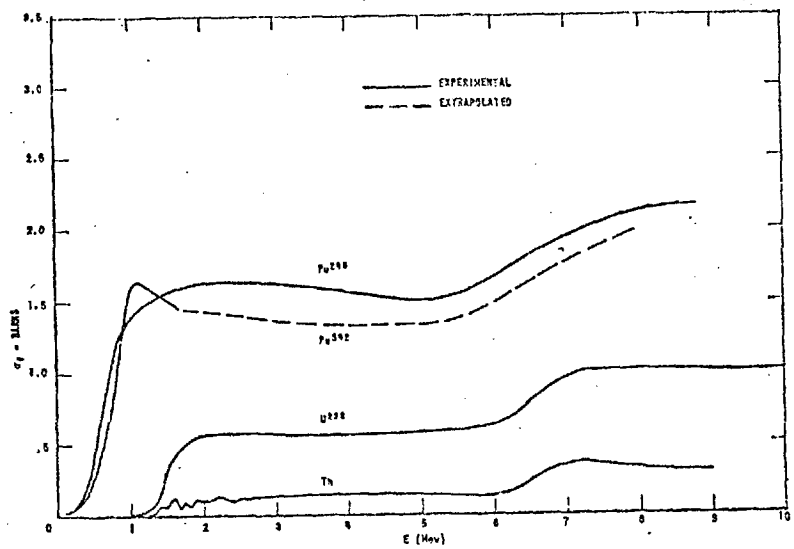

FIG. 2B Fission cross section of even-even nuclides U^{238}, Th^{232}, Pu^{240}, Pu^{242} showing extrapolated gap in Pu^{242}.

These diagrams are in Ref. 17

basis of the fission process in U_{235}. From the beginning scientists were well aware of the fast fission in U_{238} and its contribution to the reactivity. The importance of U_{238} in Nuclear Reactors was mainly due to resonance capture levels in low energies about 6.4, 21, 37, 65 and 100 ev (13), (18).

Meanwhile the availability of Thorium in nature and the discovery of many transuranic elements was a great success to this field. A great deal of research work and investigation about the properties of these elements were carried out for the purpose of finding the effect of the elements in the criticality condition as well as the possibility of using them as fuel in future Nuclear Reactors. As was mentioned earlier in section 3.1, there is a good chance of fast fission in fissile materials. This depends entirely on the design of the core. Watt's formula (20) predicts 86.8, 72.7, 59.3 and 56 per cent of fission neutrons are above U^{234}, U^{236}, U^{238} and Th^{232} fission threshold respectively. The neutron spectrum depends on how fast neutrons lose their energies in a system. Murley (23) has considered the energy spectrum of fission neutrons after having suffered one or two collisions with uranium nuclei. He has shown that about 30% of neutrons are above one Mev energy after one collision. Hicks (22) has also given diagramatically the energy spectrum of fission neutrons in uranium oxide and water lattices that are very similar. The latter is due to the low scattering cross section of hydrogen in a fission spectrum (22) see Fig. 3. It should be pointed out that the neutron spectrum in a reactor core depends on the design of the core, type of fuel and moderator. Therefore, the reaction rates which are

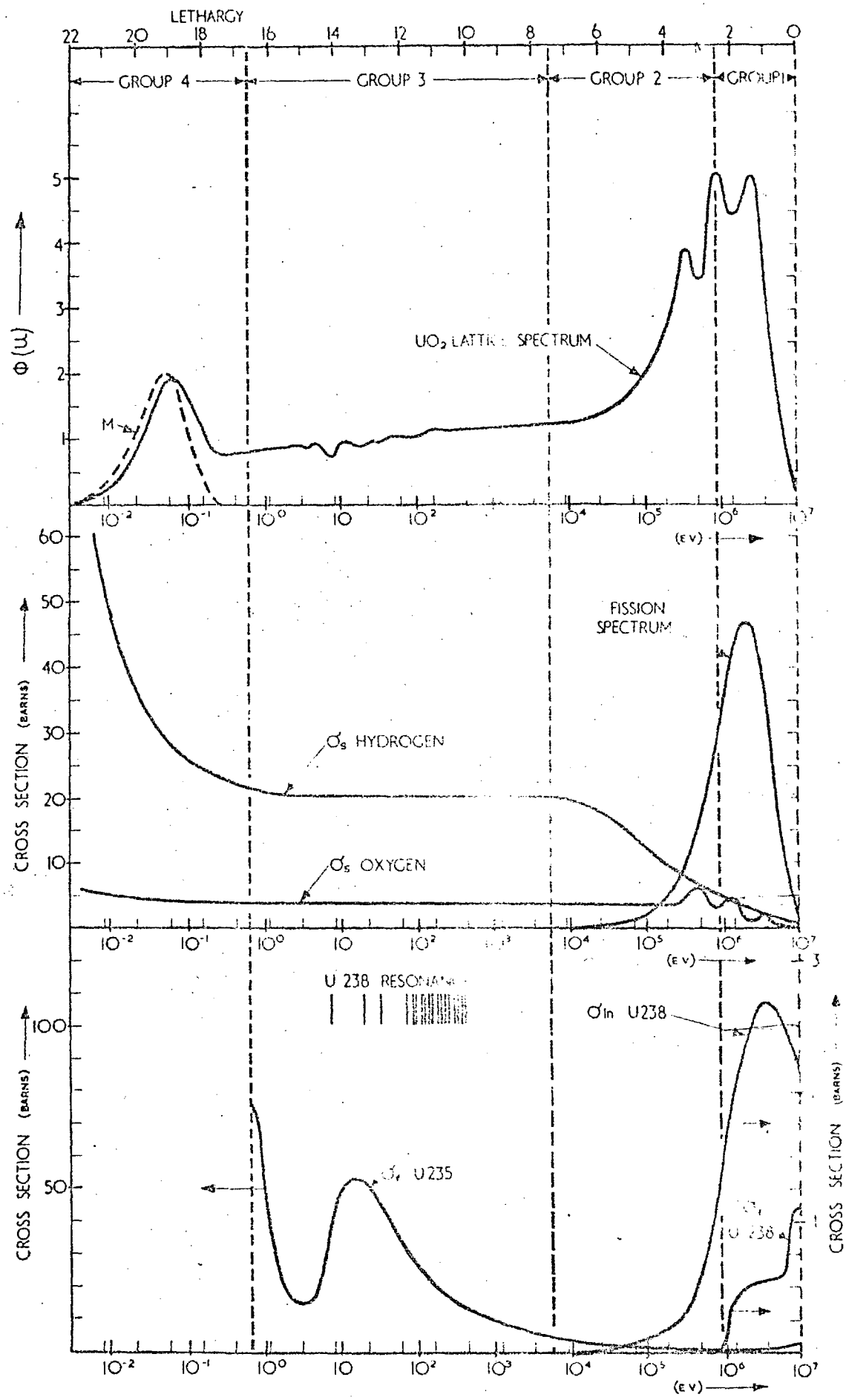

FIG. 3 NEUTRON SPECTRA AND CROSS SECTIONS (Ref. 22)

spectrum dependent have some effect on the neutron population (reactivity) and so measurements of fine and hyperfine structure of these reaction rates become essential. Naturally, in a uranium fuelled reactor it is important to know the U_{238}/U_{235} fission rate and U_{238} capture/U_{235} fission ratio. From the latter reaction Pu_{239} is produced which can undergo fission with thermal and fast neutrons. Pu_{239} has a higher value of η in the fast neutron range than u_{235} and lower in the thermal region. In thermal reactors the majority of fissions occur in the thermal region and fast fission in U_{238} is comparatively low. The contribution of fast fission to the neutron population is defined by the fast fission ratio. In fast reactors the neutron spectrum is very hard and most of the fissions occur in the fast region. In this case the fission ratio is defined as U_{238} fission relative to that in U_{235}. Fast reactor cores consist of enriched uranium 235, Pu_{239} and U_{238} and a blanket region comprising mainly of U_{238}. Therefore accurate measurements of fission ratios in the core and blanket are primary knowledge required for a fast reactor design.

3.3 DETERMINATION OF FISSION RATIO

The criterion for every critical Nuclear Reactor operating at a steady state is that the neutron population in the reactor core remains constant. This condition is inferred from the following relation:

$$K_{eff} = (\eta f\ \epsilon p)\ L_f\ L_{th} \qquad (3.1)$$

where K_{eff} is the effective multiplication factor of neutrons from

one generationto the next. η is the neutron yield per absorption in fissile material, f is the utilization factor defined as the ratio of thermal neutron absorption in the fuel to that in all materials constructing the core. P is the resonance escape probability. L_f and L_{th} are the non-leakage probability of fast and thermal neutrons respectively. This simple model is being used for convenience.

The production of neutrons is the direct result of the fission process in the uranium fuel and other fissile materials present in the reactor. This project has been directed towards the measurement of this process with the best possible accuracy.

The fissioning of U_{238} nuclei by fast neutrons contributes to the neutron population but the significance of the effect strongly depends on both fuel enrichment and the reactor design. The effect of fast fission on K_{eff} is given by the fast fission factor in four factor formula. There are several definitions for the fast fission factor which are as follows:-

(1) The number of neutrons making their first collision with moderator nuclei per number of neutrons produced per thermal fission (23). This definition was reported in Ref. 23 by Spinrad.

(2) The ratio of the number of neutrons slowing down past the U_{238} fission threshold per number of neutrons produced by thermal fission (25) (26).

(3) The number of neutrons slowing down below 0.1 Mev per neutrons produced by thermal fission (Cardvik and Pershagen in Ref. 23). Generally speaking, the definition of fast fission factor depends on the type of the reactor.

The definition can be described in terms of neutron flux and cross sections as follows:-

$$\varepsilon = 1 + \frac{\int_R dr \int_{E_{th}}^{E_o} \Sigma_f(E)\, \phi(r,E)\, dE}{\int_R \Sigma_f\, \phi(r)\, dr} \qquad (3.2)$$

where $\Sigma_f(E)$ is the macroscopic fission cross section as a function of energy $\phi(r,E)$ is the neutron flux of energy E to E + dE at point r. $\Sigma_f(E)\, \phi(r,E)dE$ is the fission rate at space point r in energy range E to E + dE. Integration of this reaction over the whole energy spectrum (in the core) yields the fast fission rate at point r. The integration of the fast fission rate over the whole core yields the total fast fission rate in the core above E_{th}. The denomenator is only the thermal fission integrated over the whole core. Equation 3.2 cannot be solved analytically because of the complexity of the cross section over the whole range of neutron spectrum. The usual procedure uses numerical integration by means of proper energy groups selection. For instance, if we divide the neutron spectrum into one thermal group and n groups above thermal, the fast fission notation becomes

$$\varepsilon = 1 + \frac{\sum_i^m \sum_{i=1}^n \Sigma_i^f\, \phi_i(r_j)}{\sum_j^m \Sigma_{th}^f\, \phi_{th}(r_j)} \qquad (3.3)$$

where Σ_i^f is the fission cross section averaged over the ith energy group, $\phi_i(r_j)$ is the average flux of ith group at point r_j,

Σ^f_{th} and ϕ_{th} the fission cross section and neutron flux respectively for thermal group - Σ^f_i in some cases is space dependent but here is assumed to be constant. If one is interested only to know fast fission at one point, integration over the space is dropped. In equation 3.3, ϵ is not a measurable quantity and therefore a quantity that is measurable and related to ϵ must be introduced. This measurable quantity is derived in the following paragraph.

The total number of fission neutrons from thermal fission is equal to

$$\nu_5 N_5 \sigma_f^5 \phi_{th} \qquad (a)$$

A fraction of the fission neutrons produced by thermal fission in U_{235}, during slowing down are absorbed in U_{238}. Of this fraction some induce fission in U_{238} and the rest are captured producing U_{239}. It should be noted that fission in U_{238} occurs with neutrons of over one Mev energy while capture, especially in the resonance region, happens in epithermal region. The net neutron gain from this process is equal to

$$\nu_8 N_8 \sigma_f^8 \phi_f - N_8 \sigma_{abs} \phi_f$$

Using definition (2) the fast fission factor is defined as

$$\epsilon = \frac{\nu_5 N_5 \sigma_f^5 \phi_{th} + \nu_8 N_8 \sigma_f^8 \phi_f - N_8 \sigma_{abs}^{\delta} \phi_f}{\nu_5 N_5 \sigma_f^5 \phi_{th}} \qquad (3.4a)$$

or

$$\epsilon = 1 + \frac{\nu_8 N_8 \sigma_f^8 \phi_f}{\nu_5 N_5 \sigma_{th}^5} \left(1 - \frac{1}{\eta_8}\right) \qquad (3.4b)$$

By introducing $\delta_{28} = \frac{N_8 \sigma_f^8 \phi_f}{N_5 \sigma_f^5 \phi_{th}}$ equation 3.4b becomes

$$\epsilon = 1 + \delta_{28} \frac{\nu_8}{\nu_5} \left(1 - {}^1/\eta_8\right) \qquad (3.4)$$

where ν_8 and ν_5 are the average number of nutrons per fission, N8 and N5 are U_{238} and U_{235} number densities, ϕ_f and ϕ_{th} are fast and thermal fluxes respectively. η_8 is the neutron yield per absorption in U_{238} - δ_{28} is called the fission ratio in uranium fuel containing N5 of U_{235} and N_8 of U_{238} atoms. δ_{28} is a measurable quantity but because of differences in fuel enrichment in different reactors F8/F5 is measured where F8 and F5 are fissions per atom in U_{238} and U_{235} respectively. The relationship below shows the fission ratio, δ_{28}, in natural uranium

$$\delta_{28} = \frac{N8}{N5} \cdot \frac{F8}{F5} \qquad (3.5)$$

where N8 and N5 are U_{238} and U_{235} number densities in natural uranium respectively.

The technique chosen of measuring δ_{28} (fission ratio) is based on foil irradiations. The experimental procedure adopted was to simultaneously irradiate two uranium metal foils of different U_{235} enrichments in a reactor. After the end of irradiationsthe foils were counted on a double NaI(Tl) detector. A block diagram of the counting system is shown in Fig. 4. The gamma activity of

each foil results from fission product activity resulting from thermal fission of U_{235} and fast fission of U_{238}. Two simultaneous equations can be written for the activity from each foil. The activity of each foil is due to fission process both in U_{235} and U_{238}. Therefore each equation consists of two parts as follows:-

$$CD(t) = N5D.F5(t) + N8D.F8(t)$$
$$CN(t) = N5N.F5(t) + N8N.F8(t) \qquad (3.6)$$

where CD(t) and CN(t) are depleted and natural foils count rates at time t corrected for weight and other necessary corrections that are discussed in chapter 6 - N5D, N5N, N8D, and N8N are the number densities of U_{235} and U_{238} in depleted and natural foils, respectively. F5(t) and F8(t) are gamma activities of the fission products of U_{235} and U_{238} per atom respectively. Considering the two equations (3.6) and substituting $\gamma(t) = CD(t)/CN(t)$ and dividing numerator and denumerator by F5(t) the following equation is obtained:-

$$\gamma(t) = \frac{N5D + N8D\,\frac{F8(t)}{F5(t)}}{N5N + N8N\,\frac{F8(t)}{F5(t)}} \qquad (3.7)$$

From this $\frac{F8(t)}{F5(t)}$ is resulted as:-

$$\left(\frac{F8(t)}{F5(t)}\right)_{\gamma} = \frac{N5N}{N8N}\;\frac{\gamma(t) - \frac{N5D}{N5N}}{\frac{N8D}{N8N} - \gamma(t)} \qquad (3.8)$$

In this equation F8(t)/F5(t) is the gamma activity fission ratio. Since the rate of fission product decay from U_{238} is different from that of U_{235}, the ratio $(F8/F5)_\gamma$ is time dependent. To correlate this ratio to the true fission ratio a calibration factor is required in order to convert the measured fission ratio to true fission ratio. The factor was obtained in an auxiliary experiment which will be discussed in detail in chapter 5. The calibration factor, defined as the ratio of the true fission ratio to the gamma activity fission ratio measured in exactly the same spectrum. The calibration factor p(t) is therefore obtained from the following equation:-

$$p(t) = \frac{(F8/F5)}{(F8(t)/F5(t))_\gamma} \qquad (3.9)$$

For determining δ28 the fission ratio is simply multiplied by N8N/N5N or by the ratio of U_{238} to U_{235} number density of the fuel.

As mentioned in section 3.4, the irradiated foils were counted alternately or if there were more than two foils they were counted periodically. Therefore a delay counting correction had to be applied to CD and CN in equations (3.6). The delay counting correction was performed by three methods:-

(1) by linear interpolation between two successive counts of each foil and calculating the count rate corresponding to the other foil counting time;

(2) by using two correction factors D5(t) and D8(t) for F5 and F8 respectively. These correction factors were found from a series of irradiations and using the set of equations (3.6) from which F5 and F8 were obtained as given below:-

$$
\begin{aligned}
F5 &= \frac{CN\,\frac{N8D}{N8N} - CD}{N5N\,\frac{N8D}{N8N} - N5D} \\
F8 &= \frac{CN\,\frac{N5D}{N5N} - CD}{N8N\,\frac{N5D}{N5N} - N8D}
\end{aligned}
\qquad (3.10)
$$

Then F5 and F8 were normalized to unity at 240 minutes after the end of irradration. A computer program, LLSQFT was written to fit a polynomial to the data by means of the method of least squares. A fourth order poly-nomial was found as the best fit. Fig. 5 shows the plot of D5 and D8 as a function of time and corresponding values are given in Appendix III followed by the polynomials. Therefore ~~if~~, for example, the depleted foil was counted at time t and the natural foil at time t' = t + Δt, Δt is the time between the two counting times. t and t' are the decay times to the middle of counting of each foils. The corrections to F5 and F8 for depleted foil counts are $\frac{D5(t')}{D5(t)}$ and $\frac{D8(t')}{D8(t)}$ respectively. Therefore, equation 3.6 become as follows:

$$
\begin{aligned}
CD &= N5D \cdot F5\,\frac{D5(t')}{D5(t)} + N8D \cdot F8\,\frac{D8(t')}{D8(t)} \\
CN &= N5N \cdot F5 + N8N \cdot F8
\end{aligned}
\qquad (3.11)
$$

From these equations the fission ratio is obtained as:-

$$
\frac{F8}{F5} = \frac{N5N}{N8N}\,\frac{\frac{CD}{CN} - \frac{N5D}{N5D}\,\frac{D5(t')}{D5(t)}}{\frac{N8D}{N8N}\,\frac{D8(t')}{D8(t)} - \frac{CD}{CN}} \qquad (3.12)
$$

(3) The third method was done by using the LISQFT program to fit a polynomial to the decay counts of depleted and natural foils. Then afterwards a set of counts at simultaneous time was calculated from the polynomials. It should be mentioned that the obtained polynomials (fourth order) for depleted count rates and natural foil count rates are different. Fig. 6 shows the polynomial fit to depleted foil and natural foil count rates with the actual counts. In order to analyze the results of irradiations and to find D5(t) and D8(t) three computer programs were written and used. The programs are FFR.I which uses the interpolation technique, FFRII uses D5(t) and D8(t) and FFRIII uses the least square routine. The programs are described in Appendix I.

It should be pointed out the order of the fitted polynomials to the depleted and natural uranium count rates depended on the length of the decay time. From 40 to 250 minutes after the end of irradiation fourth order polynomial was best. For longer times for instance 70 to 500 minutes 6th order polynomial and from 400 to 1500 quadratic or cubic on logarithmic scale was best. In this context logarithmic scale means taking logarithm of count rates and then finding the best fit.

3.4 DESCRIPTION OF DETECTOR SYSTEM

A block diagram of a double channel gamme counting system is shown in Fig. 4. The counting system for gamma counting of foils consists of two identical channels. Each channel comprises a 5 cm by 4.5 cm (dia.) NaI(Tl) scintillation detector mounted on an EMI 6097B photo-multiphier tube positioned in a lead castle. The

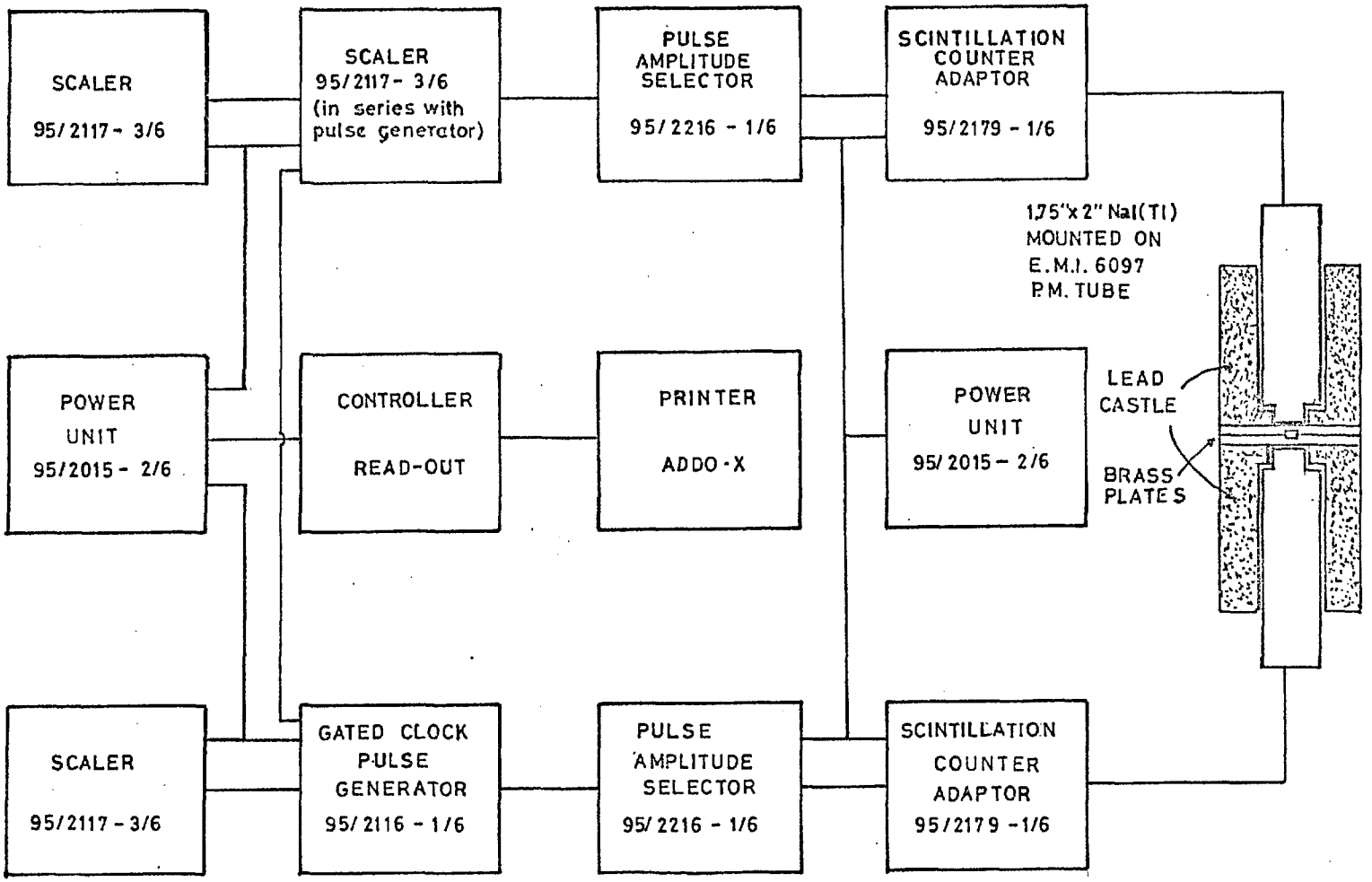

FIG. 4 BLOCK DIAGRAM OF TWO-CHANNEL GAMMA COUNTING SYSTEM.

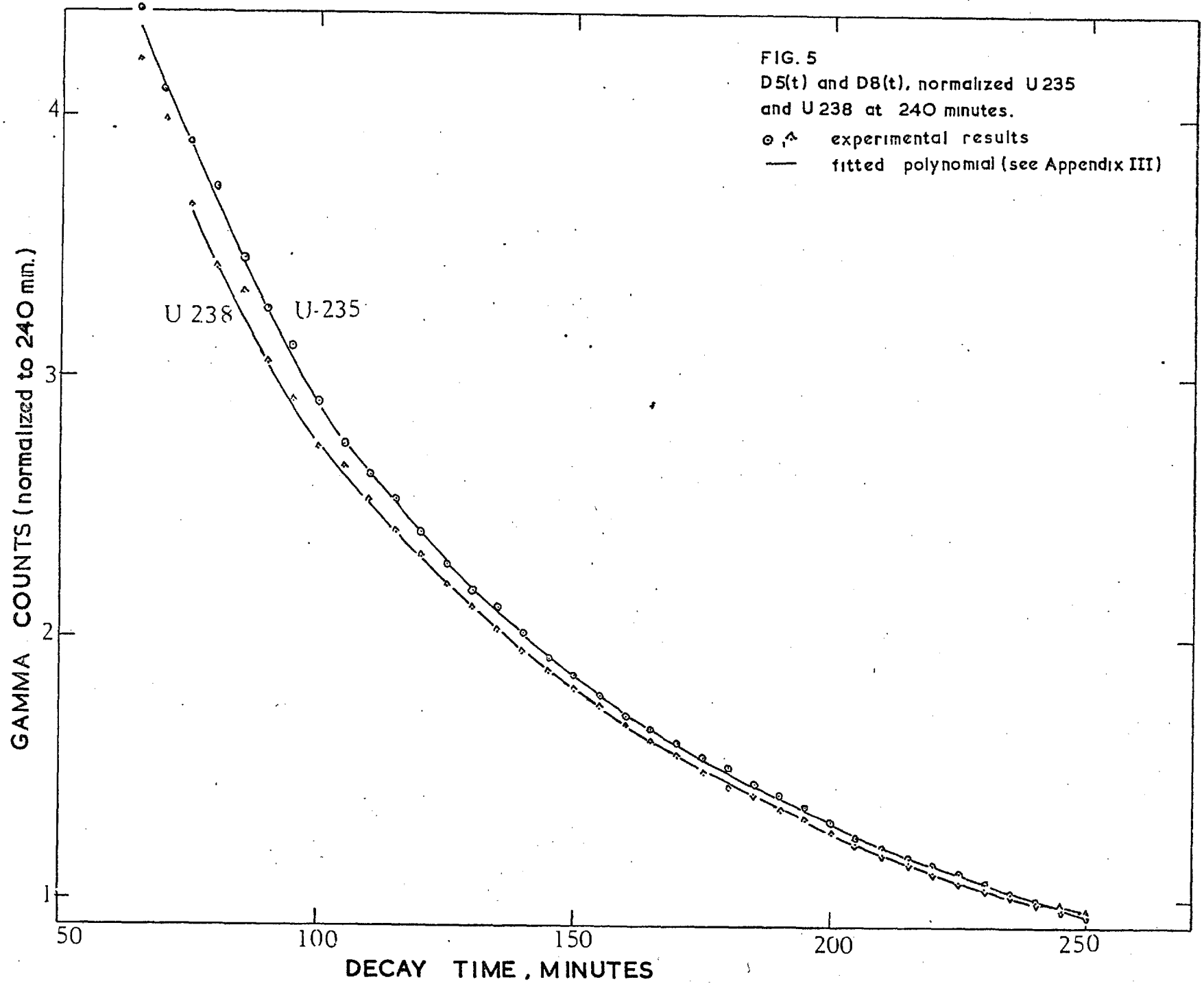

FIG. 5
D5(t) and D8(t), normalized U 235 and U 238 at 240 minutes.
⊙, △ experimental results
—— fitted polynomial (see Appendix III)

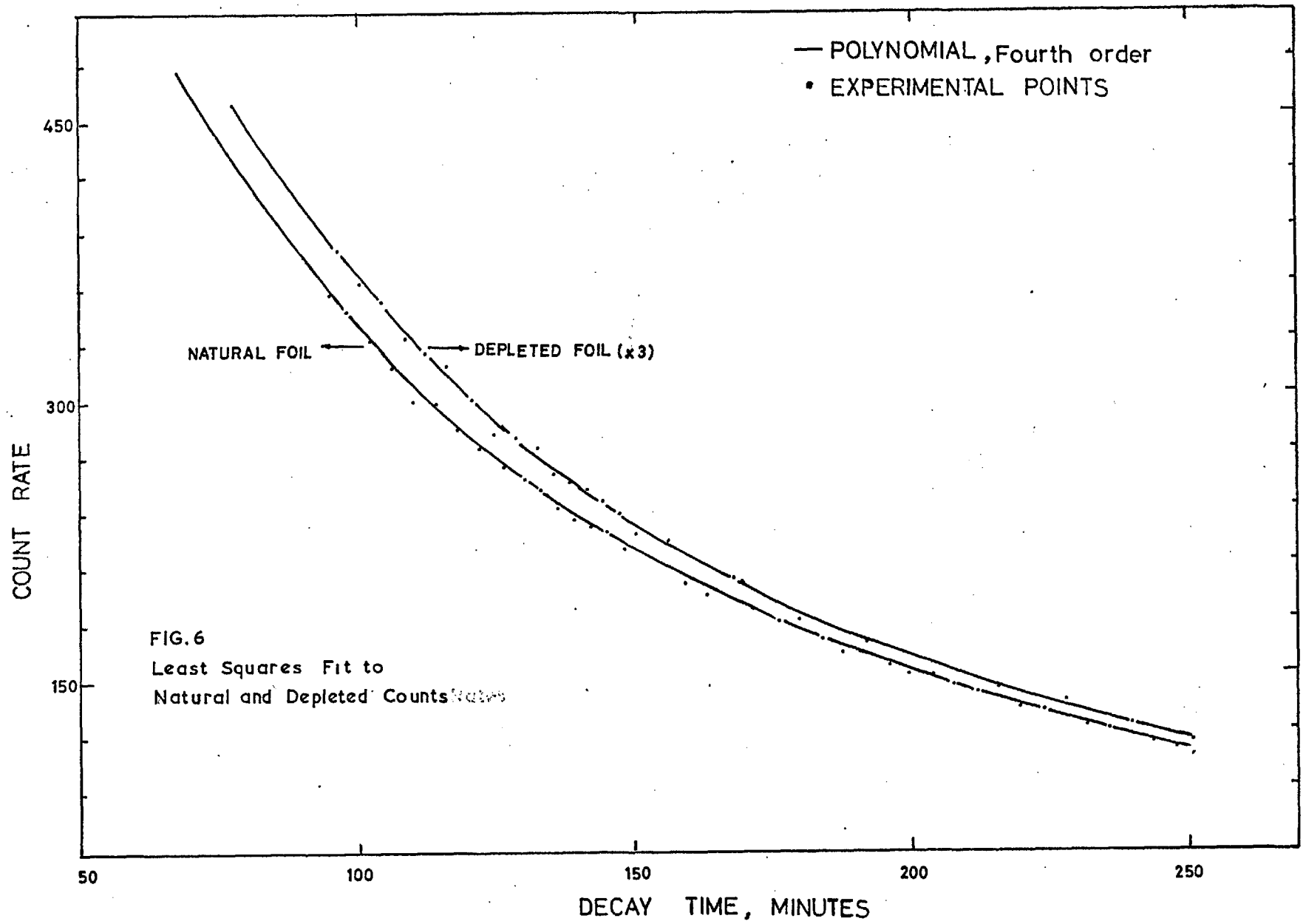

FIG. 6
Least Squares Fit to
Natural and Depleted Counts Rates

scintillation detector was followed by an adaptor unit which supplied EHT to the photomultiplier tube. The adaptor amplified the pulses received from the detector and fed them to a pulse Amplitude Selector from which standard pulses were emitted to be counted by a scaler. All units were Harwell 2000 series equipment. Two spectrometers were normally operated together with a common time control to the scaler. A pulse generator, generating 2000 cps by means of a crystal oscillator was used in conjunction with a scaler as a timer. The counts on each scaler was printed out on a paper tape through a link between the scalers and a Readout controller unit. The picture of the whole equipment is shown in plate 7.

The irradiated uranium foils o.075 mm thick and 9 mm diameter were counted on the two NaI(Tl) crystal assemblies by mounting the foils in aluminium trays and covering them with 1.5 mm thick aluminium to shield them from beta particles. Inside the trays were recessed for the foils to keep them secure in the trays (see Fig. 8B). The trays were fitted into a long brass slide, as shown in Fig. 8A, which allowed the foils to be placed in turn between the crystals. The stability of the whole equipment is highly important to meet the required accuracy in measurements. For this purpose the whole equipment was placed in a temperature controlled box. (The effects of temperature changes will be discussed in more detail in chapter 6). The box was designed to have a constant temperature with a tolerance of $\pm$ 0.1^{o}C. A temperature controller was mounted in the box to indicate and to respond to any change in the temperature. A fan and two ordinary light bulbs were used to supply heat to the detector system which was mounted in a separate compartment. The fan was always working circulating the air in the detector compartment by

sucking air from the top of the detector compartment and blowing it into the bottom of the box, see plate 7. In order to maintain a constant temperature in the box a relay was connected to the controller and to the bulbs. If the temperature inside the box dropped by $0.1^{o}C$ from the preset temperature the controller sent a signal to the relay which switched on the bulbs until temperature reached the present temperature. The bulbs were then switched off. The preset temperature was 2 to $5^{o}C$ above room temperature. A few holes were provided in the fan compartment wall to the outside air to bring cool air into the box if needed, otherwise they were always kept covered. The equipment gained stability after running for 4 to 5 hours continuously. At this stage the variation of temperature inside the box was very small and the bulbs were on for a few seconds only once every half an hour, the fan was on all the time to avoid any rapid change in the equipment temperature.

3.5 GAMMA RAY SPECTROSCOPY

It will be shown in chapter 5 that the duration of foil irradiations must be constant for all irradiations so that the results of different experiments can be compared. Irradiations of two hours duration were chosen for convenience.

Loading and unloading of foils in the irradiation hole, thermal column and the core was not possible during the reactor operation because of the high radiation level. Therefore, two hours irradiation was determined by starting the timer at 37% of the required reactor power and shutting down the reactor exactly at the end of 7200 seconds. The validity of this timing procedure was checked by placing a fission chamber in the vicinity of the core. The integrated count was then taken on a counting system and divided by the count rate at the steady state reactor power to yield the irradiation

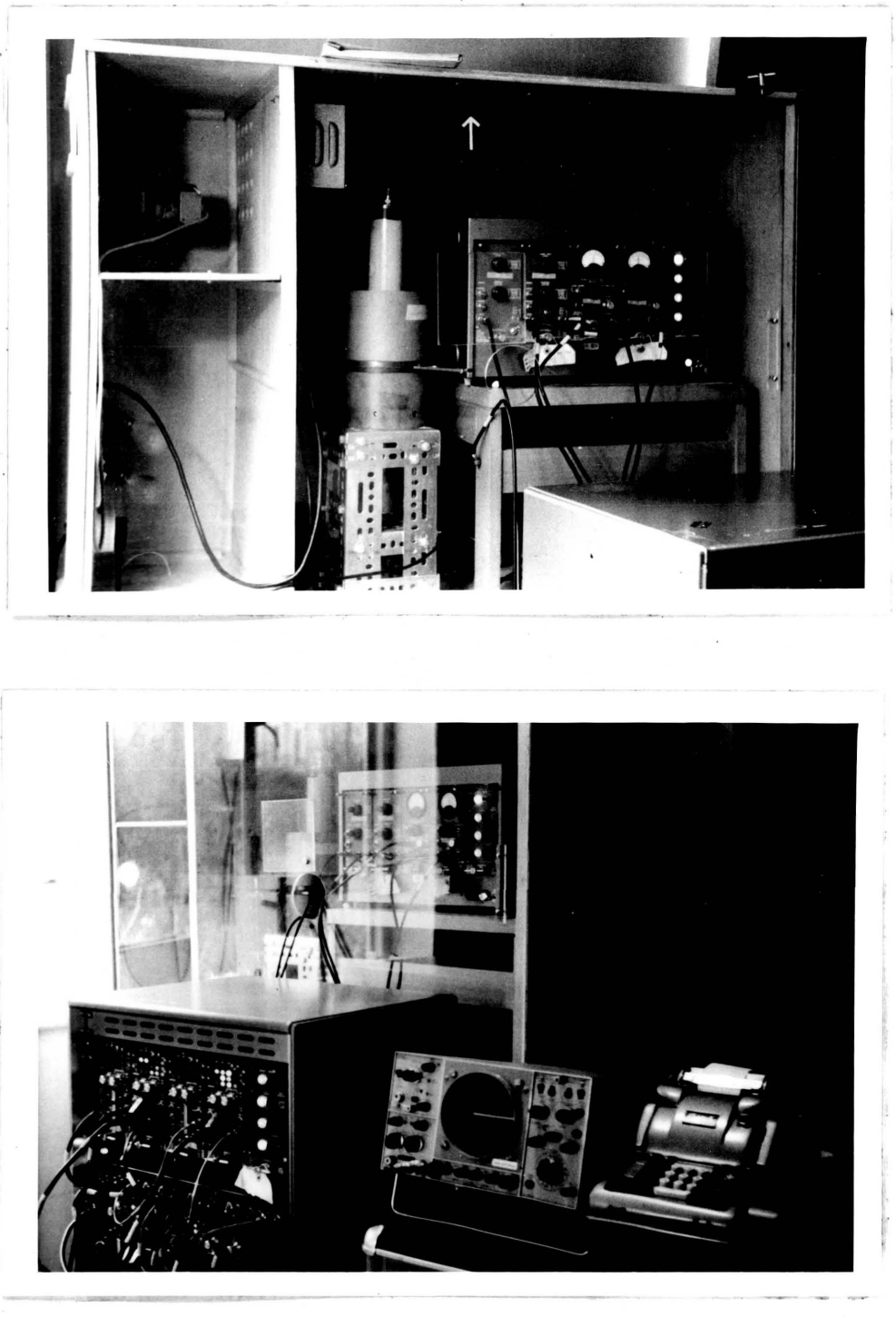

Plate 7 Gamma Counting Equipment and Temperature Box

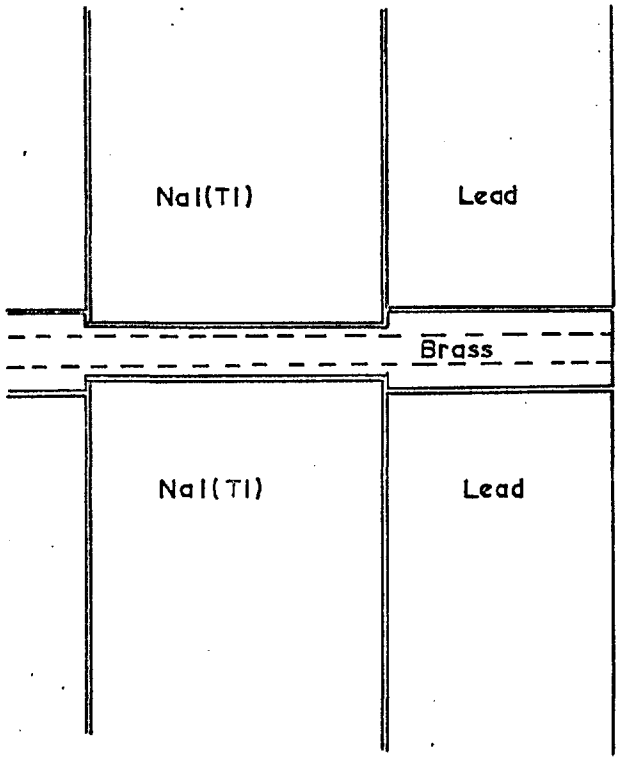

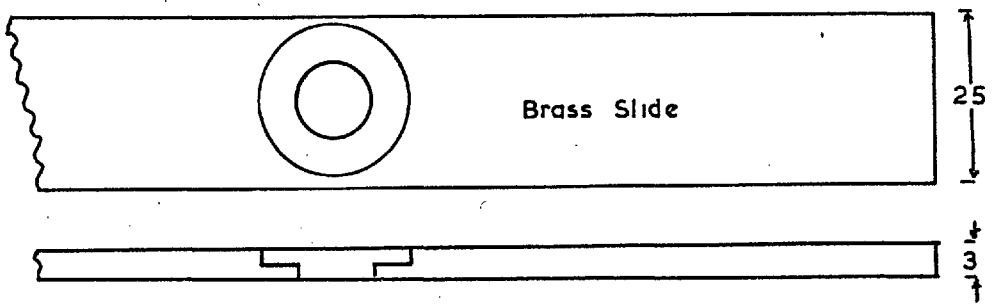

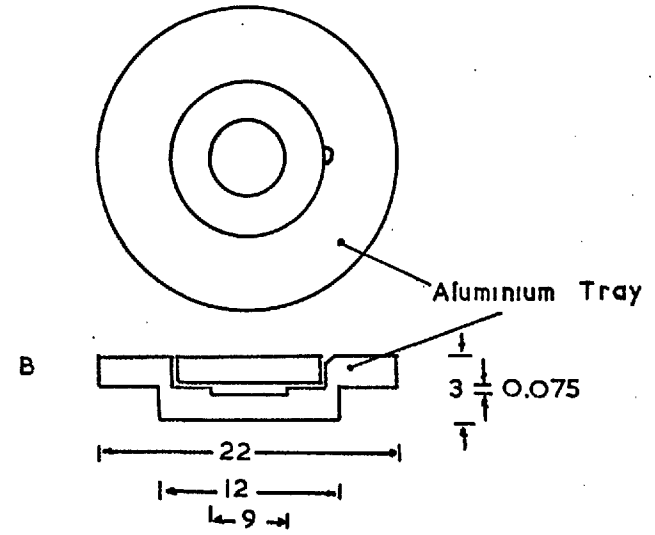

FIG.8
SCHEMATIC DEMCNSTRATION OF FOIL HOLDER IN GAMMA COUNTING.

period. The obtained irradiation period by this method was only 2 seconds more than 7200 seconds which means that the systematic error on the timing is only 0.03%.

After the irradiation was terminated the uranium foils were counted on a double NaI scintillation counting system (see section 3.4.) Depleted and natural uranium foils were used in fission ratio measurement. The depeleted foils contained 0.0355% U_{235} and natural foil 0.7196% U_{235}, and the rest was mainly U_{238}, see section 4.4. U_{238} captures thermal and epithermal neutrons and forms U_{239} which is an active nuclide and emits beta particles of maximum energy 1.20 Nev. The decay scheme and formation of U_{239} are shown in Fig. 9. The Bremsstrahlung gamma activity from 1.20 Mev beta particles can be eliminated by choosing

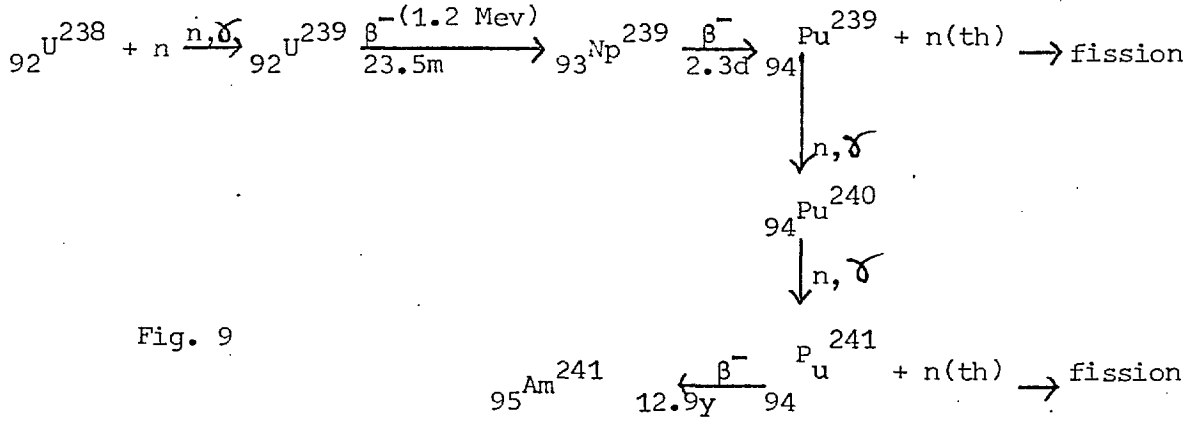

Fig. 9

an appropriate discuminator bias level. Therefore for this purpose the threshold on the pulse amplitude selector unit was set at the 1.28 Mev. photopeak of Na22. To ensure the stability of the counting equipment the integral count above 1.28 Mev. was taken to produce a method for checking the position of 1.28 Mev. peak in later countings.

The decay of Na^{22} (half life is 2.58 yr) was taken into account. A rate meter was also used for checking the threshold.

CHAPTER 4

FOIL ENRICHMENT MEASUREMENTS

4.1 INTRODUCTION

In equation (3.6) $\frac{N5D}{N5N}$ and $\frac{N8D}{N8N}$ must be known in order to determine $(F8/F5)_{\gamma}$. The method for determining the amount of U_{235} in an unknown uranium foil involves the simultaneous irradiation of two uranium foils in a thermal spectrum. The gamma activity of each foil, after the end of irradiation,is due to gamma activities of fission products of thermal fission occurring in U_{235} nuclei and capture gammas in U_{238}. As was mentioned in chapter 3.5, the Bremsstrahlung radiation is produced from beta particles emitted by U_{239}. Therefore, by setting the discriminator bias level on the counting equipment above 1.20 Mev, maximum gamma rays from U_{238} neutron capture activity are eliminated. The gamma activity of each foil above the threshold is only due to fission products of U_{235} thermal fission. The ratio of U_{235} nuclei in the two foils was found by comparing the gamma activities from the foils.

4.2 DESCRIPTION OF THERMAL COLUMN

The method of foil enrichment determination is based on the foil irradiation in a thermal flux. For this purpose an extension of the graphite stack was erected on the 270° face,Bare Face.of the University of London Reactor. The new thermal column consisted of 50 blocks of graphites each 20 cms square by 75 cms long to form a stack of 100 cms square by 150 cms long, see Fig. 10. The graphite column was 70 cm away from the 270° face of the core. Of this distance, 60 cms is graphite covered by aluminium and 10 Cm of water in the reactor tank. The aluminium covered graphite block is 95 cms square.

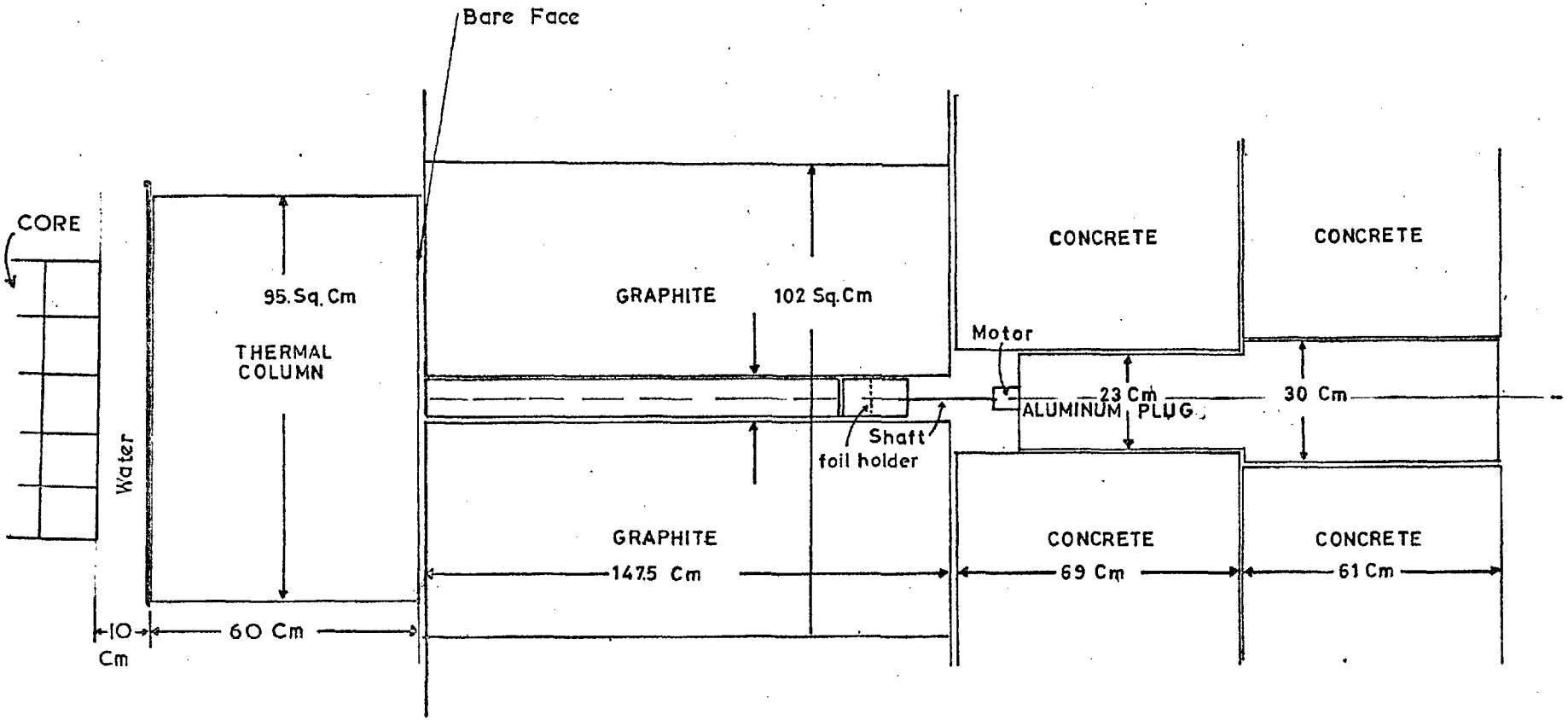

FIG. 10 EXTENSION TO THE BARE FACE OF THE UNIVERSITY LONDON REACTOR

A hole of 10 Cms diameter in the central block of the thermal column was filled with graphite pieces 23 cms long. A hole of about 6.5 mm diameter in the centre of these pieces facilitated access of the fission chambers.

4.3 REACTION RATE MEASUREMENTS IN THE THERMAL COLUMN

A series of measurements were carried out in the thermal column in order to determine the nature of the neutron spectrum and the flux distribution. Two fission chambers containing Pu-239 and U-235 were used for these measurements. The fission chambers made by 20th Century Electronics Ltd., were 131 cms long with 1 cm active length and 6 mm diameter. The measurements were performed on the central axis of the graphite column. The measurements with both fission chambers started from the bare face moving outwards. As the fission chambers moved outwards, the 10 cm diameter graphite pieces were replaced by solid ones to prevent neutron streaming through the central hole of 6.5 mm diameter. The measurements with both fission chambers were carried out alternately. The Pu239/U235 fission ratio measurements were plotted in Fig. 11. It should be mentioned that the Pu/u measurements were not corrected for mass of deposits, i.e. they are not fission/atom. It is seen that the fission ratio is constant to within one per cent from 20 to 120 cms from the bare face. It should be noted that Pu-239 and U-235 have similar types of fission cross sections over the thermal region except that Pu-239 has a strong resonance at 0.3 ev. Therefore Pu239/U235 fission ratio indicates the degree of neutron thermalization in the medium in which the measurements have been carried out. The Pu239/U235 fission ratio measurement along the thermal column indicated that the thermal neutron

FIG. 11 PU 239/U 235 FISSION RATE IN THERMAL COLUMN

(Error at each point is ± 2%)

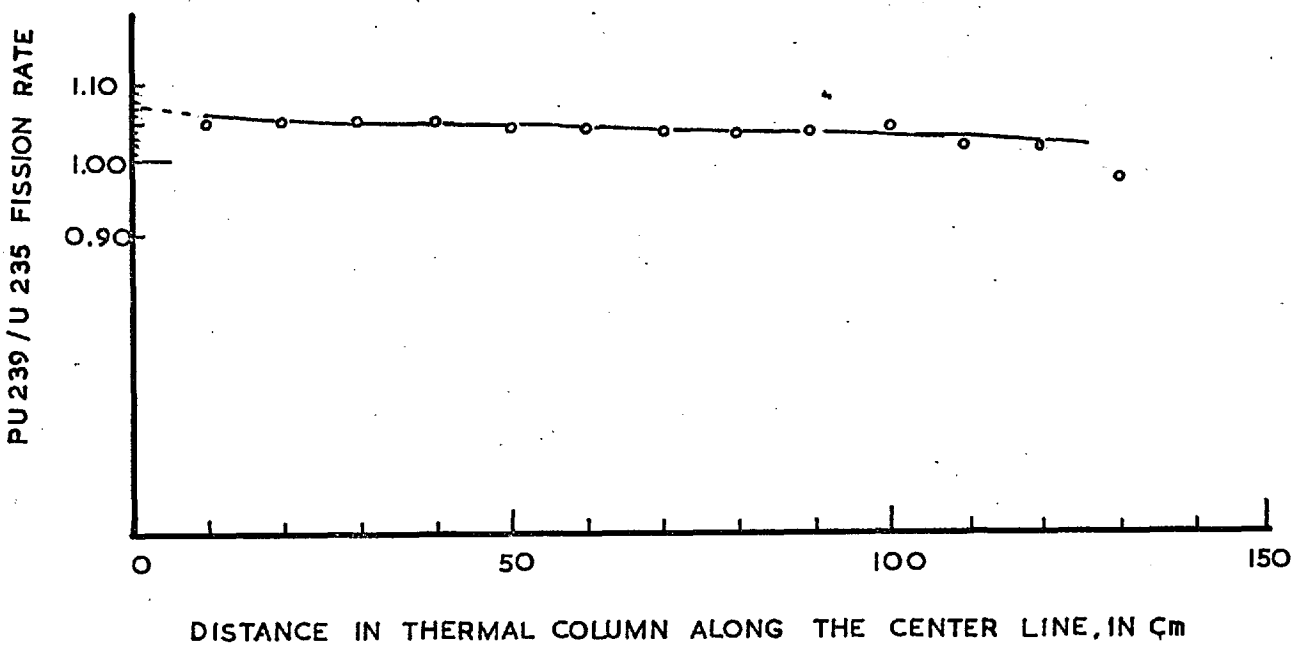

spectrum is nearly unchanged in the mentioned region.

The cadmium ratio was also measured in the thermal column using a fission chamber and a Boron Trifluoride Counter covered with 0.5 mm thick cadmium. The central hole in the graphite was enlarged to fit the cadmium covered fission chamber and cd-covered BF3 counter. The BF3 counter was 1.2 cms diameter and 25 cms long. It was found from this measurement that the highest cadmium ratio was at 100 cms, from the bare face. This measurement also confirmed that the amount of epithermal neutron in the thermal column is not significant. The thermal flux and epicadmium flux are shown in Fig. 12, using the fission chamber.

4.4 DETERMINATION OF FOIL ENRICHMENT

In fission ratio measurements it is necessary to know the enrichment of the foils. These were determined by irradiating the foils simultaneous in a thermal neutron spectrum along with a foil of natural uranium, and gamma counting for U_{235} fission product activity on a double NaI(Tl) counting system, see Section (3.4). Knowing the enrichment of the natural foil and the weights of all the foils, the enrichments were calculated to an accuracy of better than $\pm$ 1%. Possible sources of errors in this measurement are discussed in chapter 6. The results of foil enrichment measurements with a depleted foil along with a mass specrometric analysis carried out at AWRE (Aldermaston) are given in Table 1.

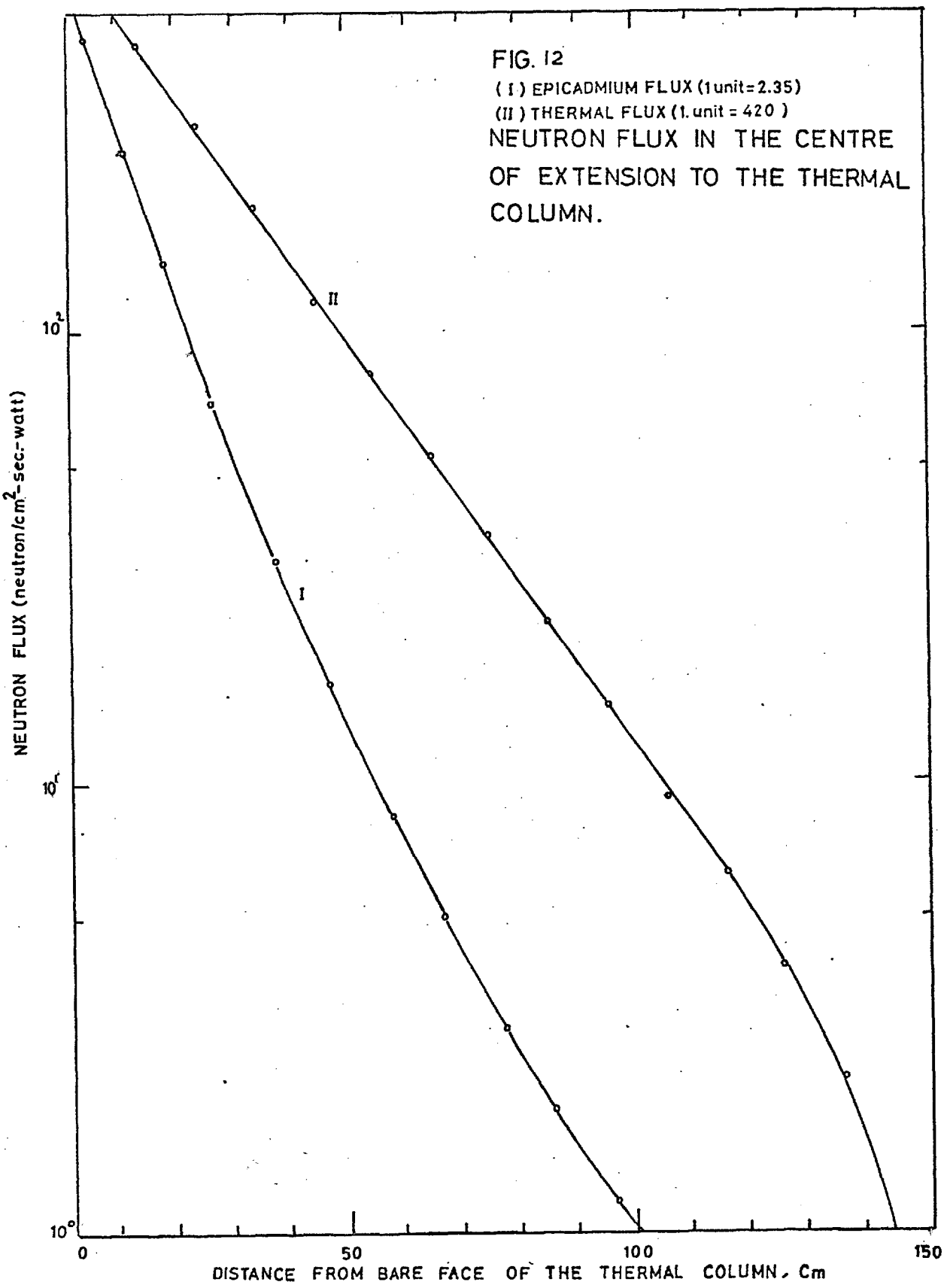
FIG. 12
(I) EPICADMIUM FLUX (1 unit = 2.35)
(II) THERMAL FLUX (1 unit = 420)
NEUTRON FLUX IN THE CENTRE OF EXTENSION TO THE THERMAL COLUMN.
II
I
NEUTRON FLUX (neutron/cm²-sec-watt)
10²
10¹
10⁰
0
50
100
150
DISTANCE FROM BARE FACE OF THE THERMAL COLUMN, Cm

The foils were irradiated in a flux about $10^{8n}/cm^2$-sec for two hours. The foils were irradiated under the same conditions by mounting them between two cylindrical graphite pieces which were connected to the shaft of an electric motor, see Plate 13 (A and B). The centre of the two graphite pieces were threaded and a graphite spigot held them tight together. The motor rotated the graphite assembly at a speed of 4 rpm during the irradiation in order to expose the foils to the same flux. The motor was mounted on an aluminium shaft so that the foils could be positioned at 48 cms from the outside edge of the thermal column, this position being one meter from the bare face. Plate 13 (A and B) shows the Al-plug, motor and the graphite rotator. The two hours irradiation was chosen so that the normalized U_{235} decay of this measurement could be compared with the normalized decays obtained from fission ratio measurements in the reactor spectrum. All decays were normalized to unity at 240 minutes after the end of irradiation in order to compare them to one another.

A Fortran IV computer program ENRICH was written to calculate the percentage of U_{235} in the unknown foil (see Appendix I for detail of the computer program). The enrichment determination was based on a value of $0.7196 \pm 0.0036\%$ (26) U_{235} for the enrichment in natural uranium, see Table 1.

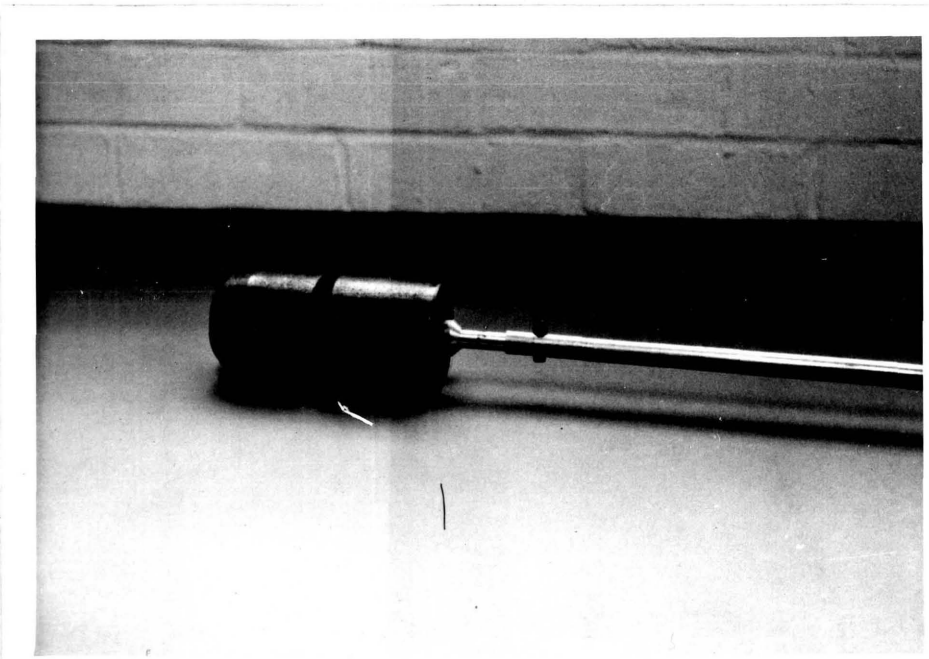

Plate 13A Graphite Rotator(foil holder)

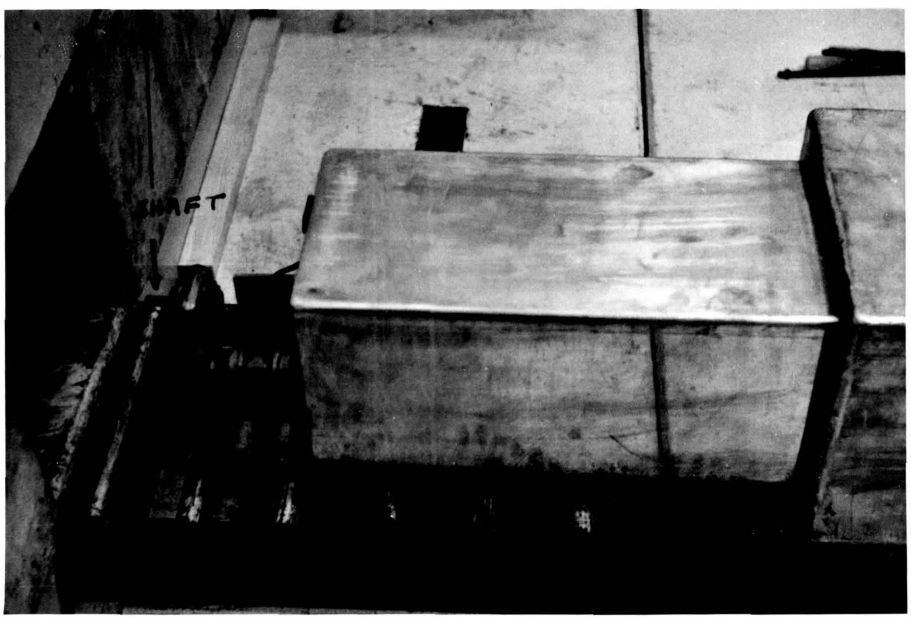

Plate 13B Aluminium Plug and Electric Motor

TABLE 1 - SPECIFICATION OF FOILS

	$\frac{U_{234}}{U_{238}}$ %	$\frac{U_{235}}{U_{238}}$ %	$\frac{U_{236}}{U_{238}}$ %
*Mass Spectrometry (Depleted foil)	0.000347 ±6	0.0354 ±2	0.000321 ±9
*Mass Spectrometry (Natural foil)		0.7253 ±32	
	U_{234}%	U_{235}%	U_{236}%
Present work (Depleted foil)		0.0355 ±3.0	
Natural foil (19)	0.0056	0.7205	
Natural foil (26)		0.7196	

*The mass spectrometry was performed by J. Roberts at AWRE, Aldermaston.

The procedure for irradiating foils in the thermal column was to expose all foils to the same neutron flux. Each foil was guarded between two identical foils to prevent loss of fission products from the measuring foils. Flux perturbations will be discussed in chapter 6.

CHAPTER 5

CALIBRATION FACTOR p(t)

5.1 INTRODUCTION

p(t) is a factor which is required to convert the gamma activity fission ratio to the true fission ratio is given as:-

$$p(t) = (F8/F5)/(F8/F5)_{\gamma} \qquad (5.1)$$

The true fission ratio is a constant quantity and the fission ratio $(F8/F5)_{\gamma}$, is a time dependent function. Time in this context is referred to decay time (see equation 3.6). The uranium foils were counted on a double NaI(Tl) counting system whose discriminator bias was set at the 1.28 Mev photo-peak of Na.22. The gamma activity fission ratio obtained from equation 3.8 depends on the ratio of $CD/CN.(F8/F5)_{\gamma}$ decreases with decay time as CD/C^{N} does. Therefore p(t) is a time dependent parameter. p(t) also varies with discriminator bias level, geometry of the detector, size of foils and length of irradiation. However, it should be noted that foils from reactor irradiations were counted on the same system as that used for the p(t) measurements and so the dependence of p(t) on bias level, detector geometry, etc., cancels. p(t) is also dependent on the neutron spectrum to a small extent and this is discussed in detail in chapter 6.

5.2 DESCRIPTION OF THE DOUBLE FISSION CHAMBER, IRRADIATION FACILITY AND FISSION COUNTING SYSTEM

A double fission chamber manufactured by 20th Century Electronics Ltd., was used for the determination of the p(t). Details of the fission chamber are shown in Fig. 14. The fission chamber was loaded with two

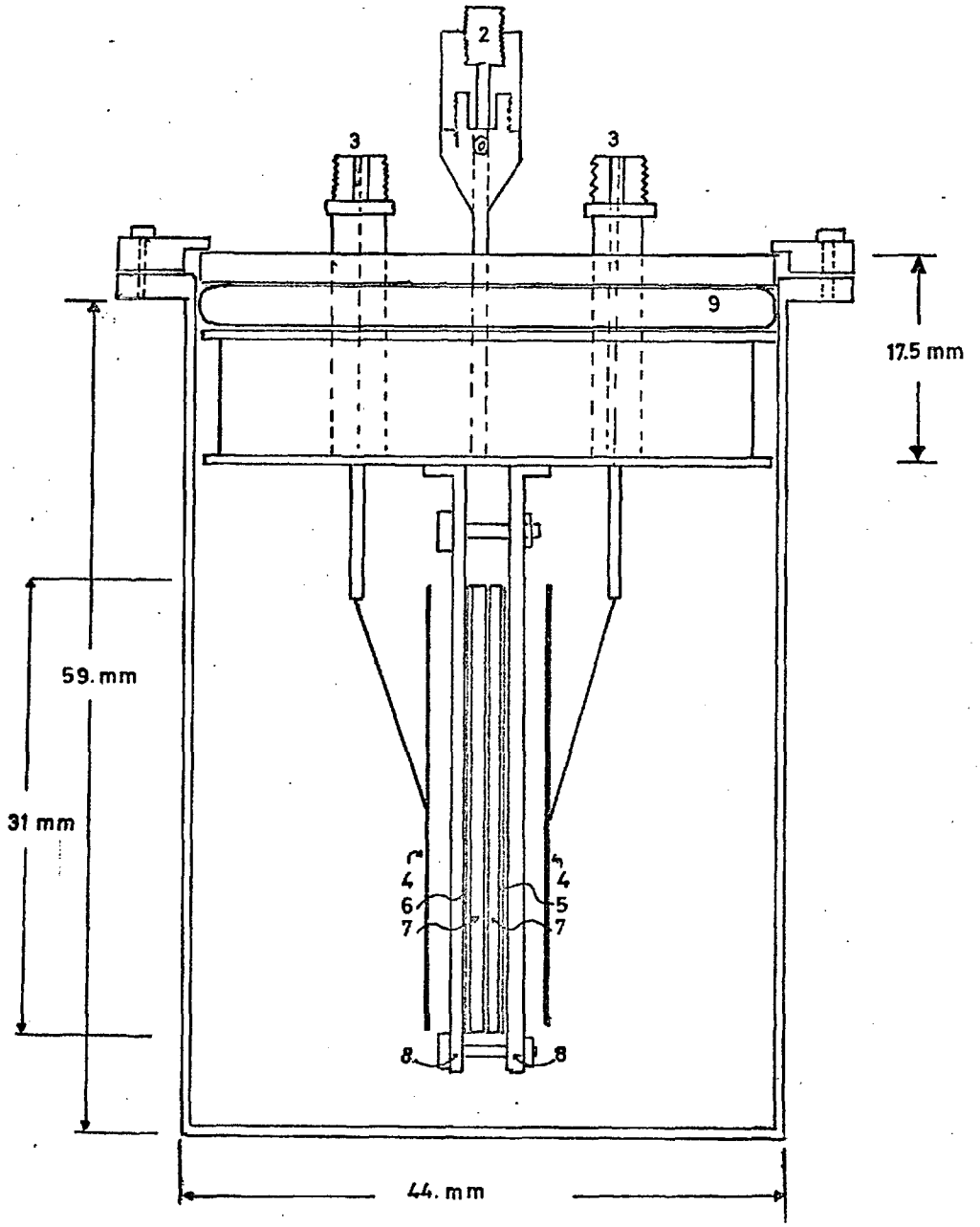

1- GAS FILLING PIPE.
2-PLUG.
3-P.E.T. SOCKETS.
4-COLLECTORS.
5-U-235 DEPOSIT (0.504 mg/cm 2, U308)
6-U-238 DEPOSIT (1.993 mg/cm^2, U308)
7-PLATINUM BASE (each 0.005" thick)
8-FOIL/DEPOSIT HOLDER.

FIG. 14 DOUBLE FISSION CHAMBER

uranium deposits in the form of U_3O_8. The deposits were painted by a special brush on a platinum backing, 0.125 mm thick and 4.4 cms diameter on an area of 3.2 cms diameter. The painted deposits were then baked in a furnace to become U_3O_8. In the second set of deposits depleted and natural uranium were painted on aluminium backing 0.125 mm thick and 3.2 cms diameter. The deposits were prepared at Harwell in the same fashion mentioned above. The specifications of the deposits are given in Table 2. It should be mentioned that the deposits are demountable and can be replaced with any deposits of proper size. The weights of the deposits were assessed by alpha counting in 2π geometry

TABLE 2. SPECIFICATIONS OF THE DEPOSITS

Deposit	Mass $\mu g/cm^2$	U_{234} %	U_{235} %	U_{236} %	U_{238} %
U_{235}	63		92.95		5.68
U_{238}	245		0.001		100
*Depleted Uranium	110	0.000347 $\pm$6	0.0354 $\pm$2	0.000321 $\pm$9	99.96
*Natural uranium	109	0.0056	0.7196		99.28

at Harwell. The weights of the deposits have been measured to better than 1.5% accuracy.

The fission chamber was filled with an argon/methane mixture in the proportion, 90% Argon and 10% Methane, at two atmosphere pressure. The fission chamber had an excellent voltage plateau an optimum operating position chosen at 500 volts, see Fig. 15. The operating bias level was obtained by determining the fission products pulse height amplitude spectrum using a single channel analyzer. The operating bias was positioned above the alpha cutoff energy. Fig. 16 shows the fission products energy spectrum together with the bias curve.

A second fission chamber exactly similar to the double fission chamber was used for foil irradiations so as to produce the same spectrum condition as in fission counting.

The most suitable place for the p(t) determination in the University of London Reactor was found to be the irradiation holes on the 0° face of the Reactor. The position of the holes is shown in the general layout of the core and its surroundings (Fig. 17). The hole that was chosen for the p(t) measurement is a 7 cms square passing 37 cms from the 90° face of the core through the mid-height plane of the core. Access to the hole is through a round hole, 15 cms diameter which was filled with aluminium cased concrete plugs. The fission chamber was fixed to a piece of sindanyo being held by an aluminium tube. The aluminium tube was fixed to an aluminium concrete plug by four screws. The assembly is shown schematically in Fig. 18. It is shown in the diagram that a mechanical device was used for repositioning the plug in the irradiation hole so that it was in the same position for every irradiation. Three pieces of P.E.T. strips were attached to the outside surface along the plug to ease the movement of the assembly in the hole. Using this arrangement the fission chamber was placed on the horizontal central axis of the core. The

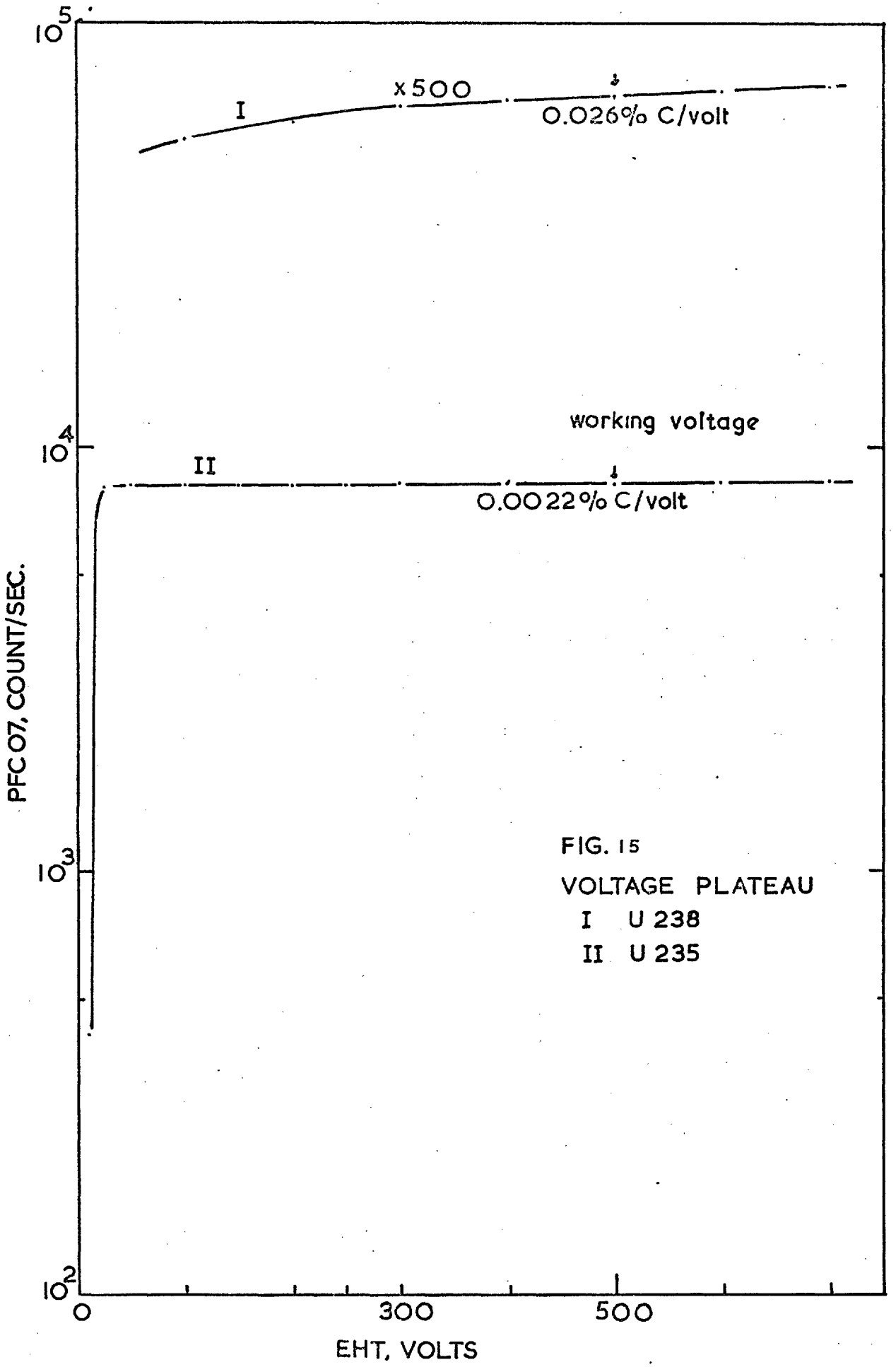

FIG. 15

VOLTAGE PLATEAU

I U 238

II U 235

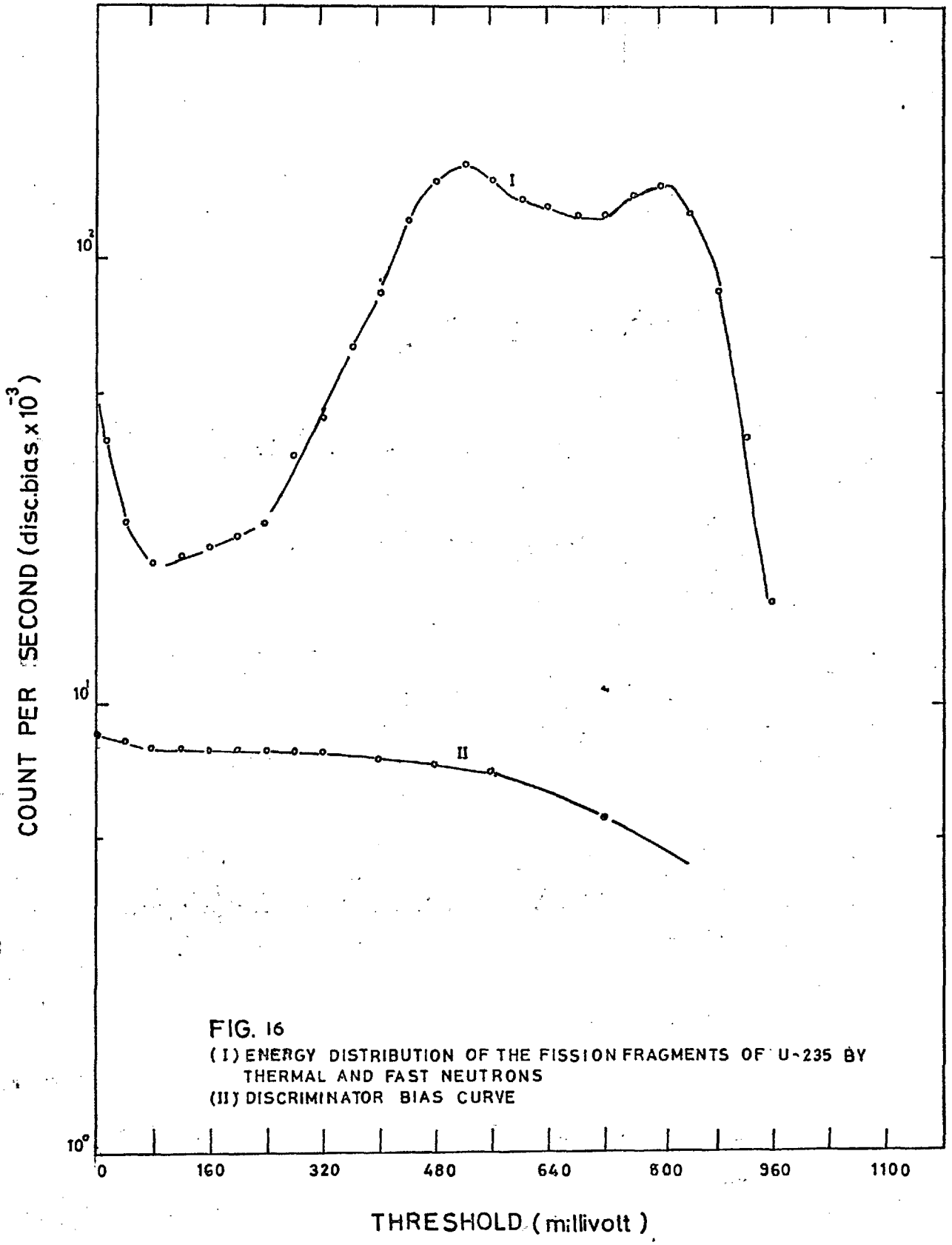

FIG. 16
(I) ENERGY DISTRIBUTION OF THE FISSION FRAGMENTS OF U-235 BY THERMAL AND FAST NEUTRONS
(II) DISCRIMINATOR BIAS CURVE

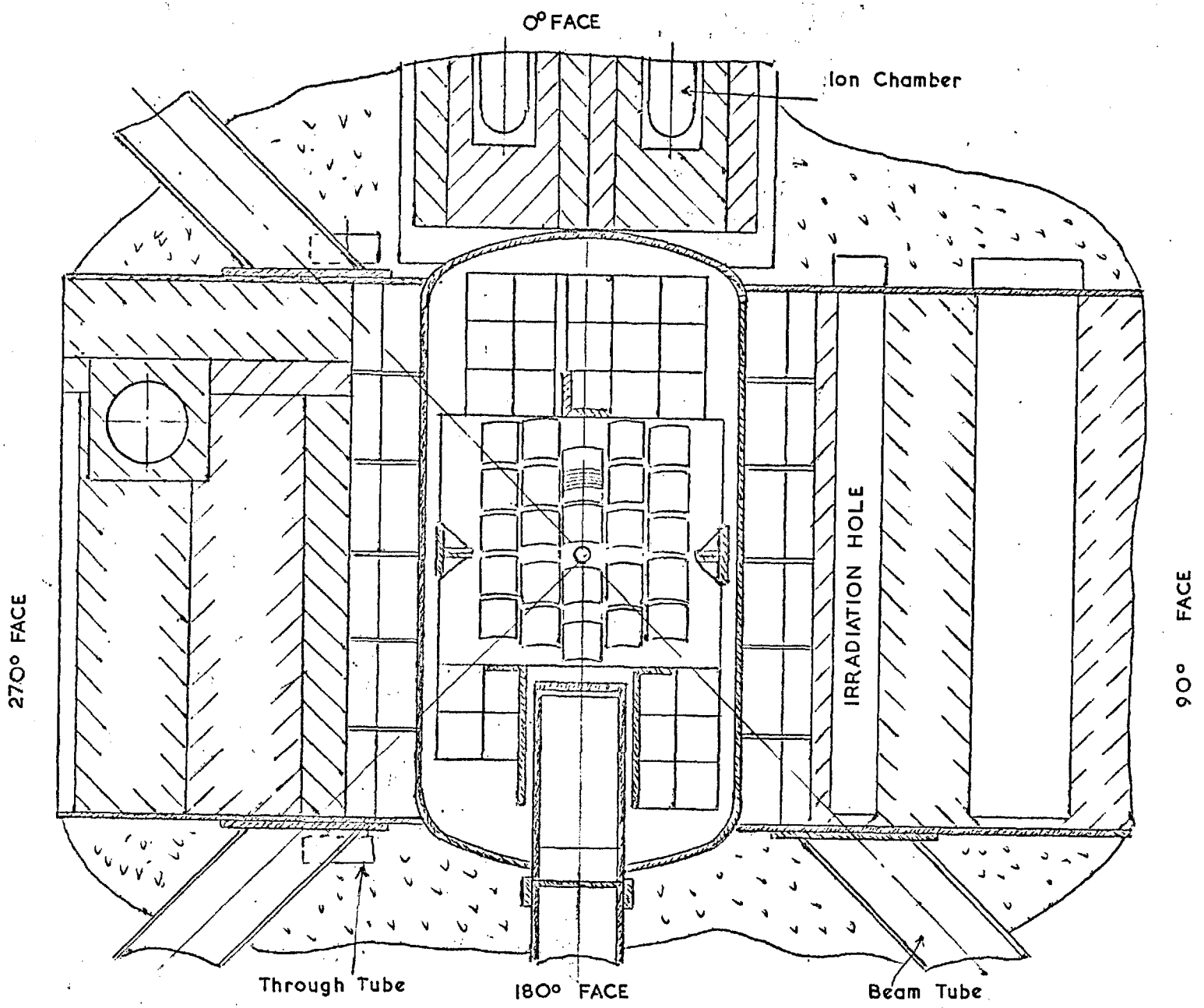

FIG. 17 GENERAL LAYOUT OF THE REACTOR CORE

The four meter long EHT and signal cables were passed through a hole on the Al-tube and located in the grooves milled on the Al-concrete plug see plate 19. A monitor fission chamber was fixed inside the aluminium tube and was used in conjunction with fission counting and foil irradiation to check the flux level fluctuation and for timing the irradiation period. In some cases the second output of the main amplifier was used to monitor the flux change. The procedure of the experiment was to irradiate the double fission chamber for fission counting, then replace the chamber with the dummy fission chamber loaded with uranium foils for a foil irradiation. The uranium foils sandwiched between two identical foils were taped by aluminium tape on platinum or aluminium discs, whichever the backing of the deposits were in the fission counting. These discs were exactly identical to the backing of the deposits. The dummy fission chamber had air at atmospheric pressure. The gamma activity of the foil irradiation in the dummy fission chamber filled with argon at two atmosphere pressure was compared with the identical irradiation with air at atmospheric pressure in the chamber. No difference more than statistical fluctuation was observed.

A cadmium sleeve was used to cover the double fission chamber and the aluminium tube. The cadmium sleeve was made a tight fit to the tube, see Fig. 18.

The fission counting was performed with Harwell 2000 service equipment. A block diagram of the counting system is shown in Fig. 20.

The irradiation period was two hours as usual in this work.

An experiment was performed in the irradiation hole to see the flux shape from the centre of the hole to the outside face of the reactor, that is the 0° face. The measurement showed a gradual drop in the flux followed by a sharp decrease near the edge of the core.

1- Double Fission chamber
2- Perspex or Sindanyo
3- Cadmium sleeve.
4- Aluminium tube.
5- Slot for cables
6- Monitor fission chamber.
7- Aluminum plug.
8- Grooves

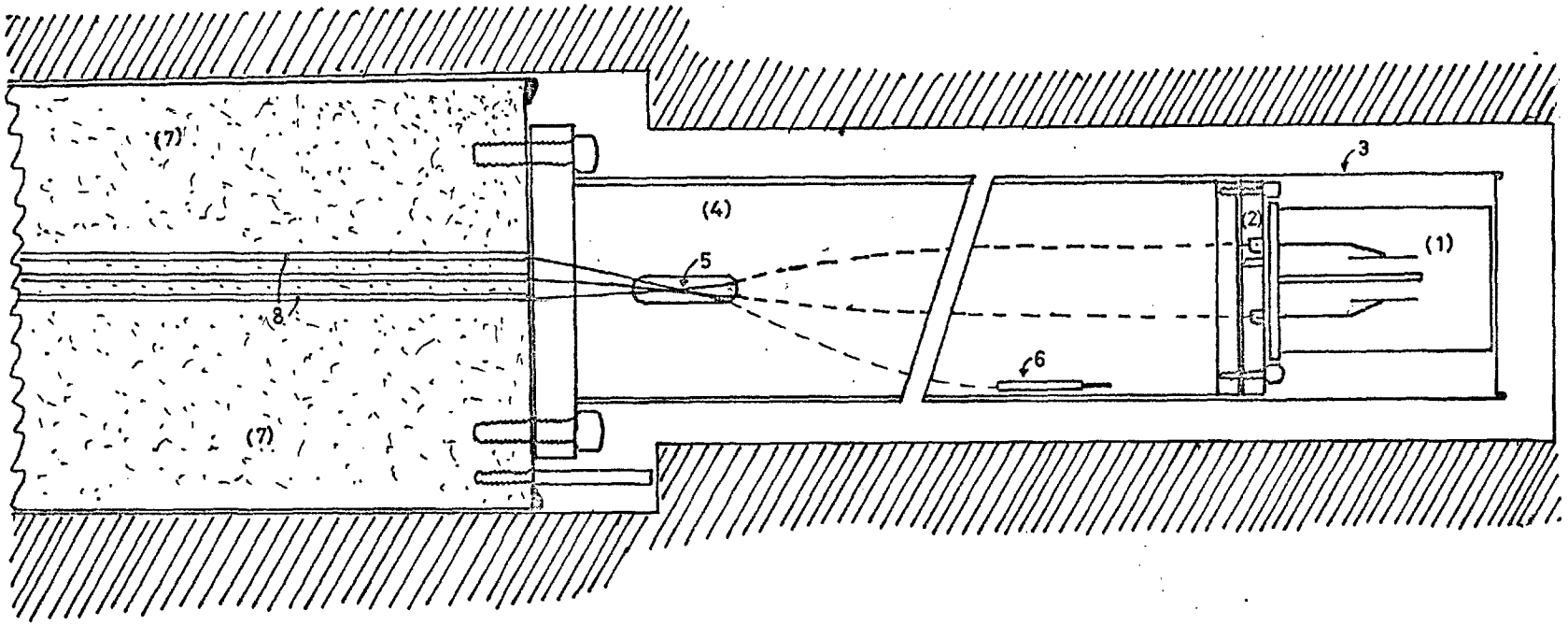

FIG.18 DOUBLE FISSION CHAMBER AND PLUG ASSEMBLY IN IRRADIATION HOLE.

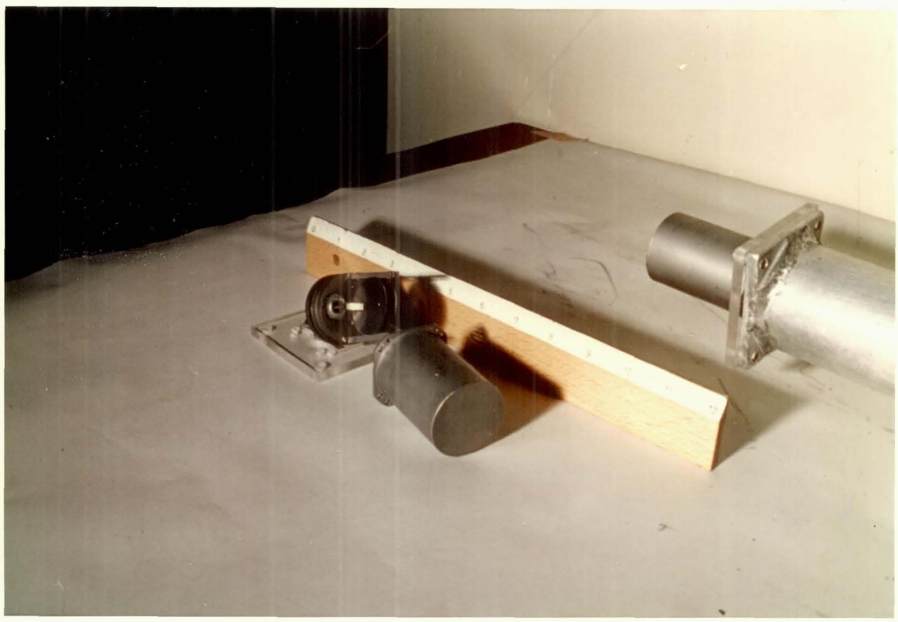

Plate 19 Aluminium cased Concrete Plug and Double Fission Chamber.

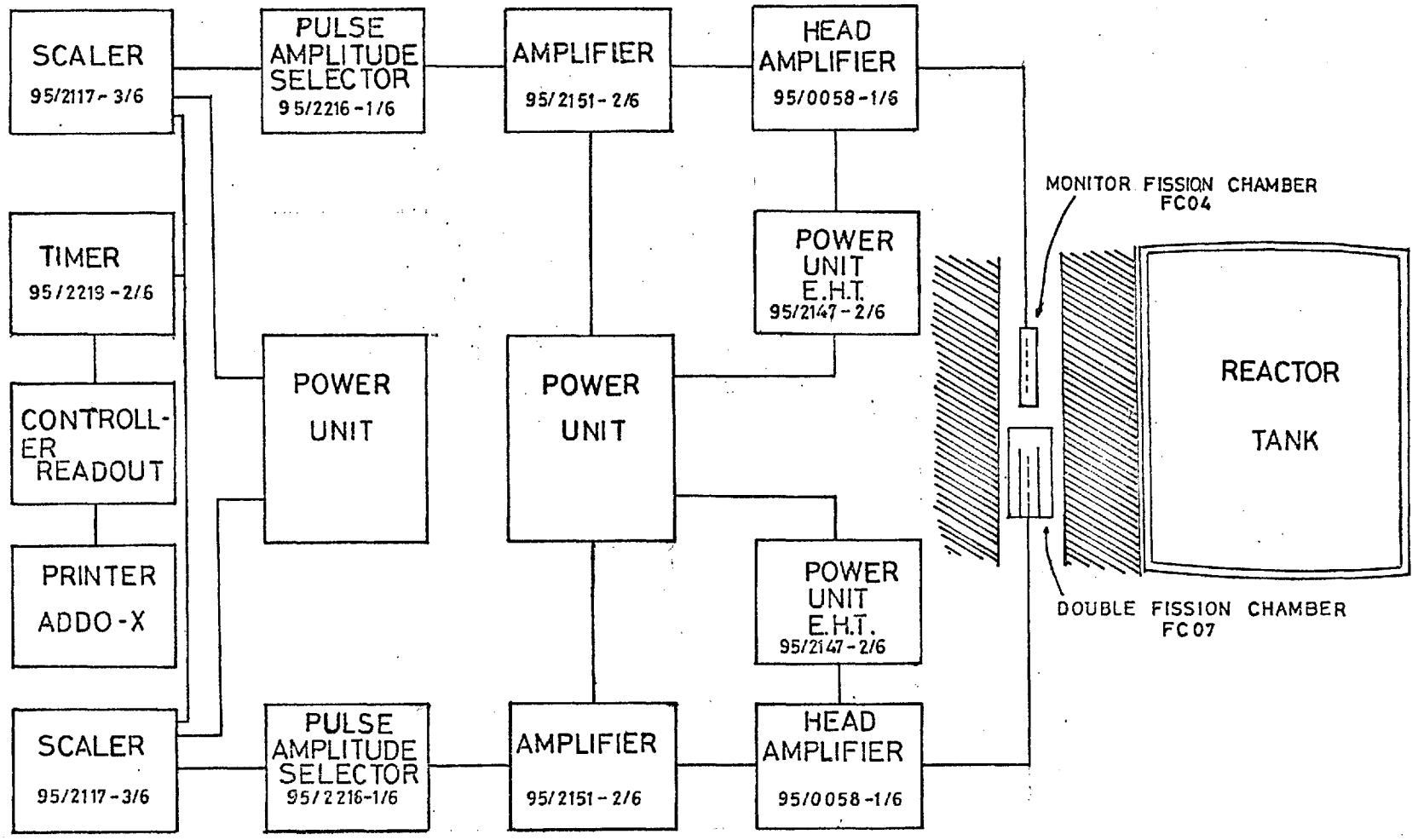

FIG. 20 A BLOCK DIAGRAM OF FISSION COUNTING SYSTEM

5.3 DETERMINATION OF p(t) BY FISSION CHAMBER

The experimental arrangement for the calibration factor measurement, which was conducted with a double fission chamber, and was discussed in section 5.2, is shown in Fig. 18. Thin deposits of U_{235} and U_{238} painted on 0.125 mm thick platinum discs were used as the anode coating for the two halves of the fission chamber. Also depleted and natural uranium deposits painted on aluminium discs were used for further experiments. See Table 2 for deposits specifications. The choice of the deposits and foils for these measurements will be discussed in chapter 6. The fission counts were measured from both halves of the fission chamber and knowing the masses of the deposits and composition of the coatings the true fission ratio was obtained. $(F8/F5)_\gamma$ was obtained from gamma counts of the irradiated foils using equation 3.8. Thus the calibration factor was calculated simply by dividing the true fission ratio by the gamma activity fission ratio. F8, F5 and also $(F8/F5)_\gamma$ are time dependent. F8 and F5 normalized to unity at 240 minutes are shown in Fig. 5 and $(F8/F5)_\gamma$ is shown in Fig. 21. It can be seen from Fig. 21 that p(t) varies with decay time and passes a maximum at about 360 minutes from the end of the irradiation. Some p(t) values are given in Table 3 determined at 240 minutes after the end of irradiation. Some other p(t) values using the double fission chamber are given in chapter 6 in Table 6. The counts of depleted and natural foils and fission counts obtained from the fission chamber were fed into the computer program FFRIII. The program will be discussed in Appendix 1.

FIG. 21
GAMMA ACTIVITY FISSION RATIO
CALIBRATION FACTOR, P(t)

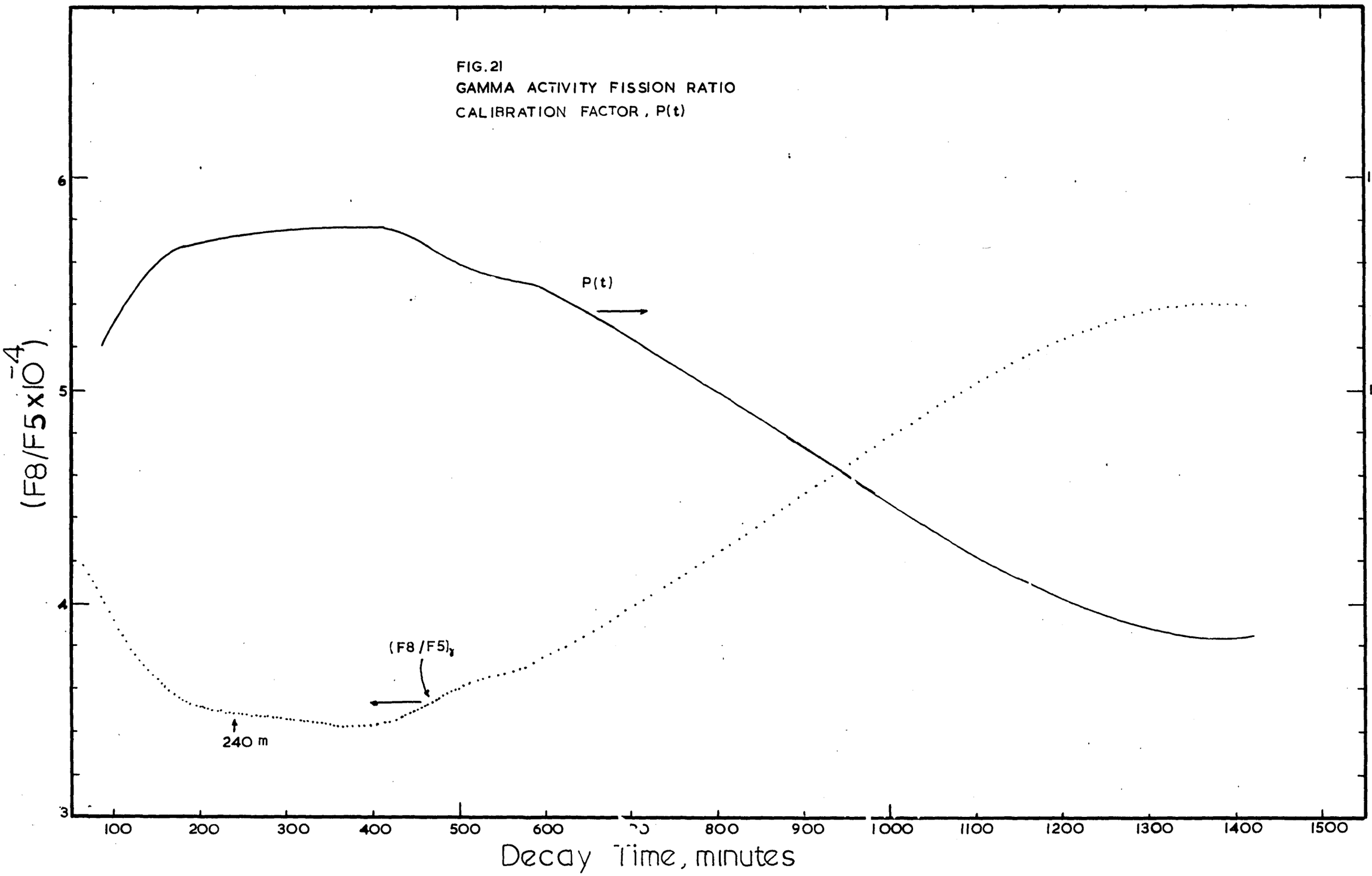

FIG. 22 P(t) vs TIME AFTER THE END OF IRRADIATION.

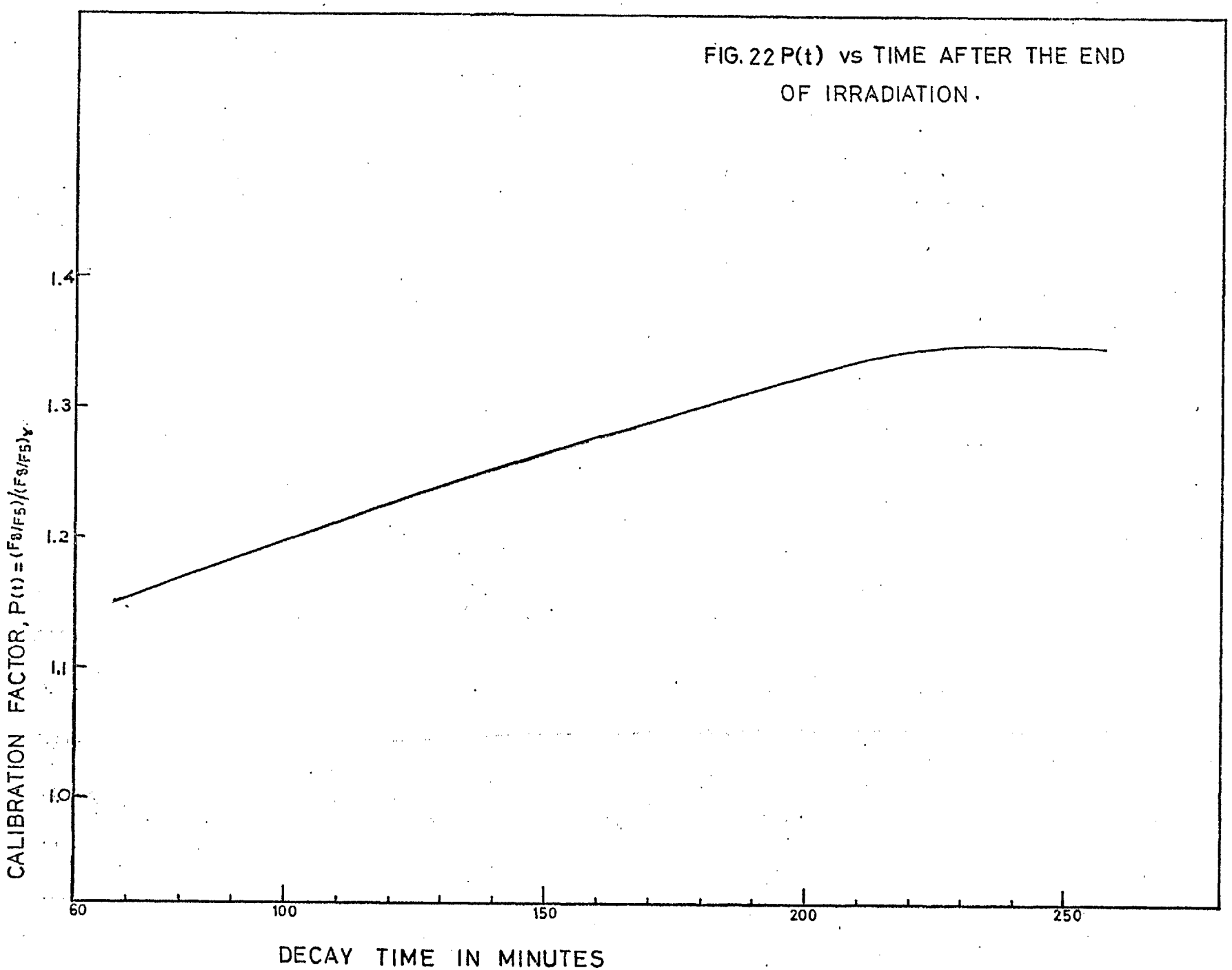

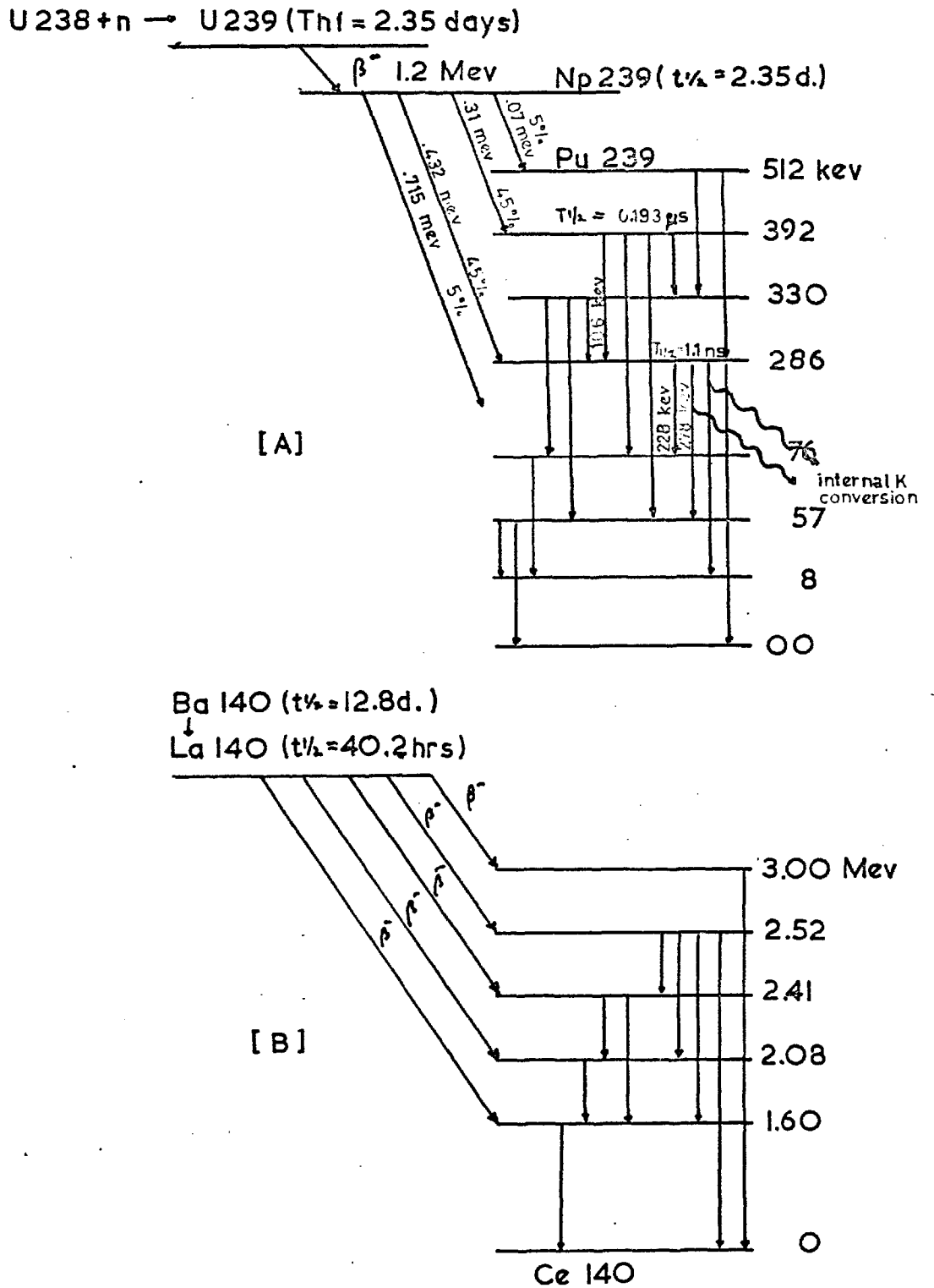

FIG. 23

DECAY SCHEME OF

[A] U239

[B] La 140

TABLE 3. CALIBRATION FACTOR AT 240 MINUTES

Method	Place of Irradiation	Number of Experiments	p(t)	Experimental Error %
Fission	Irradiation			
Chamber (5.3)	Hole	5	1.33	± 1.6
La-140	"	1	1.33	4
La-140(5.4)	Core	1	1.31	± 3
Fission	Irradiation			
Chamber (5.3)*	Hole	2	1.32	1.1%
5.4	V. de G* ±	1		
	T.C.**	1	1.34	1

*In this experiment two foils natural and depleted and two deposits natural and depleted same as foils 100μg/cm^2 thick were used.

*±V. de G = Van de Graaff

**T.C. = Thermal Column

5.4 p(t) DETERMINATION USING La-140

One of the uranium fission products is $_{54}Xe^{140}$ and it decays to a stable isotope $_{58}Ce^{140}$ through a sequence of decay as follows:-

$$_{54}Xe^{140} \xrightarrow[16^s]{\beta^-} {}_{55}Cs^{140} \xrightarrow[66^s]{\beta^-} {}_{56}Ba^{140} \xrightarrow[12.8^d]{\beta^-} {}_{57}La^{140} \xrightarrow[40.2h]{\beta^-} {}_{58}Ce^{140} \text{ (stable)} \qquad (5.2)$$

In this decay scheme Barium builds up very rapidly because of its long half life and the short half life of $_{55}Cs^{140}$ the predecessor isotope. Barium decays to Lanthanum with a half life of 12.8 days. La-140 emits several gamma rays including a 1.60 Mev photopeak that brings 96% (26) dissipated of the energy of the excited nucleus to the ground state. The decay scheme for La-140 is shown in Fig. 23. Other gamma rays are 2.52 and 3.00 Mev which contribute only a few per cent to the energy release of the excited nucleus. The fission product gamme spectrum of a natural uranium foil was obtained using a Ge(Li) detector and a 400-channel LABEN analyzer and is shown in Fig. 25 with the 1.60 Mev peak in a low background. The half life of La-140 is 40.2 hours, but because of the 12.8 days half life of its parent, Ba-140, the effective half life of La-140 is virtually 12.8 days.

For determining p(t) by the La-140 method a series of irradiations of depleted and natural foils were carried out. The foils were counted on a Ge(Li) detector after a delay of one week, using the 400 channel analyzer. The total count under the 1.60 Mev peak for the depleted and natural foils was due to the fission product La-140 resulting from thermal fission in U_{235} and fast fission in U_{238}. Therefore by determining the integral counts under this peak and knowing

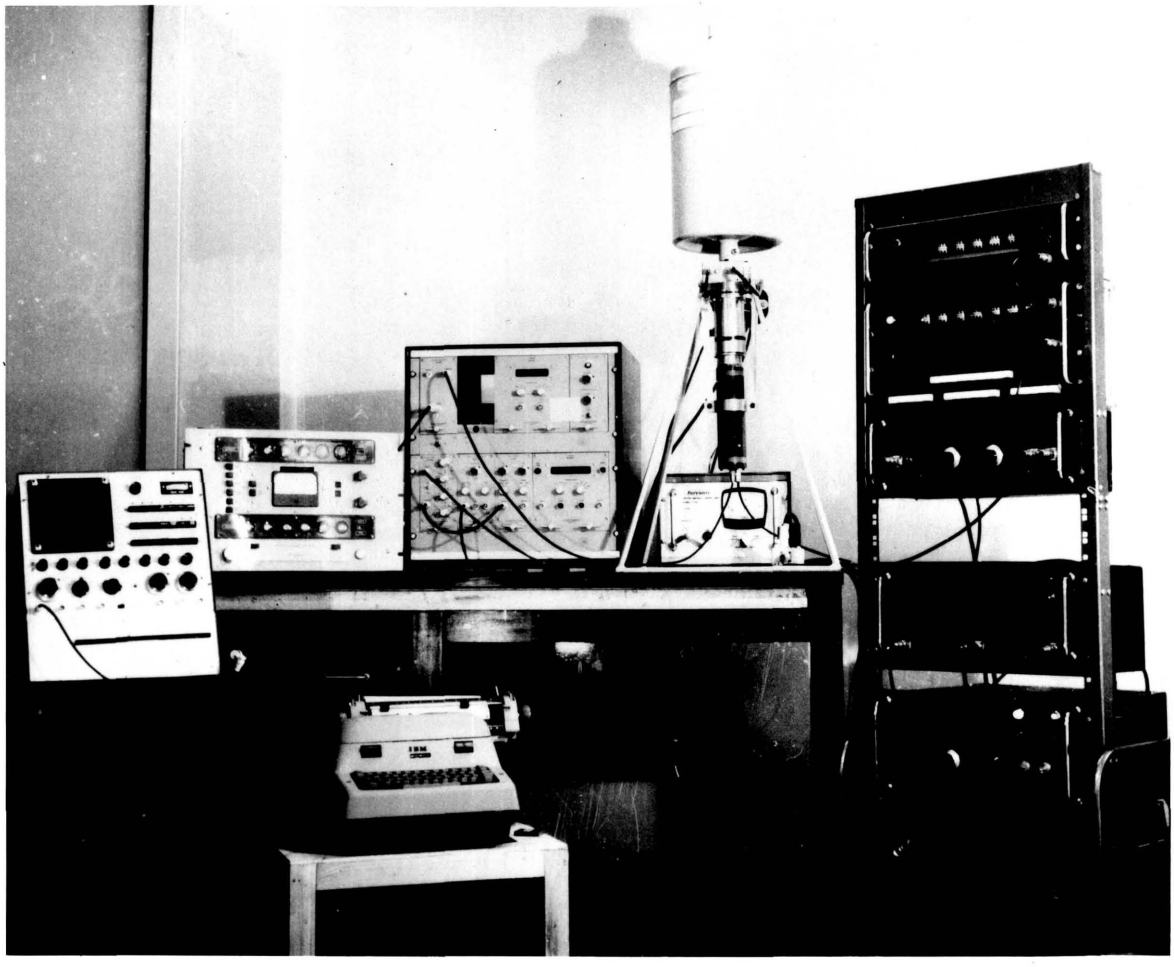

Plate 24 Ge(Li)-NaI(Tl) Detector Assembly and Counting System

the La-140 fission yields in thermal and fast fission, the true fission ratio was obtained.

The following two equations may be written for the count rates from the foils:-

$$CN.f = N5N.\ F5.\ y5 + N8N.\ F8.\ Y8$$
$$CD = N5D.\ F5.\ y5 + N8D.\ F8.\ y8 \qquad (5.3)$$

where CD and CN are the integral counts under the 1.60 Mev peak of La-140 of the depleted and natural foils respectively. CD and CN are the corrected count rates for weight of foils, deadtime of analyzer and position of foils. The latter point will be discussed later in this section. N5N, N5D, N8N and N8D are the number densities of U_{235} and U_{238} in natural and depleted foils respectively. y5 and y8 are La-140 fission yields for thermal fission in U_{235} and fast fission in U_{238}. They are given as (27)

$$y5 = 6.40 \pm 0.12 \qquad y8 = 6.15 \pm 40$$

and the ratio is $\frac{y5}{y8} = 1.034 \pm 2\%$

f is a factor used to correct counts for delay in counting.

The true fission ratio obtained from equations 5.3 is given by:-

$$\left(\frac{F8}{F5}\right) = \frac{N5N}{N8N}\,\frac{y5}{y8}\,\frac{\frac{CN}{CD}\,f - 1}{1 - f\,\frac{CN}{CD}\,\frac{N8D}{N8N}\,\frac{N5N}{N5D}} \qquad (5.4)$$

In this measurement two sets of foils natural and depleted were fixed to a perspex strip and inserted between the fuel plates of fuel element F where the fission ratio per atom was 0.8×10^{-3}. This value was obtained from the results of the foil irradiations in the fuel elements in order to determine fission ratio in each fuel element. These measurements are discussed in chapter 7. The first set was irradiated for two hours at low flux (10^{8} n/Cm^2-sec) and the second set for two hours at a higher flux (10^{11}n/Cm^2-sec). Timing of the irradiation was as before, starting at 37% of the required Reactor Power and terminating by quick shut-down. The first foil set was counted on the double scintillation detector assembly shown in Fig. 4. The gamma activity fission ratio was obtained from depleted and natural foils counts using equation 3.8. The second set was left until the activity of short lived fission products diminished. After one week the foils were then counted on the Ge(Li) counting system. Two foils natural and depleted were counted for six weeks. Since the intrinsic efficiency of the Ge(Li) detector ($\epsilon = 1.6 + 10^{-3}$ [31] for 1.60 Nev gamma) was low compared to the NaI(Tl) crystal efficiency for the same gammas ($\epsilon = 5.5 * 10^{-2}$) [31] the foils were counted on a NaI(Tl) crystal 4.4 Cms by 5.0 Cms height starting four weeks after the irradiation, see Fig. 25.

The gamma spectrum of fission products is shown in Fig. 26. The gamma rays are monoenergetic but because of the nature of absorption in the detector and random phenomena the output pulses are spread over a range of energy which determines the resolution of the detector assembly. The output pulse ~~shape~~ photopeak can be represented by a Gaussian distribution. It is shown in the gamma spectrum, see Fig. 26, that the 1.60 Mev peak is superimposed on a background that

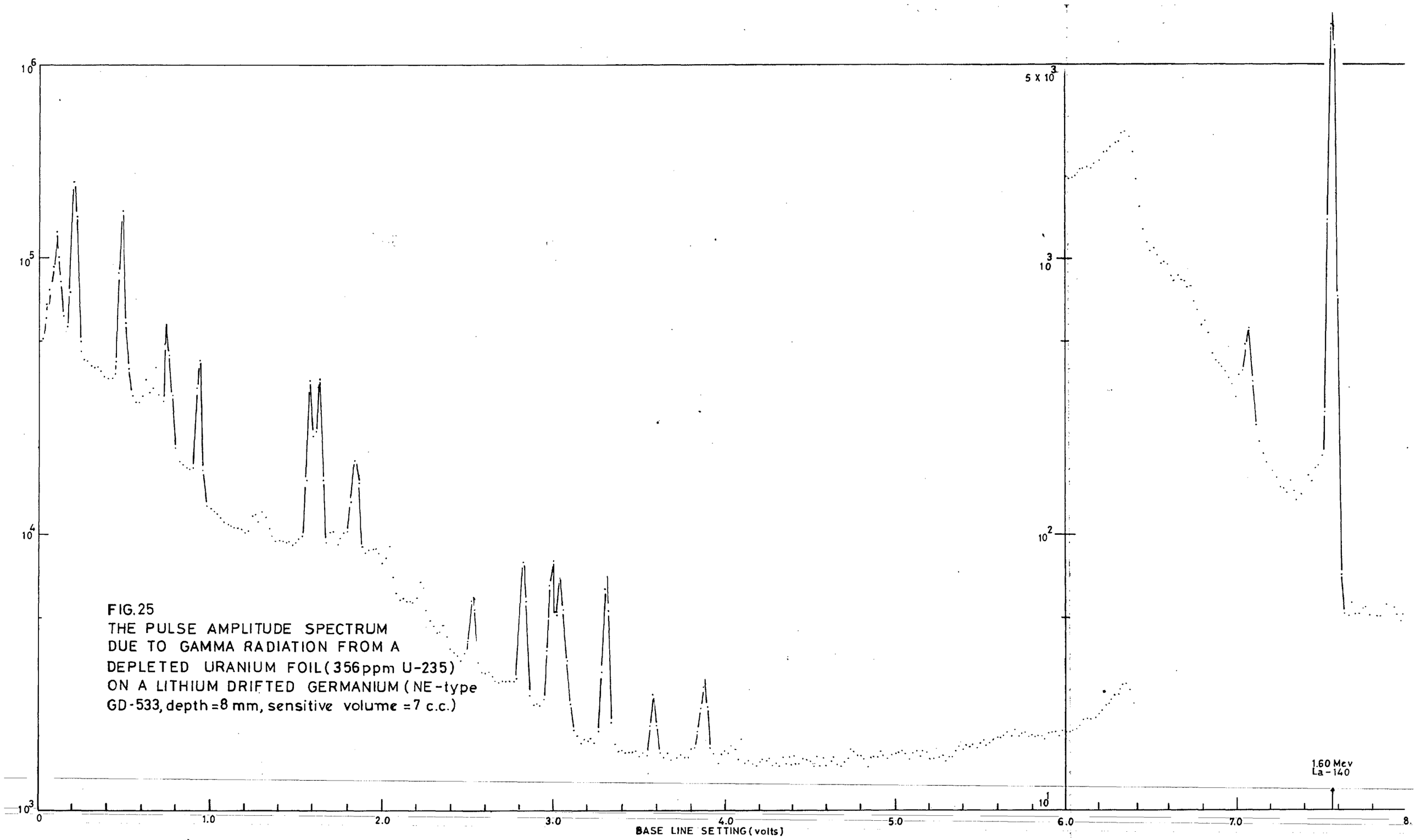

FIG. 25
THE PULSE AMPLITUDE SPECTRUM DUE TO GAMMA RADIATION FROM A DEPLETED URANIUM FOIL (356 ppm U-235) ON A LITHIUM DRIFTED GERMANIUM (NE-type GD-533, depth = 8 mm, sensitive volume = 7 c.c.)

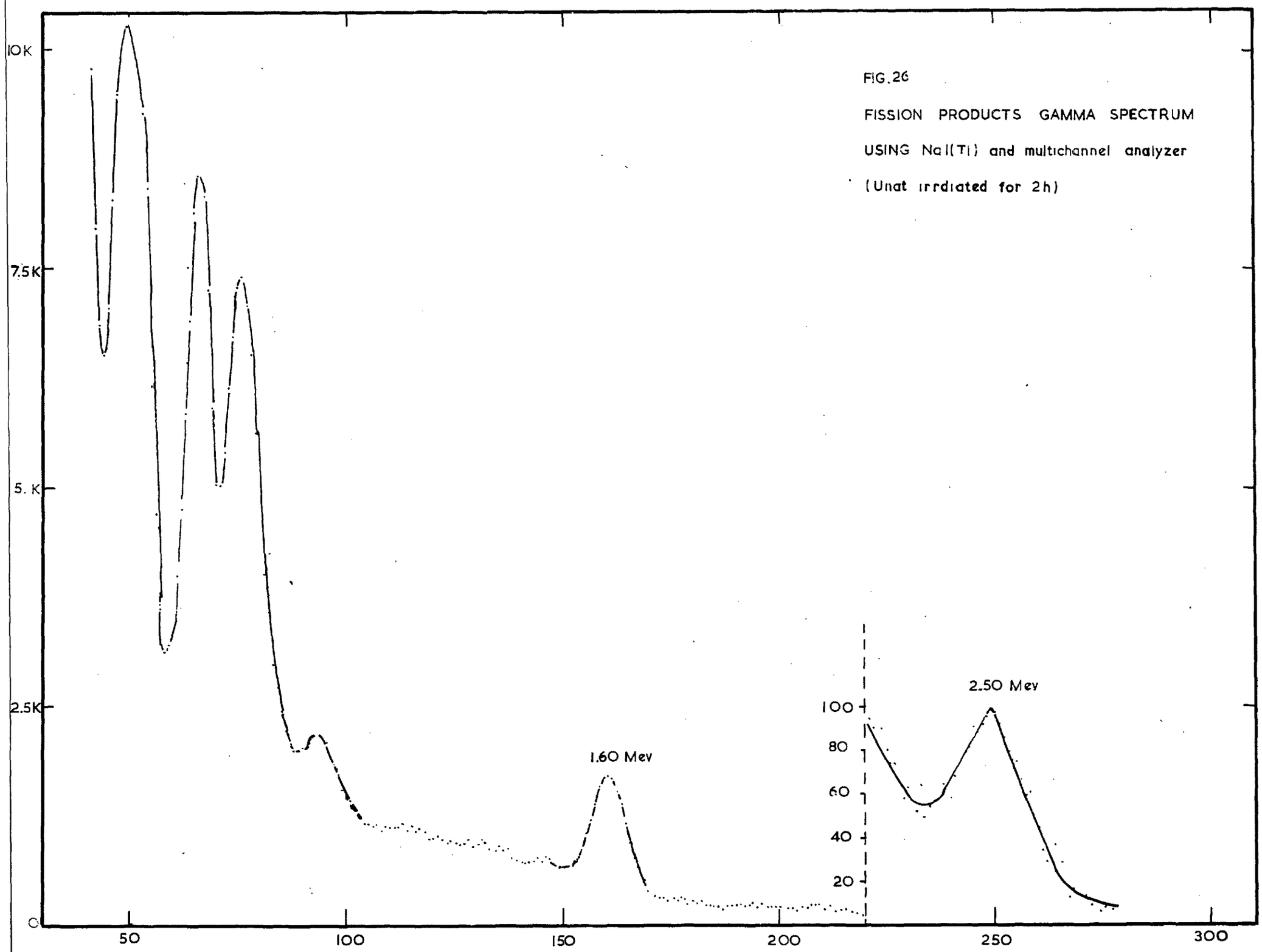

FIG.26

FISSION PRODUCTS GAMMA SPECTRUM USING NaI(Tl) and multichannel analyzer (Unat irrdiated for 2h)

comes from other fission products and this background can be represented by a straight line. Therefore the total can be shown as a Gaussian plus a straight line. A computer program Photo-Peak-Analysis PPA, (28) was used to fit a Gaussian plus a straight line to the observed count per channel. The equation is represented by

$$y = A + Bx + Ce^{-E(D-x)^2} \qquad (5.5)$$

where A and B are empirical constants which account for interferehce with the Gaussian distribution. C, D and E can be related to the Gaussian terms of the following equation

$$W(x) = \frac{(2\pi)^{-\frac{1}{2}}}{\sigma} \exp\left(-\frac{(m-x)^2}{2\sigma^2}\right) \qquad (5.6)$$

By comparison with equation 5.5, C, D and E are found as :-

$$C = \frac{1}{\sigma\sqrt{2\pi}}$$

$$D = m$$

$$E = + \frac{1}{2\sigma^2}$$

In equation 5.6 σ and m designate the standard deviation and the true mean respectively. Figs. 27 and 28 show the observed 1.60 Mev photopeak from NaI and Ge(Li) with PPA result for each case.

A computer program LANTA was written to calculate the true fission ratio using equation 5.4. The correction factor, which was mentioned earlier, to allow for different positions of the

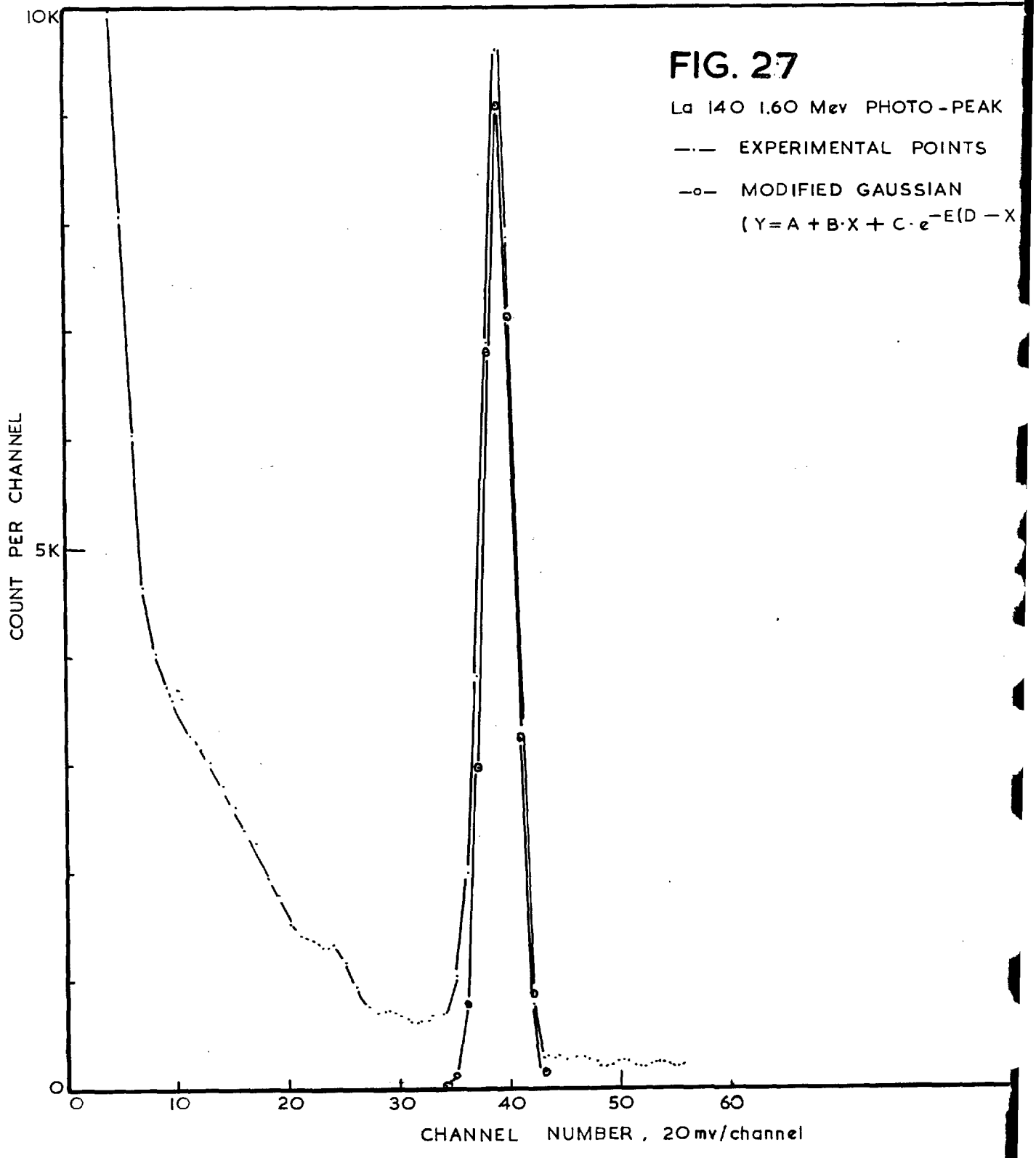

FIG. 27

La 140 1.60 Mev PHOTO-PEAK

—·— EXPERIMENTAL POINTS

—o— MODIFIED GAUSSIAN

$(Y = A + B \cdot X + C \cdot e^{-E(D-X}$

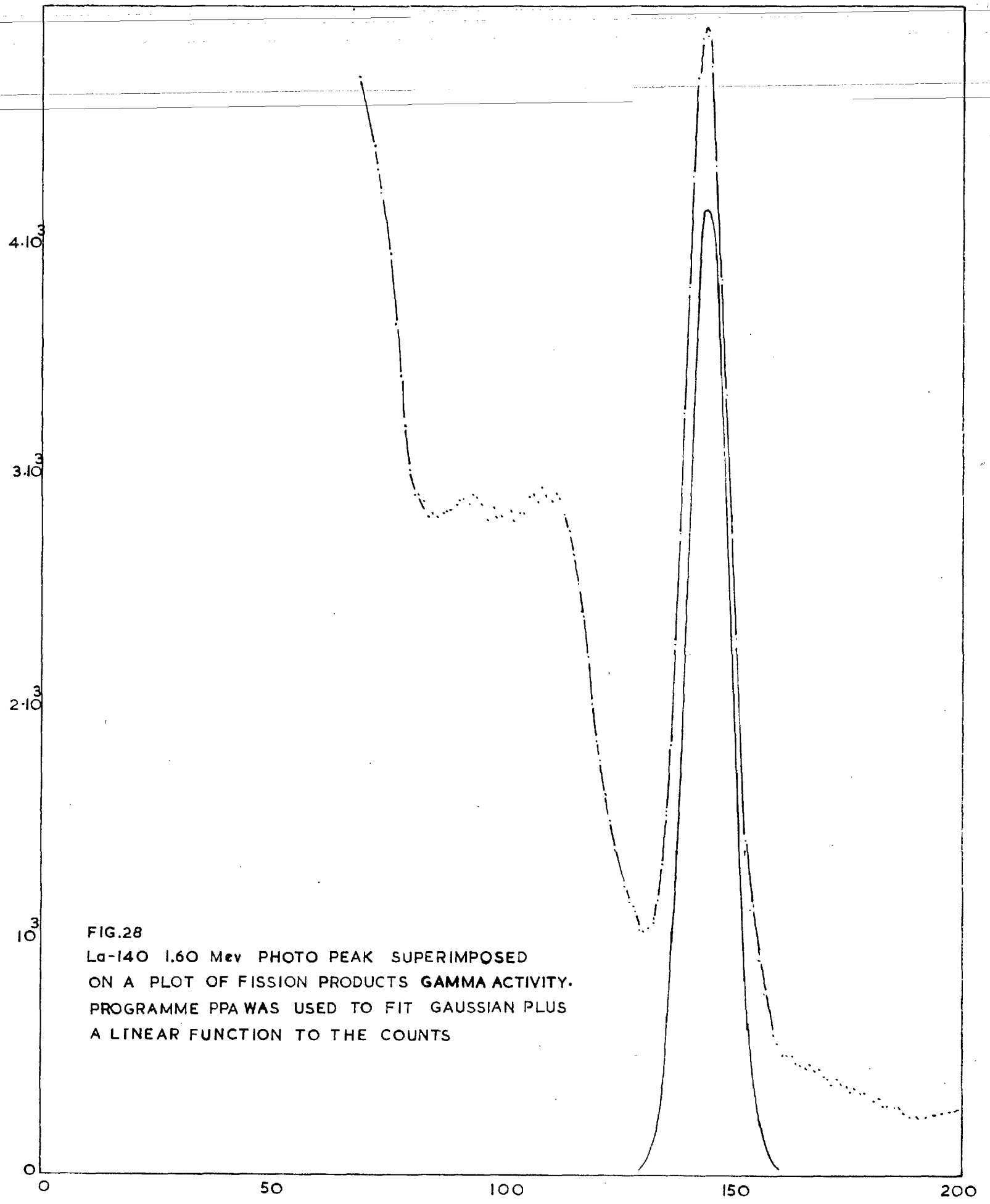

FIG.28
La-140 1.60 Mev PHOTO PEAK SUPERIMPOSED ON A PLOT OF FISSION PRODUCTS GAMMA ACTIVITY. PROGRAMME PPA WAS USED TO FIT GAUSSIAN PLUS A LINEAR FUNCTION TO THE COUNTS

TABLE 4. La-140 RESULTS

Decay Time Min.	Depleted Count	Counting Period Sec.	Decay Time Min.	Natural Count	Counting Period Sec.	Count Ratio	Fission Ratio x 10^{+3}
311.5	4922	3600	286.50	31540	3600	0.1534	0.829
338.2	4426	7680	336.5	30150	3840	0.1443	0.7482
409.50	3743	9000	411	25440	3600	0.1446	0.75111
431.5	4763	7260	434	33870	7260	0.1382	0.6950
456.	3469	10800	457.5	23910	7200	0.1426	0.7335
505	3052	18060	501	21270	10800	0.141	0.7194
527	2916	18180	531	20350	9060	0.1408	0.7181
552.7	2735	18000	548	19410	14400	0.1385	0.6976
577.20	2545	18000	580.5	17230	7380	0.1452	0.25617
602.3	2428	20400	597.5	17130	10920	0.1393	0.7048
624.8	2294	20400	629.2	15760	9000	0.1430	0.7375
649.5	2199	19860	644.7	15160	10800	0.1426	0.7334
766.5	1751	16200	770	12150	7380	0.1416	0.7246
795.2	1621	16200	790.5	11340	10800	0.1404	0.7149

The calibration factor was determined by dividing averaged fission ratio by the gamma activity fission ratio. The calibration factor is, p(240) = $1.31 \pm 3\%$.

natural and depleted foils was determined by simultaneously irradiating two natural foils in two recessed holes on the perspex foil mounting strip, see Fig. 29. The correction factor obtained from this experiment was 1.021 ± 0.005 (random error). The true fission ratio was calculated from equation 5.4. The results are tabulated in Table 4. It can be seen that the depleted to natural foil count ratio does not change more than statistical fluctuation with decay time.

The lanthanum technique has some limitations which are as follows:-

(1) To obtain good accuracy in counting the foils have to be irradiated in a high flux. This condition is not always permissible because of high induced activity in the fuel element and in the foils.

(2) Uncertainty in the fission yields. Ba-140 is on the second tip of the fission product mass distribution, and the fission yield should not therefore change very much with neutron energy. The change, however, is significant for accurate measurements. Table 5 demonstrates this change by giving the ratio of the fission yield compared to thermal fission (27).

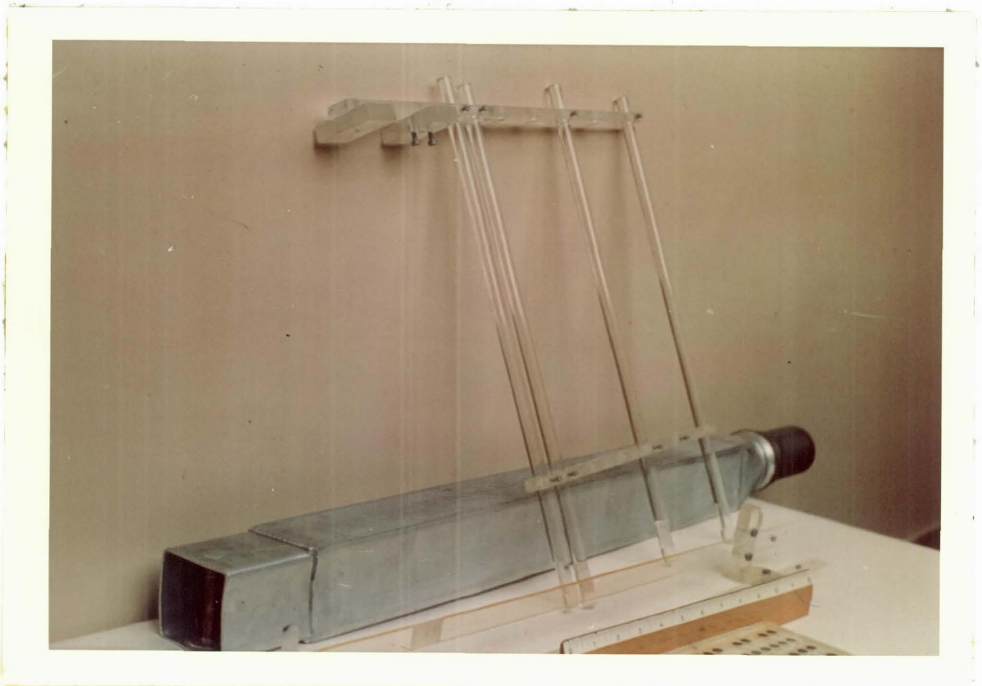

Plate 29 Perspex Strips and Perspex Frame for Foil Irradiation in Consort Reactor Fuel Elements and outside the Core.

TABLE 5. La-140 FISSION YIELDS FOR U_{235} AND U_{238} BY NEUTRONS OF VARIOUS ENERGIES

Neutron Energy	U_{235} Yield		U_{238} Yield
	Compared to Thermal	Yield	
Fast Fission Spectrum	0.926	5.80 ± 0.5	6.15 ± 0.40
	0.921		
	0.941		
Fast Reactor	0.953		
	0.944		
	0.940		
Thermal Neutrons	1.000	6.36 ± 0.12	

However, this method has several advantages:-

(1) The foils can be placed anywhere in the core without causing too much depression in the flux.

(2) The fission product Ba-140 because of having less energy than her counterpart does not escape from the foil surface easily.

5.5 DETERMINATION OF p(t) USING THERMAL AND FAST SPECTRA

This method involves irradiating a depleted foil and a depleted deposit in the thermal column and in a fast neutron spectrum. In the first irradiation thermal fission occurs only in U_{235} nuclei and in the second irradiation is a hard spectrum fast fission occurs in U_{238} and U_{235}. The contribution of fast fission of U_{235} to total fissions is negligible since only 0.036% of the uranium is U_{235} and fast fission cross section of U_{235} is not much larger than U_{238} fission cross section. In order to determine p(t) by this method one depleted deposit 100 $\mu g/Cm^2$ and a depleted foil mounted in the double fission chamber, were irradiated in the thermal column for two hours. The fission counts were taken and foil was counted on the double NaI(Tl) counting system. For the fast neutron irradiation the depleted deposit plus a depleted and a natural foil were irradiated in the beam of neutrons emitted from the 6 Mv Van de Graaff at AWRE (Aldermaston). The irradiation lasted for two hours and fission counts were taken and the foils were counted on the same counting system as in the first experiment. A depleted and a natural foil were used to find out the nature of the fast spectrum. The corrected count ratio, $^{CD}/_{CN}$, was 0.98. This ratio indicates that spectrum is very hard and two per cent difference in activity is due to the fast fission in U_{235} in natural foil. Knowing the enrichment of natural foil, 0.7196%, and of the depleted foil, 0.036%, the contribution of fast fission in U_{235} in depleted foil was estimated less than 0.2%. The advantages of this method are numerous such as no correction for deposit weights and fission products absorption in the coating are required. In this case the calibration factor is defined as:-

$$p(t) = \frac{\left(\frac{C8}{c8}\right)}{\left(\frac{C5}{c5}\right)} = \frac{\left(\frac{F8}{f8}\right)}{\left(\frac{F5}{f5}\right)} \qquad (5.7)$$

where C8 and C5 are fast fission and thermal fission counts from fission counting. c8 and c5 are gamma counts of fast and thermal fission of the depleted foils counted on the double NaI(Tl) counting system. Because no correction for mass of the deposit is required and after having corrected c8 and c5 for the weight of the foils the calibration factor is obtained as in equation (5.7). The data of this experiment was analyzed by the programme FFR-III after introducing a new subroutine NEWPT and dropping subroutines pT and ERROR. One of the big advantages of this method is the low systematic error in the measurement, see Table 3. However, this method is only applicable where a very hard spectrum is present.

CHAPTER 6

ERROR EVALUATION AND CORRECTIONS

This chapter is mainly concerned with the analysis of errors and corrections involved in the fission ratio measurements. In the measurements two types of errors were considered, random error and systematic errors. For calculating random errors in F8/F5, p(t), F8 and F5 determination because they are time dependent functions, two sets of normalized decays for U_{235} and U_{238} were obtained. These two sets were resulted from a series of natural and depleted foils irradiations. The two sets are plotted in Fig. 5 and tabulated in Appendix III. After multipying fission ratio and p(t) by $\frac{D5(t)}{D8(t)}$ and $\frac{D8(t)}{D5(t)}$, F8 and F5 by $\frac{1}{D8(t)}$ and $\frac{1}{D5(t)}$ respectively the following equation was used to calculate the root mean square error (R.M.S.).

$$R.M.S. = \frac{1}{N}\left[\sum_{i=1}^{N} (\nu_i - \bar{\nu})^2\right]^{\frac{1}{2}} \qquad (6.1)$$

where $\bar{\nu}$ is the average value of ν_is and ν_i is the i^{th} value.For the systematic errors evaluation the following equation was used:-

$$(\Delta F)^2 = \left(\frac{\partial F}{\partial \nu}\Delta\nu\right)^2 + \left(\frac{\partial F}{\partial y}\Delta y\right)^2 + \ldots \qquad (6.2)$$

where F is a function of ν, y . . . and ΔF, $\Delta\nu$, Δy . . . are the absolute errors on F, ν, y, etc. $\frac{\partial F}{\partial \nu}$, $\frac{\partial F}{\partial y}$, etc. are the partial derivatives of F with respect to ν, y, etc., respectively.

6.1 DEADTIME AND PULSE PILEUP EFFECT

Deadtime is a common effect and well known in counting systems.

The deadtime of the double NaI(Tl) counting system and also fission counting equipment were determined by using a CALNE Electronic, PG101 double pulse generator. The pulse duration and the time between two pulses were adjustable. The method of measuring the deadtime was by feeding the double pulses to the input of the equipment and gradually increasing the time between two pulses until the count rate doubled. The pulse duration of the pulse generator was adjusted to that of the detector. The measured deadtime, $T = 1.9 \pm 0.05$ μ sec per pulse was in good agreement with the deadtime given by the manufacturer, 2 μ sec. The term pulse pileup is referred to the process when more than one pulse arrives during a time interval of the pulse duration and as a result produce a larger pulse. The effect can be reduced by reducing the rise time and the resolution time of the pulse. Therefore pulse pileup depends on type of the detector, amplifier and the analyzer or discriminator whichever was used. The threshold and discrimination bias level has also some effect in total number of the pulse pileup.

The following experiment was carried out to determine the effect of pulse pileup in count rates. By the same method as enrichment measurement two foils, natural and depleted uranium metal, were irradiated in the thermal column in a high flux for two hours. Immediately after the end of irradiation the foils were removed from the thermal column and counted on a double NaI(Tl) counting system. It was observed from the computer results that the ratio of depleted foil to natural foil count rate increased as the natural foil count rate decreased. The change was due to the pulse pileup of the gamma pulses of energies below the threshold level. The threshold was set at 1.28 Mev peak of Na22. In this way of counting, 95% of the total counts are below the threshold. The number of extra pulses counted above 1.28 Mev

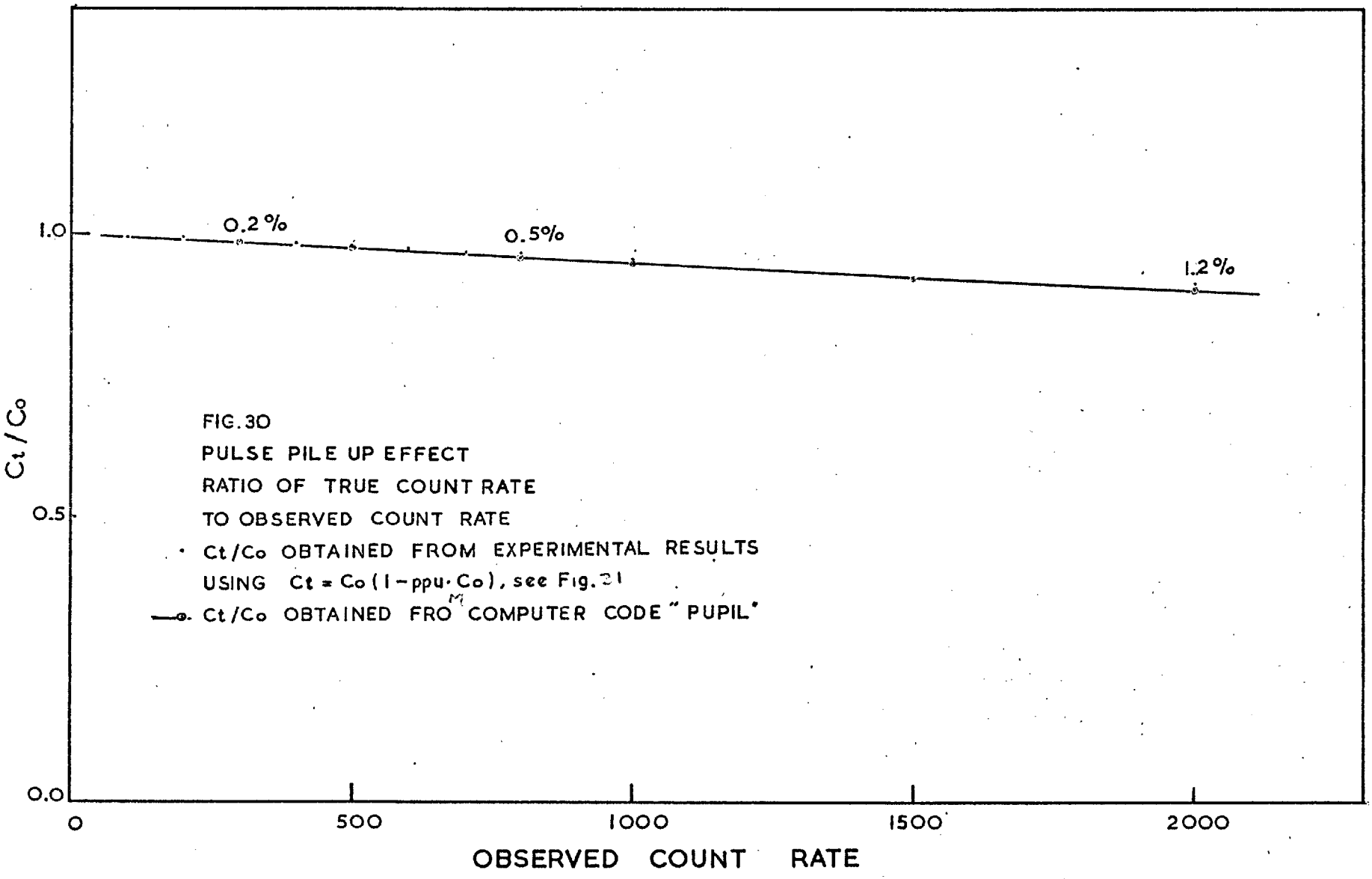

FIG. 30
PULSE PILE UP EFFECT
RATIO OF TRUE COUNT RATE
TO OBSERVED COUNT RATE
· Ct/Co OBTAINED FROM EXPERIMENTAL RESULTS
USING $Ct = Co(1 - ppu \cdot Co)$, see Fig. 31
—o— Ct/Co OBTAINED FROM COMPUTER CODE "PUPIL"

threshold due to pulse pileup below 1.28 is much higher than the pulses lost as a result of the effect above 1.28 Mev. By the method of the least squares using program LISQFT, a linear equation was fitted to the data, CD/CN against CN, from which the following equation was derived

$$C_t = C_o \ (1 - \text{ppu.}\ C_o) \qquad (6.3)$$

$$\text{ppu} = 31.5 \pm 1.5 \ \mu \text{ sec/count}$$

where C_t and C_o are true and observed count rates and ppu is the pulse pileup measured from the experimental result. Fig. 31 shows the ratio of CD/CN against CN. A computer program PUPIL (Brown) pulse pileup was used to estimate the effect of the pulse pileup in the present work. In Fig. 30 experimental results using equation 6.3 and the output of PUPIL are given. The quoted values are the percentage difference on predicted values as compared with the experimental results.

6.2 p(t) AS A FUNCTION OF NEUTRON ENERGY of U^{235}

The fission products mass distribution is shown in Fig. 32. The yield curves for U_{235} fission products by thermal and 14 Mev neutrons are given in the diagram. Each curve has two peaks corresponding to the two fission fragments.

The lowest point in the thermal fission yield distribution in the valley of the curve is 0.01% whereas the corresponding point with 14 Mev neutrons is 1%. The other changes are small in the peak yields

FIG.31 PULSE PILE-UP

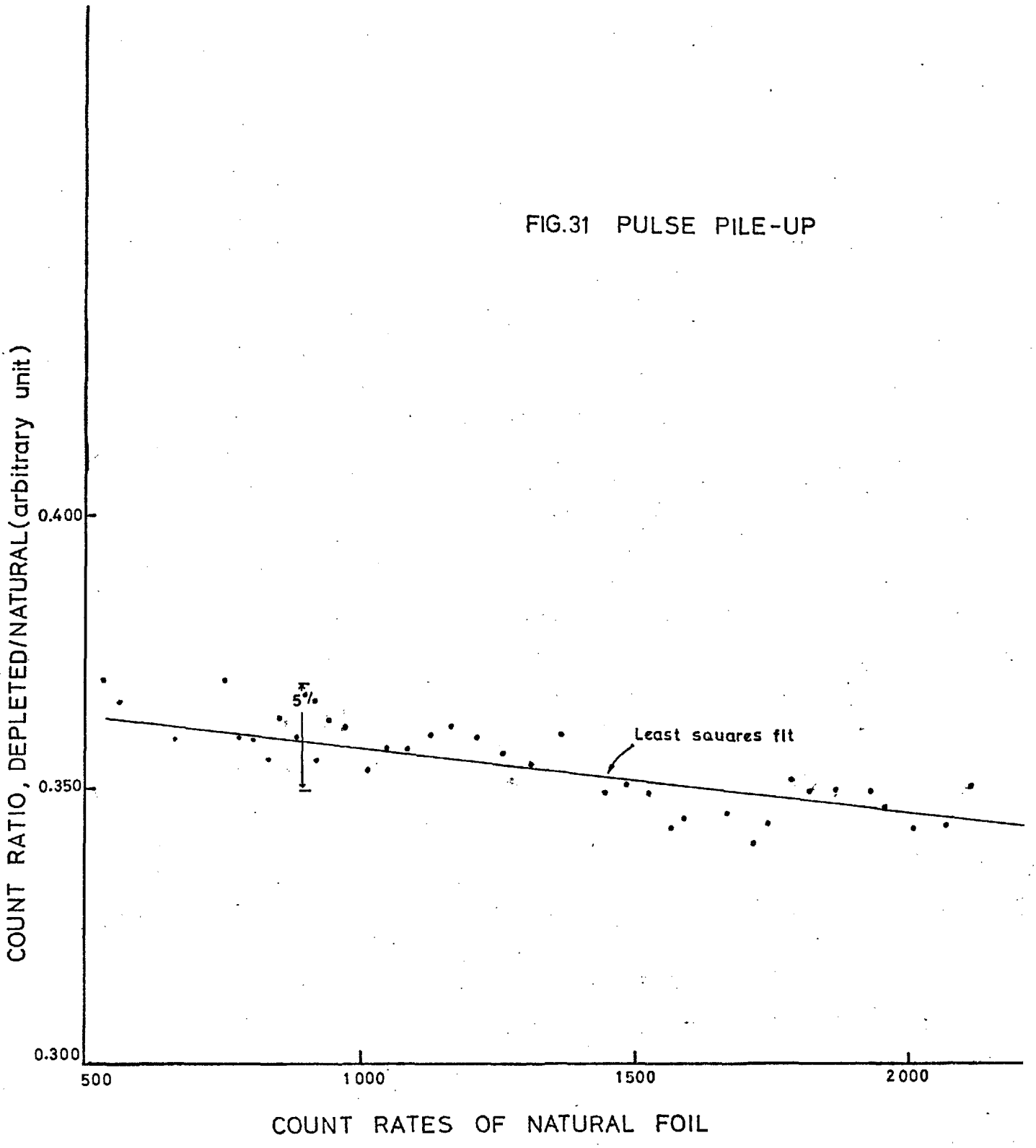

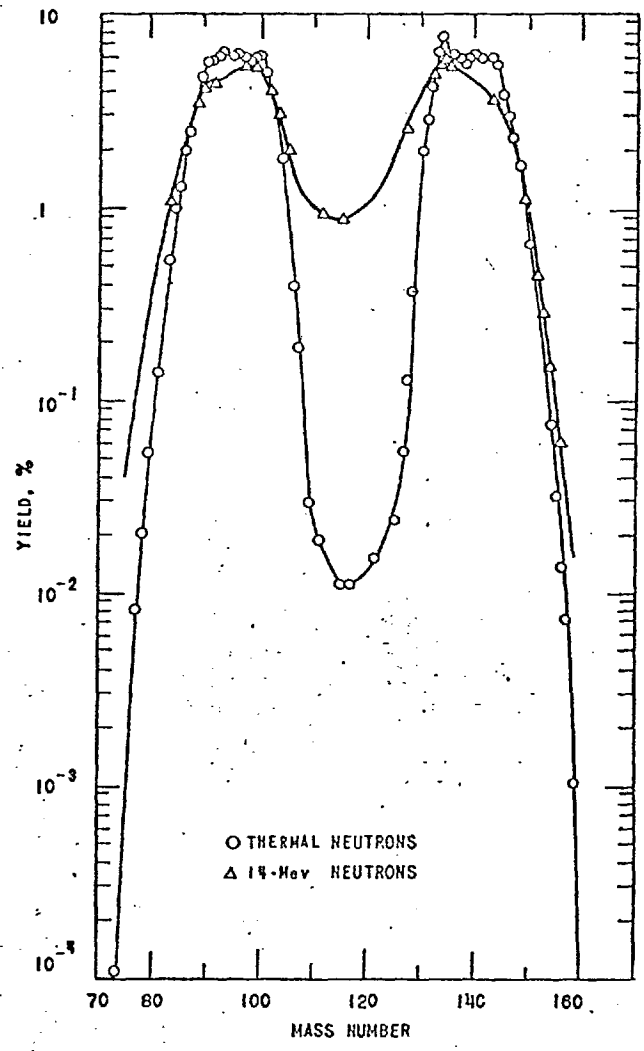

FIG. 32 YIELD vs MASS NUMBER FOR U235 FISSIONS AS A FUNCTION OF INCIDENT NEUTRON ENERGY.

and moderate increase in asymmetric mode of fission i.e. rise in the wings of the curves. As the neutron energy increases the probability of symmetrical fission products also increases. With neutrons of 90 Mev energy only one peak in fission products mass distribution is observed, at this energy the symmetrical fission is most probable mode.

In the p(t) measurement technique besides other considerations discriminator bias level was set at 1.28 Mev photopeak of Na.22 in order to eliminate 1.2 Mev Bremsstrahlung radiation produced by 1.2 Mev betas emitted by excited U_{239} nucleus. The fission products contributing to the observed gamma activity has been plotted in Fig.33. The principal fission products contributing to the gamma activity after about four hours from the end of irradiation are $_{92}Sr$, $_{135}I$, and $_{88}Kr$ (9). In the fission process by various neutron energies the percentage of the fission products yields changes (Leachman, Hemmedinger) gamma activity of individual fission product therefore varies because of changes in concentration of each fission product. Moreover that the decay mode of the different isotopes are different. On this account the integrated gamma activity beyond a certain energy may be different. p(t) is the ratio of the true fission ratio to gamma activity fission ratio. The true fission ratio is assumed to be independent of neutron energy and the fission counter counts only number of fission events irrespective of the neutron energy inducing fission. However, the total gamma activity as mentioned earlier may alter as a result of the changes in the fission products yield. Consquently the calibration factor may be neutron spectrum dependent.

The effect of neutron energy on p(t) was determined by measuring

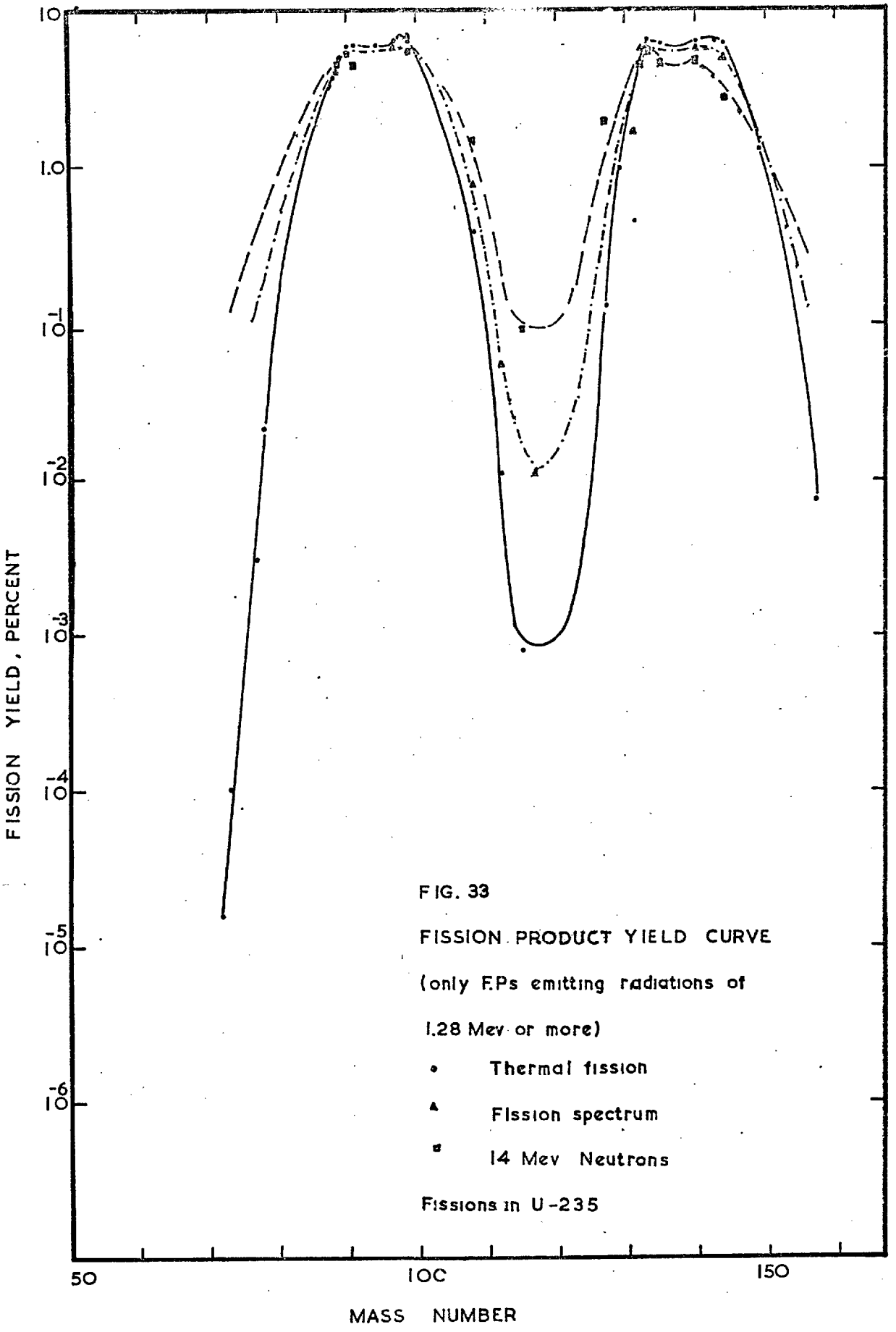

FIG. 33

FISSION PRODUCT YIELD CURVE

(only F.Ps emitting radiations of 1.28 Mev or more)

• Thermal fission

▲ Fission spectrum

▪ 14 Mev Neutrons

Fissions in U-235

p(t) in a number of different spectra. It was difficult to assess the neutron spectrum in each case but fission ratio measurements gave an indication of the neutron flux above U_{238} fission threshold to the total neutron flux.

The first experiment was carried out in the irradiation hole at 0^{o} face of the University of London Reactor. The second experiment was done on a fission plate placed on thermal column and the third experiment was performed at AWRE Aldermaston using the 6MV Van de Graaff.

In the first experiment two measurements were carried out with a bare and cadmium covered fission chamber (PFCC7). The details of this experiment are given in 5.2. Covering the fission chamber with cadmium cuts off majority of thermal neutrons below cadmium cutoff energy. The cadmium sheet was 0.5 mm thick and the effective cutoff energy is 0.533 ev (31). A fission plate was used in the second experiment. The fission plate was composed of 24 uranium aluminium alloy strips 5 cms wide, 15 cms long by 0.5 mm thick placed adjacent to one another. The U-Al pack was fixed between two 35 cms square aluminium sheets surrounded by pieces of aluminium. A cadmium sheet 0.5 mm thick was placed beneath the top aluminium plate to stop thermal neutrons passing through the fission plate. The details of the fission plate are shown in Fig. 34. The fission plate was placed on the horizontal thermal column at the 90^{o} face of the University of London Reactor in a cave 1 m square by 1.5 m height. The floor of the cave was covered with cadmium 0.5 mm thick with a 30 cms square opening in the centre. The thermal flux at the opening was estimated to be $10^{9n}/Cm^{2}.sec$. The fission plate was surrounded by 0.5 mm thick cadmium to prevent thermal neutrons reaching the fission chamber placed on the fission plate. In one measurement the double fission chamber (see Fig. 14)

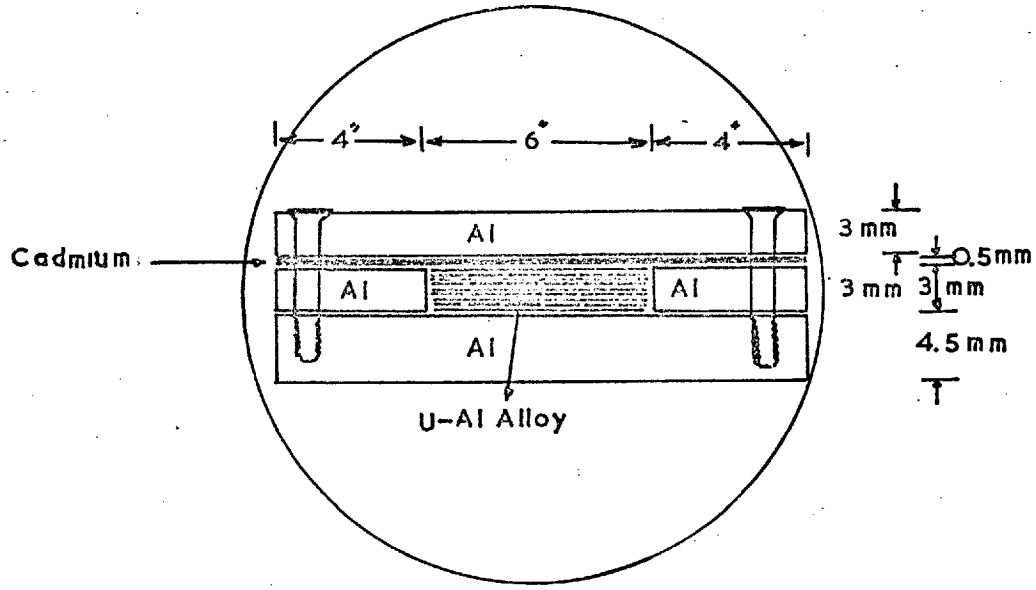

a

FISSION PLATE

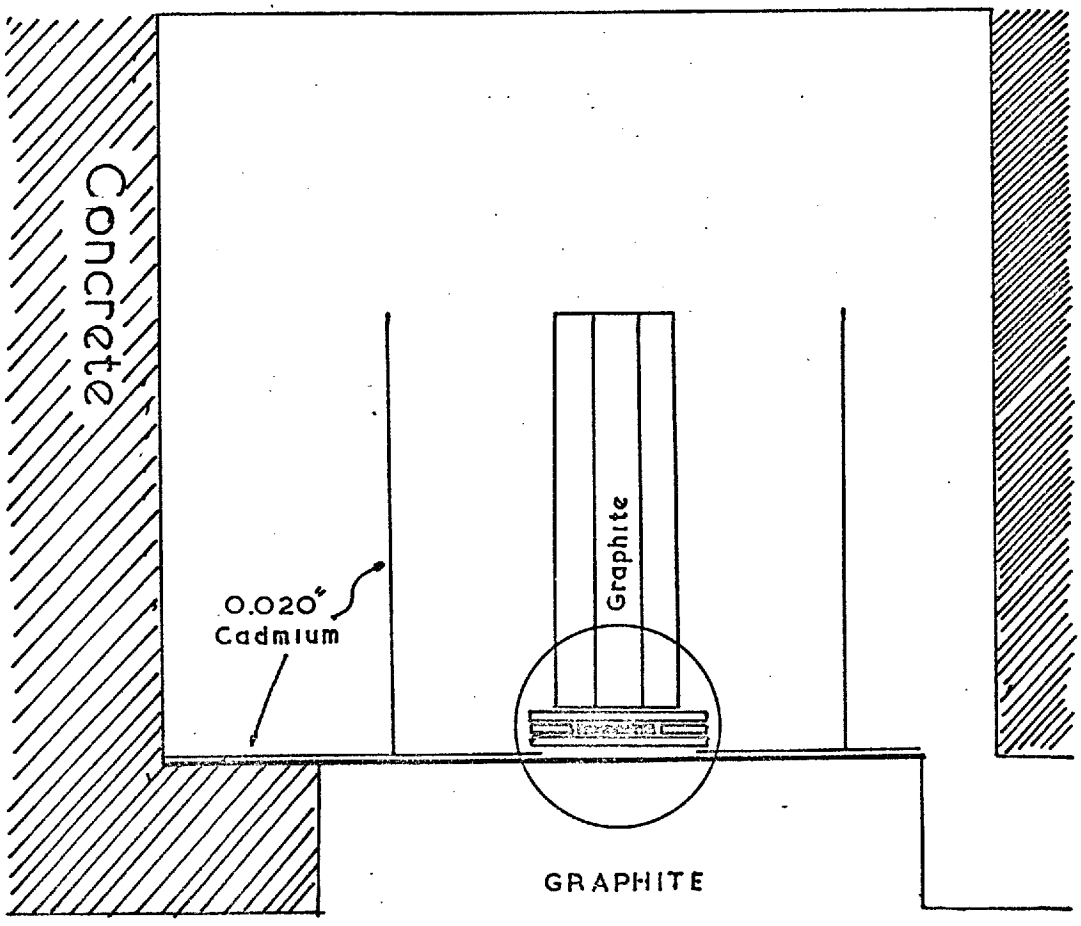

FIG. 34 POSITION OF FISSION IN THE CAVE AT THE 90° FACE OF THE LONDON UNIVERSITY REACTOR.

was placed on the fission plate and p(t) determined. In the second measurement a graphite block 20 cms square by 75 cms long was placed on the fission plate, see Fig. 34, and the double fission chamber was positioned in the graphite block one centimeter above the fission plates. In the third experiment fission counting and foil irradiations were performed on the 6 Mv Van de Graaff at AWRE Aldermaston. Neutrons emitted from a Berylium target as a result of $_4Be^9(D,n)_5B^{10}$ reactions were allowed to impinge on the face of a graphite block in which the fission chamber was placed. The graphite block 20 cms square by 75 cms long was 13 cms away from the target. The actual terminal voltage of the Van de Graaff was 5.2 MV and current 4μa. The total neutron yield was estimated to be 5×10^{10}n/sec (Olive et al). In this experiment and the former one natural, depleted and U-Al alloy 93% enriched U_{235}, foils were irradiated. From the Van de Graaff irradiation the ratio of depleted to natural foil gamma activity was obtained 0.98. This ratio shows how hard the neutron spectrum was in the position of the fission chamber. It should be reminded that depleted and natural foils contained 0.0355 and 0.72% U_{235} respectively.

The following list of reactions occurs in aluminium by neutrons is to present a fact that none of the reactions does not contribute any significant gamma activity to the fission fragments gamma activity in this experiment (Kaplan).

$$_{13}Al^{27} + {}_0n^1 \ (8 \text{ Mev}) \rightarrow ({}_{13}Al^{28}) \rightarrow Na^{24} + {}_2He^4$$

15 hrs

$$_{13}Al^{27} + {}_0n^1 \ (5.3 \text{ Mev}) \rightarrow ({}_{13}Al^{28}) \rightarrow {}_{12}Mg^{27} + {}_1H^1$$

9.5m,

$$_{13}Al^{27} + _{1}n^{1}\ (\text{fast}) \rightarrow (_{13}Al^{28}) \rightarrow {}^{6.5\ sec}_{13}Al^{26} + {}_{o}n^{1} + {}_{o}n^{1}$$

$$_{13}Al^{27} + {}_{o}n^{1}(\text{th}) \rightarrow (_{13}Al^{28}) \rightarrow {}^{2.3\ m}_{13}Al^{28} + \gamma + Q$$

The result of these experiments were analyzed using program FFRIII. The obtained results are given in Table 6 and plotted in Fig. 35.

TABLE 6. p(240) IN DIFFERENT SPECTRA

PLACE OF IRRADIATION	FISSION RATIO	p(t)	EXPERIMENTAL ERRORS
Irradiation Hole	0.0008	1.34	± 3
Irradiation Hole	0.0032	1.32	± 1.1
Irradiation Hole	0.0038	1.33	± 1.1
Graphite on fission plate	0.015	1.29	± 1.1
Fission plate	0.02	1.24	± 1.1
V. de G.	0.18	1.30	± 3

FIG. 35

CALIBRATION FACTOR IN

DIFFERENT SPECTRA.

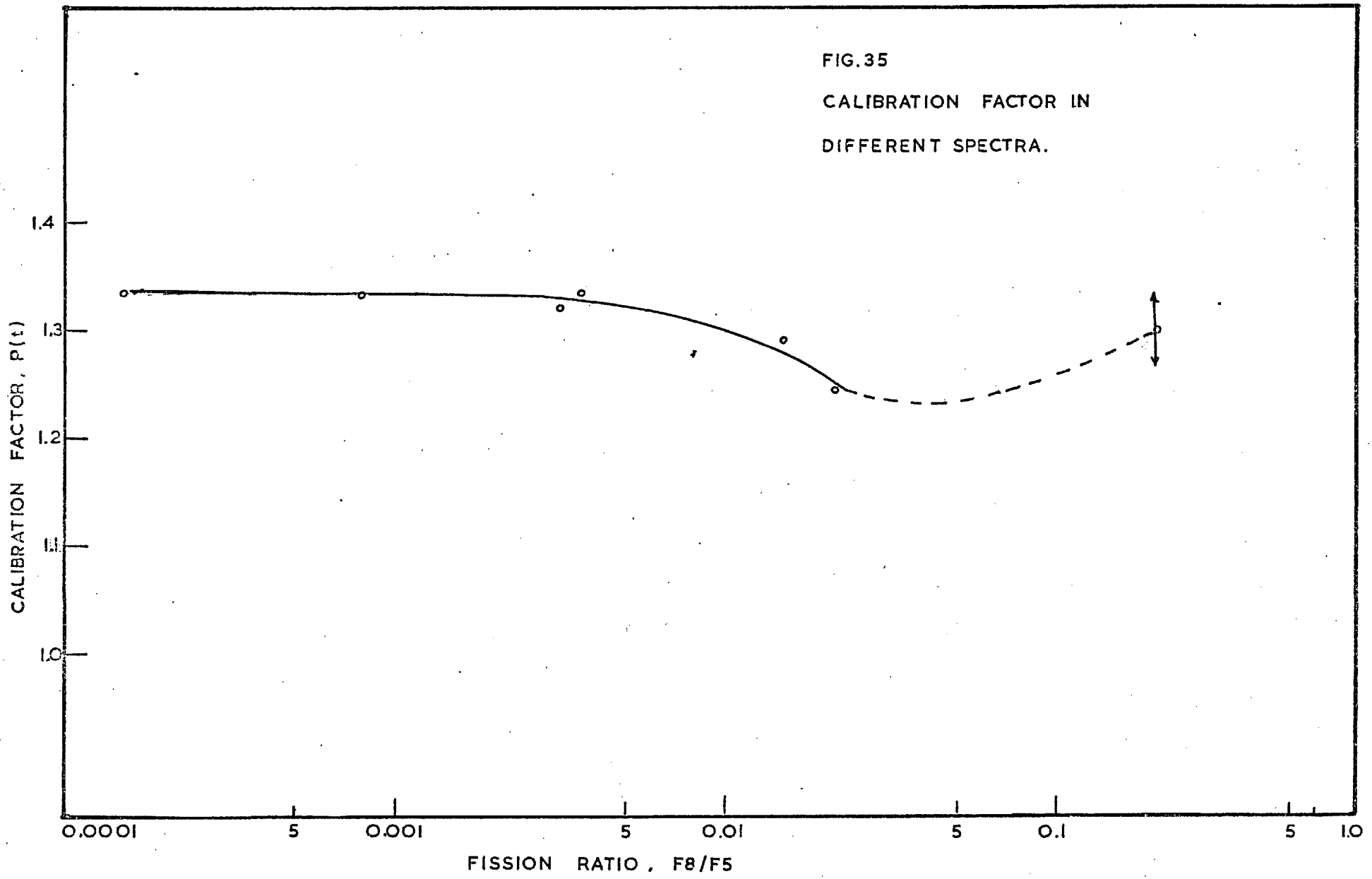

6.3 OTHER ERRORS

In equation 3.8 the ratio of CD/CN compared to $\frac{N5D}{N5N}$ in the numerator and $\frac{CD}{CN}$ compared to $\frac{N8D}{N8N}$ in denomerator have a significant effect on the gamma activity fission ratio measurement. Using depleted and natural foils in a soft spectrum the corrected count ratio is very close to N5D/N5N or similarly irradiating the foils in a hard spectrum the count ratio is very close to $\frac{N8D}{N8N}$. The implication is that in these extremes the more accurate parameters are required in order to obtain high accuracy in the gamma activity fission ratio measurement. For this purpose the differential of the logarithm of equation 3.8 with respect to the count ratio was taken as

$$\frac{dFR}{FR} = \frac{R8 - R5}{(RC-R5)(R8-RC)} \qquad (6.4)$$

where Rc, R8 and R5 are count ratio, $\frac{N8D}{N8N}$ and $\frac{N5D}{N5N}$ respectively. The plot of equation 6.4 is shown in Fig. 36 and it is seen from the graph that the variation of fission ratio with count ratio is minimum where count ratio is about 0.5. Therefore, the count ratio between 0.3 and 0.7 has minimum effect on the fission ratio variation and as a result on p(t) variations. Beyond these limits the fission ratio and the calibration factor are very vulnerable to unexpected changes with high random and systematic errors. In the fission ratio measurements in hard spectra three foils natural, depleted and highly enriched, were used to achieve the above criterion and find the nature of the spectrum from depleted and natural foils gamma activities.

(2) Furthermore to decrease the random error in the computer program FFR, see Appendix I, the subroutine LISQFT was used to fit a polynomial to the count rates. By this method some improvement was achieved in decreasing statistical fluctuation as well as extraneous error in count rates due to linear interpolation between successive counts which was adopted in first calculation of p(t) in FFR.I. Fig. 6 shows the actual count rates of depleted and natural foils and the fitted polynomials. Usually a fourth order polynomial gave the best fit to the count rate between 40 to 250 minutes. The results of one of the fits to the count rates are given in Appendix III.

(3) One of the main factors in count rates fluctuation is the stability of the counting system, especially photomultiplier tubes, amplifiers, discriminators and EHT supply. This requirement is necessary because of the threshold at 1.28 Mev photopeak of Na.22. To demonstrate this point the gamma spectrum of fission products at different decay times are shown in Figs. 37 and 38. These spectra were obtained by using the Ge(Li) detector and LABEN 400 channel analyzer. It is seen from the spectra that the 1.28 Mev threshold is positioned in a valley between two peaks and after four hours from the end of irradiation the 1.28 Mev photopeak of I135 emerges and it becomes more distinct in the later decays. Since the threshold is placed at 1.28 Mev, any such instability in the counting system causes the threshold varies between two peaks. To keep the count rates constant within the statistical fluctuations it was found necessary to have the ambient temperature of the counting system constant within $\pm$ 0.1^{o}C. After 240 minutes from the end of irradiation the total observed gamma activity above 1.28 Mev is contributed mainly by three nucleon K_r88, S_r92, and I135. Some of the observed I135 gamma activity appears as a gamma ray

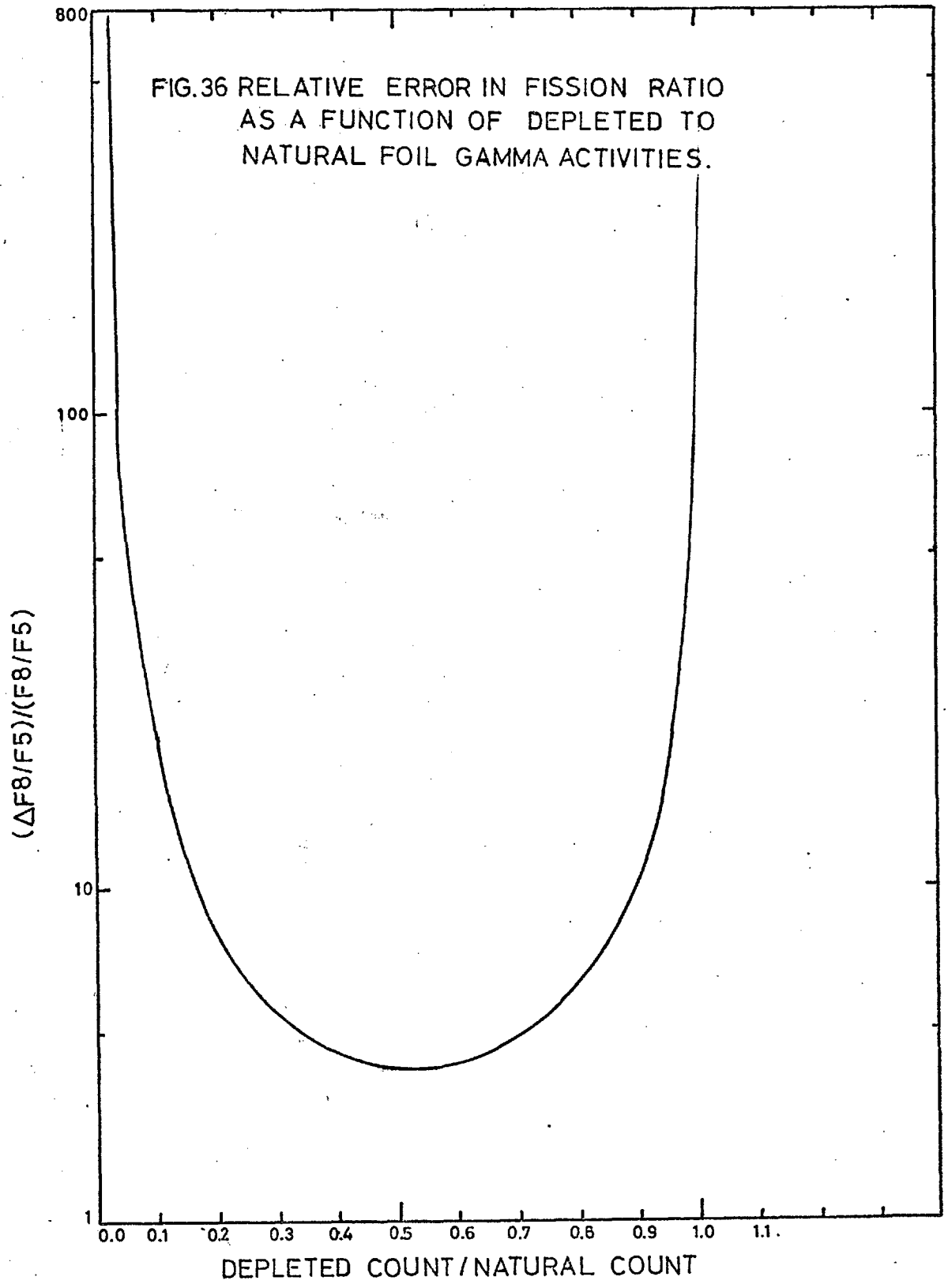

FIG. 36 RELATIVE ERROR IN FISSION RATIO AS A FUNCTION OF DEPLETED TO NATURAL FOIL GAMMA ACTIVITIES.

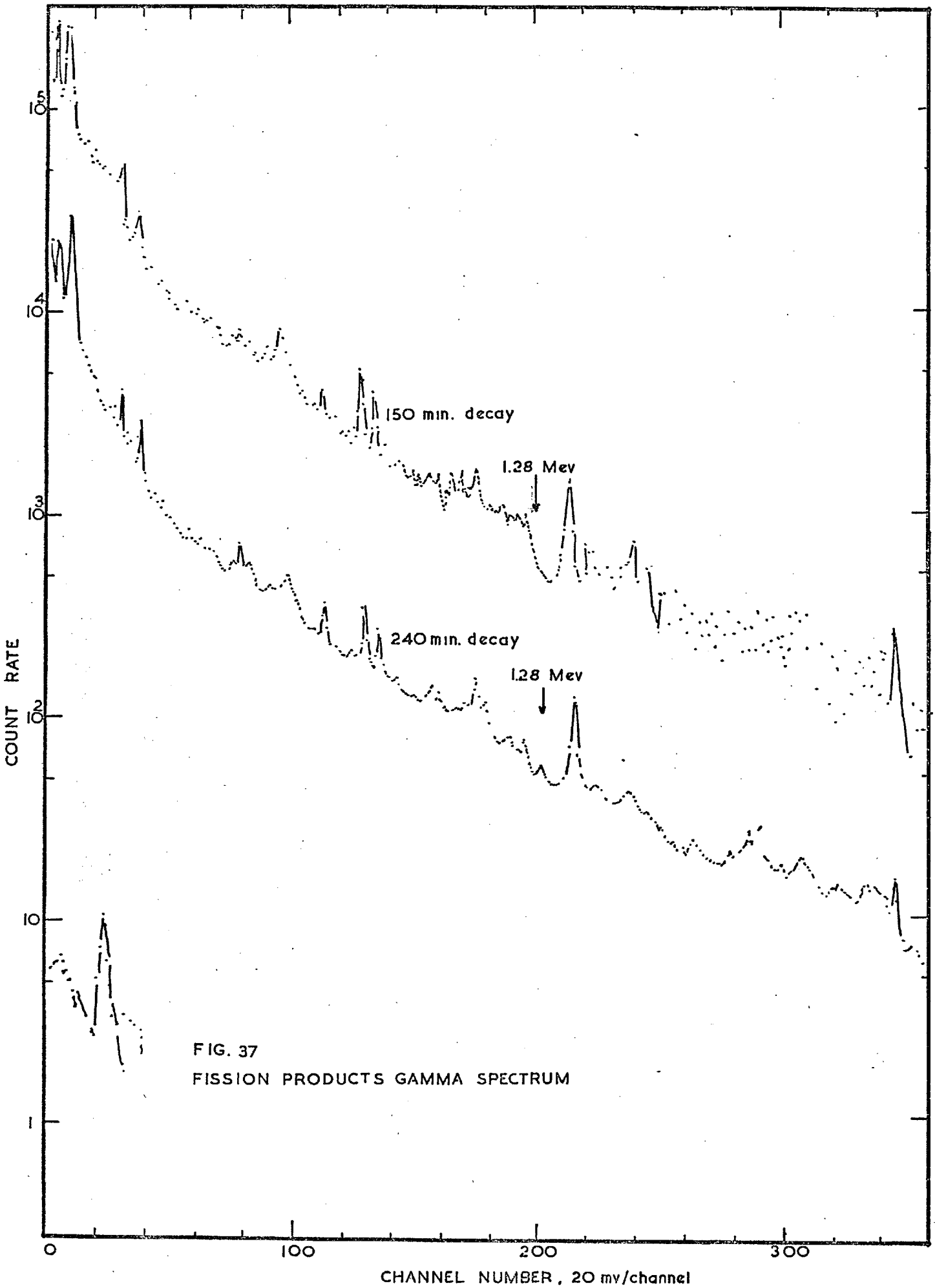

FIG. 37
FISSION PRODUCTS GAMMA SPECTRUM

of 1.28 Mev which is the bias level of the counting system. Therefore after 240 minutes the stability of the counting equipment is extremely important in the measurement of the U_{238}/U_{235} fission ratio. Figs. 37 and 38 show the fission product gamma spectrum at different decay times and the position of the 1.28 Mev bias level. For this purpose a temperature controlled box was made big enough to contain the whole counting equipment. The temperature controlled box is described in chapter 3.

(4) The purpose of using two scintillation counter head-to-head was to eliminate any effect in count rates due to twist in the foils during the handling.

The foils were carefully washed in acetone and weighed on a microbalance before the irradiation and the oxidation on the surface of the foils was removed by dipping them into the dilute nitric acid.

(5) Flux Perturbation: In the method of determining p(t) using the double fission chamber very thin deposits were virtually replaced by uranium foils. The specification of deposits and foils are given in Table 7. Because of differences in size, thickness and amount of U_{235} in deposits compared with uranium foils, flux perturbation in fission counting was different from that in foil irradiations. In the calibration factor p(t) determination in the irradiation hole, because of the low fission ratio 0.0034, flux depression was due to thermal neutron absorption in U_{235}. A series of irradiations were carried out in the hole using 0.025 mm thick natural uranium foils sandwiched between different thicknesses of the identical foils in order to measure the flux perturbation. From this experiment the flux perturbation was estimated to be less than 1% for the present work.

TABLE 7

DEPOSITS AND FOILS SPECIFICATIONS

Deposits	U_{235} $\mu gm/Cm^2$	U_{238} $\mu gm/Cm^2$	Coating Diameter (Cms)	Total Mass U_3O_8 mg	U_{235} %	U_{238} %
U_{25}	49.24	2.96	3.2	0.504	92.95	5.68
U_{28}	0	210	3.2	1.993	0	100
Depleted	0.03176	89.467	2	105.5	0.0355	99.9645
Natural	0.556	76.7	2	91.1	0.7196	99.28
FOILS	mg/foil	mg/foil	foil dia.	weight		
U-Al	3.157	0.243	0.9	17	93	6
Depleted	0.287	77.2	0.9	80	0.0355	99.9645
Natural	5.757	74.3	0.9	80	0.7196	99.28

In order to improve the accuracy on p(t) measurement two deposits depleted and natural uranium of equal thickness, 2 Cms. diameter were used. The deposits were made of the same material as the foils in order to eliminate systematic errors due to fission products loss in the coating as well as a flux perturbation correction in fission counting. Five foils were irradiated in the irradiation hole in order to determine the magnitude of flux gradients. Four foils were positioned crosswise and one at the centre on an area equal to the deposit coating as shown in Fig. 39. The corrected count rate of the foils indicated that the foils had been irradiated in a

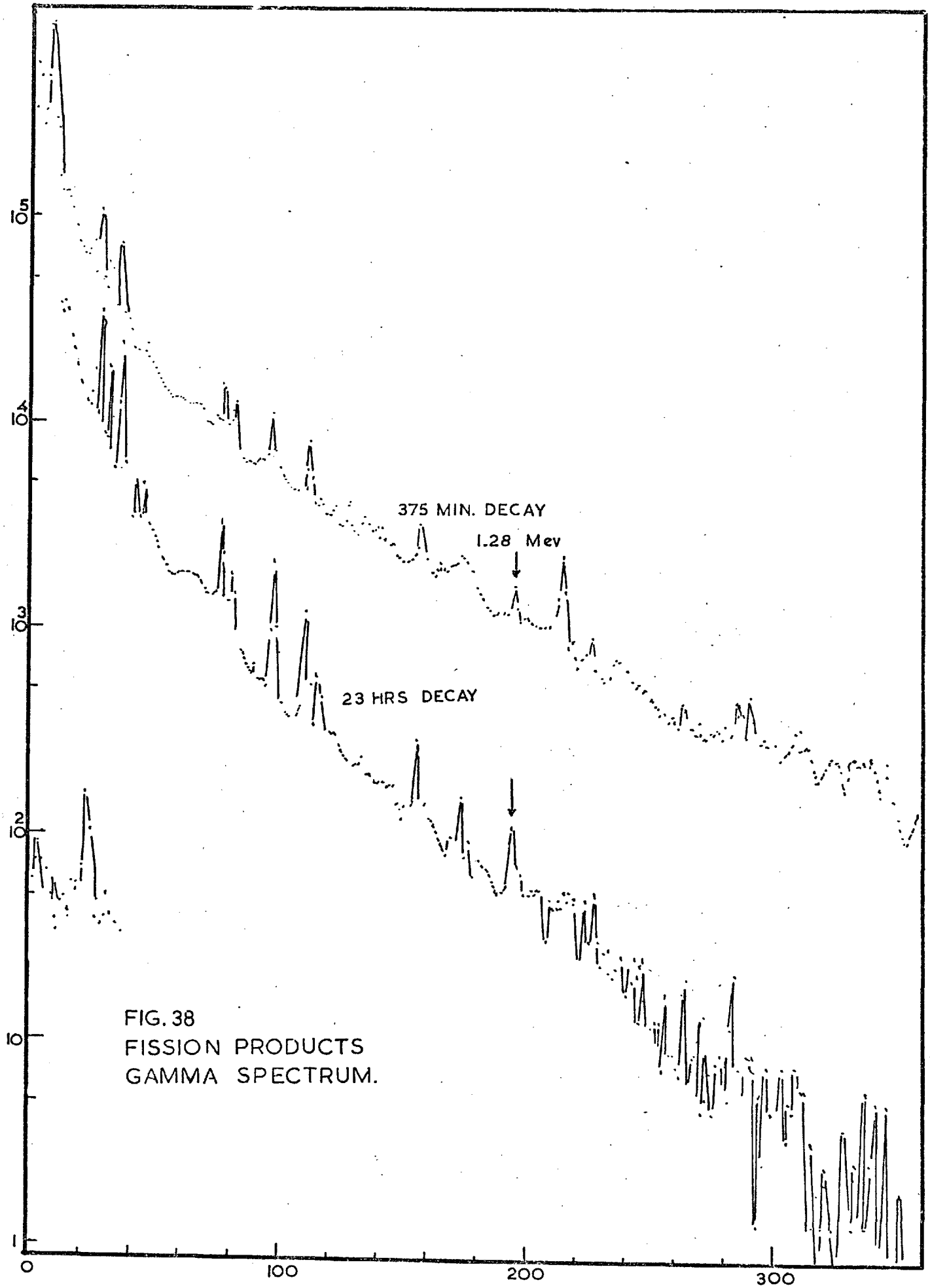

FIG. 38
FISSION PRODUCTS
GAMMA SPECTRUM.

uniform flux. The difference in the foils activities was within the experimental error. The counts were fed into the program FLUX. The program after performing all necessary corrections using a linear interpolation method, produced a set of decays for each foil. Then the decays of peripherial foils were divided by centre one and the averaged ratio was obtained for each of four foils. Equation 7.1 was used from which the random error was calculated and was about 1% for each set.

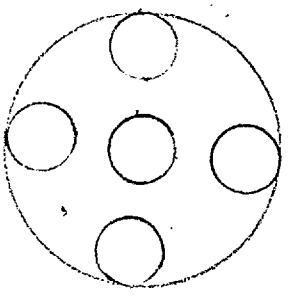

Fig. 39

Following is a list of sources of error with estimated error:-

TABLE 8

	Percentage of Error
(1) Uncertainty in the weight of foils	0.025
(2) Background and natural activity of the foils	< 0.1
(3) Foil holder calibration factor	negligible
(4) Feed through (manual)	negligible
(5) Deadtime	2.5
(6) Pulse pileup	2.5
(7) Uncertainty in deposit weights by alpha counting	1.5
(8) Uncertainty in the ratio of deposit weights by fission counting in thermal column	< 1
(9) Flux perturbation	< 1
(10) Fission products absorption in fissile coating	0.5

CHAPTER 7

EXPERIMENTAL MEASUREMENT OF FISSION RATIO IN LONDON UNIVERSITY REACTOR CORE

7.1 PURPOSE OF EXPERIMENT

The purpose of the experiment was to measure the fission ratio, thermal flux and fast flux above 1 Mev in each fuel element in the core. Fission ratio measurements were carried out in two fuel elements I and L using depleted and natural foils, see Fig. 40. Fuel elements H and F were assumed to have similar fission ratio distributions as I and J because of their complementary positions to elements I and L. Fuel element L located between two fuel elements H and F has a different situation in comparison with the others and was expected to have symmetrical fission ratio distribution and flux shape about the central plane of the fuel element. The results of the experiments are shown in Fig. 41 and the positions of the fuel elements J, I, H, L and F are indicated below the curves for clarity. From the experiment F8, F5, F8/F5 and δ28 were obtained where F8 and F5 are U_{238} and U_{235} gamma activity fission rate per atom in U_{238} and U_{235} nuclei respectively. F8/F5 and δ28 are fission ratios per atom and natural uranium respectively. The corresponding values are indicated in the graph. In a series of irradiations only one natural uranium was used to display the general variation of the flux in the core and outside the core. The result of this experiment is shown as a continuous line in the diagram.

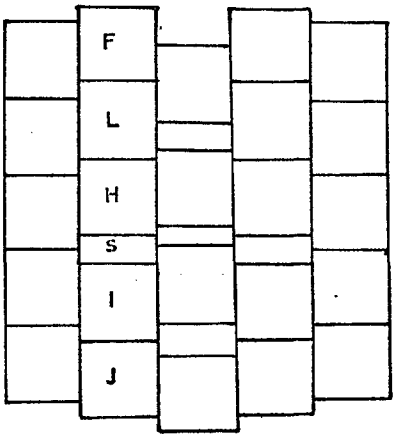

BLOCK DIAGRAM OF
UNIVERSITY LONDON
REACTOR CORE

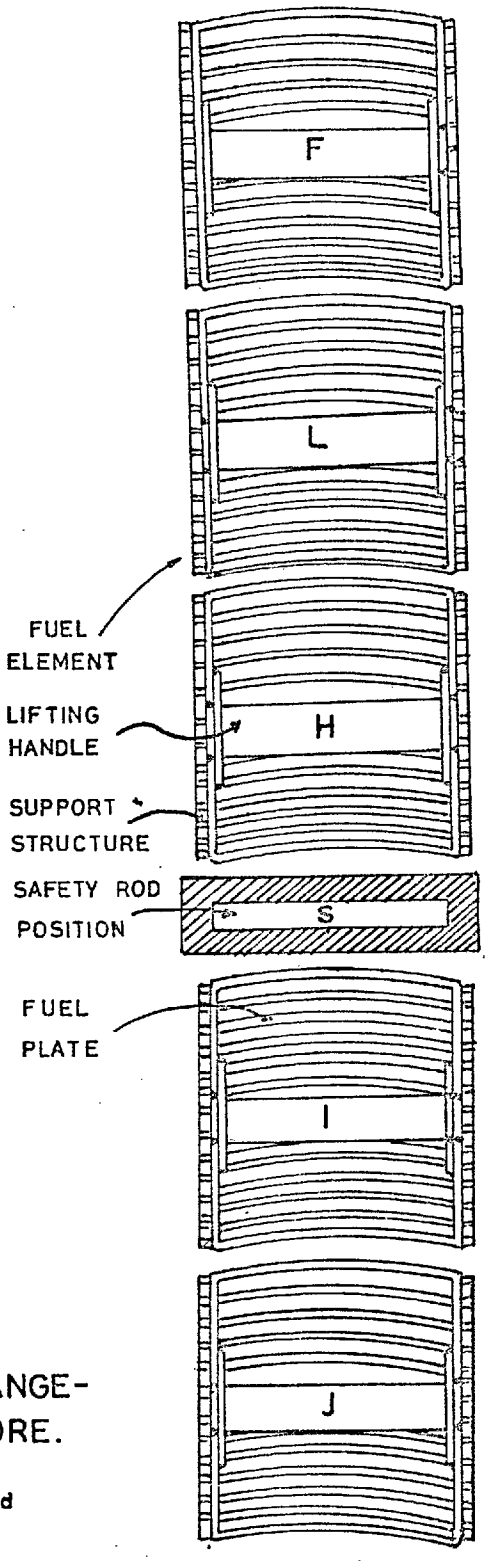

FIG. 40
FUEL ELEMENT ARRANGE-
MENT IN REACTOR CORE.

scale : half size
uranum foils were irradiated
between fuel plates.

7.2 CORE STRUCTURE AND THE EXPERIMENTAL PROCEDURE

The London University Reactor Core consists of twenty-four UKAEA Standard MTR type fuel elements. The general layout of the core and surroundings are shown in Fig. 17. A block diagram of the core and a half scale size of one row of fuel elements are shown in Fig. 40. The position of the safety rod is indicated by letter "S", coarse rods by "C", fine rod by "FINE" and pneumatic facility by "O". The twenty-four fuel elements sit in an aluminium frame in the Reactor tank.

The core is about 35 Cms square by 60 Cms high. Each fuel element comprises of twelve slightly curved aluminium fuel plates. Each fuel element is 7.2 Cms by 6.4 Cms. Fuel plate thickness varies between 1.42 and 1.50 mm, and fuel plates are between 3.72 and 4.1 mm apart. Twelve fuel plates are secured in a fuel can to form one fuel element. Fuel meat in the form of uranium alluminium alloy nominally 0.5 mm thick is rolled between two aluminium claddings. The uranium is 80% enriched U_{235} and each fuel element has nominally 138 gm of U_{235}(33). The core is controlled by two coarse rods and a fine rod. A safety rod is provided for emergency or quick shutdown.

Fission rate measurements were made with natural and depleted foils, 0.0762 mm thick, 9 mm diameter. The foils were fixed in recessed holes on a perspex strip by waterproof polythene tape, see plate 29. The strip was lowered by a long aluminium rod, threaded on one end to hold the strip, so that the strip became locate between two fuel plates. The thickness of the strip was so chosen to fill the water gap. The length of the strip was such that the foils were located at half the depth of the fuel elements where

the flux gradient is small. A slightly curved aluminium strip was fastened in a slot to the end of the perspex strip to keep it moving sideways in the fuel plates spacing and also add extra weight to keep it from floating. For irradiating foils outside the core a perspex frame was made to hold the foils at the same level as incore irradiations, see plate 29.

The row of fuel elements JIHLF was chosen for the fission ratio and flux measurements since it was readily accessible for loading foils. During the Reactor operation the safety rod was always out, the two coarse rods half-way out and only fine rod was used to control the Reactor power level. The two hours irradiation was adopted as before in order to be able to find the true fission ratio using pre-determined value of p(t). The irradiation period was counted from 37% of the required Reactor power, 100 watts, to the time of shutdown. Foils were removed about half an hour after the end of irradiation. Since doing all irradiations simultaneously was impossible because of many reasons such as number of perspex strips, amount of uranium introduced into the core (because of reactivity change), and the counting problems of the foils irradiations were carried out in many runs. The maximum number of foils could be counted was five foils, therefore whole experiment was performed in several days. To normalize all irradiations a reference foils was needed to be used with every irradiation. For this purpose a natural foil was irradiated in the centre of the core concurrently with each set of foils for monitoring the flux level. The foils were counted on a double NaI(Tl) counting system shown in Fig. 4, with the discriminator bias set at 1.28 Mev peak of Na^{22}

FIG.41

⊙ NATURAL FOIL GAMMA ACTIVITY(X 2.5×10^{3})

^ $(F8/F5)_{\gamma}$ ($\times 10^{3}$)

▫ U-235 GAMMA DECAY ($\times 10^{15}$)

Δ U-238 GAMMA DECAY ($\times 10^{18}$)

× $[d_{28}]_{\gamma}$ ($\times 10$)

To obtain true Fisson Ratio multiply the corresponding value by 1.33, P(t).

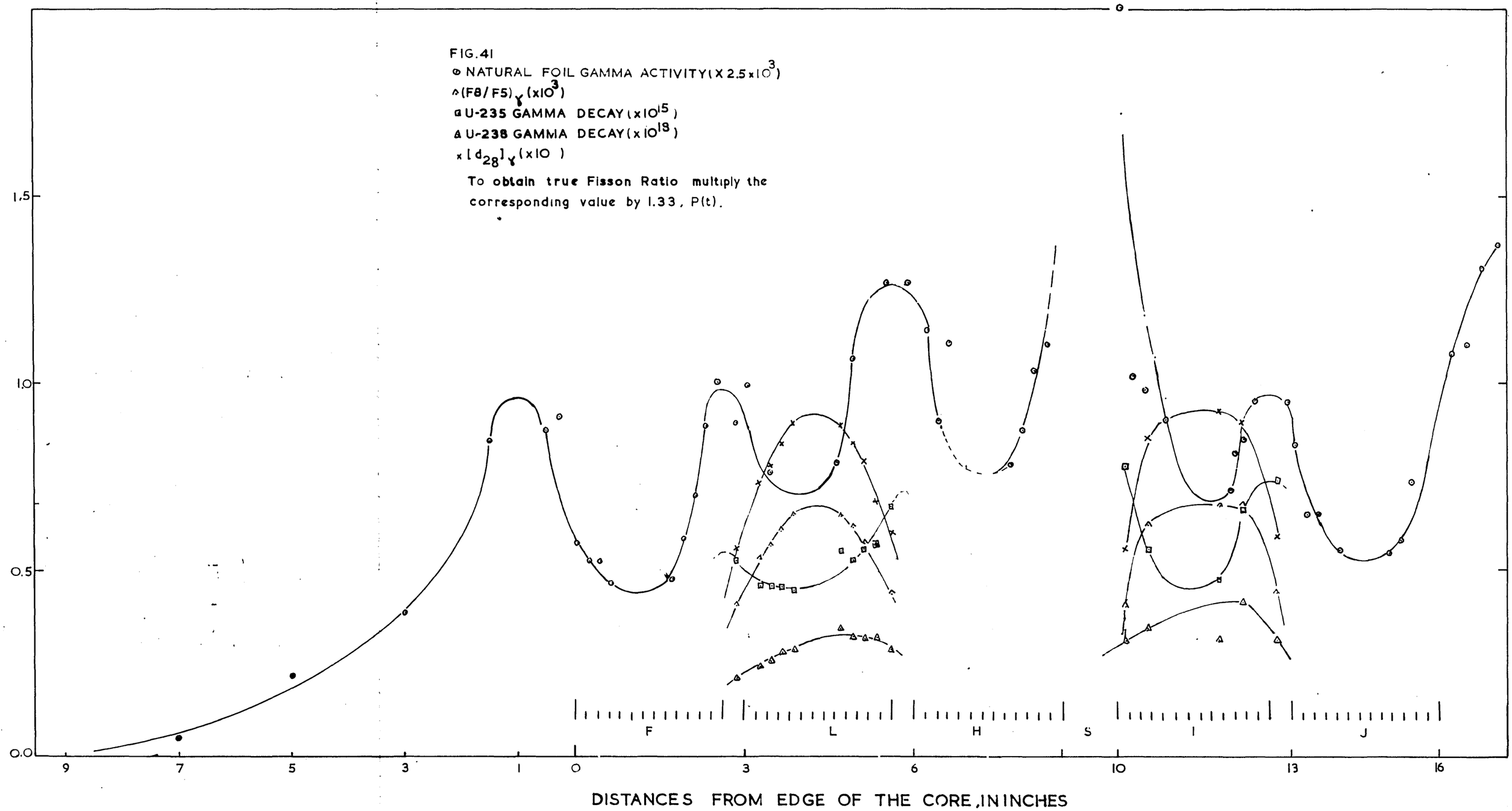

7.3 FINE AND HYPERFINE STRUCTURE.

From the experimental results the largest value of fission ratio, δ28 is 0.08 in the middle of fuel elements and the smallest is less than 0.04 between two fuel elements. Therefore the gamma activity of natural foil across the core shown by solid line in the diagram, see Fig. 41, can be taken as proportional to the thermal neutron flux. The effect of reflector was noticed on the edge of the core as the activity of the natural foils irradiated on the edge of the core rises, see Fig. 41. The rise of the thermal flux within the fuel elements is due to neutron moderation and low absorption rate in water compared with the fuel element. In the position of the safety rod thermal flux has appreciably increased, which is due to the large spacing between the two adjacent fuel elements I and H and being close to the centre of the core. The high level thermal flux in this position signifies the importance of the safety rod in reactivity change for the shutting down the reactor. As shown in Fig. 41, the general trend in the flux distribution is the one usually expected, high in the centre and low near the edge of the core. In fuel element L fission ratio distribution is symmetrical about the centre plane of the fuel element, but U_{235} and U_{238} gamma activity distribution are not symmetrical. This is again due to higher flux in the centre of the core than the edge. In fuel element I because of the position of the safety rod there is more chance for neutron to slow down than the other gaps between fuel elements.

It is seen from diagram 41 that thermal flux gradient is greater than fast flux gradient. This is because of the fact U_{238}, a threshold detector with threshold energy more than one Mev, was used

to measure the fast flux. The scattering cross section of hydrogen and oxygen above one Mev is less than 4 b in comparison with 20 b for H below .5 Mev, as such fission neutrons have a great chance to travel from one fuel plate to the others inducing fission in U_{238} in fuel meat, while thermal neutrons are easily absorbed, mainly in uranium. From the thermal flux shape in each fuel element U_{235} burnup can be estimated that is very higher in outer plates than inner plates.

Since the foils irradiations have been carried out within the fuel plate gaps and there is not access to measure the fission ratio and the neutron flux in the fuel plates, a computer code RIPPLE (34) was used to predict the decrease in the thermal flux in the fuel plates and increase in fission ratio. RIPPLE calculation is based on collision probability, a brief description of the method is given in Appendix II for detail of the method consult (34), (35) and (36). The RIPPLE structure of thermal flux in the fuel elements between the fuel plates is shown in Fig. 42. From the graph the ratio of the flux in the fuel plates spacing where the foils were irradiated to the flux in the fuel meat is 1.05 ± 0.01. One per cent error is due to uncertainty of the position of the foils in the water gap. Therefore, thermal flux and fission ratio in the fuel meat are by 5% different from the measured values. Whereas the fast flux distribution in each fuel element due to low cross sections of materials in the core has a small variation. As such the fast neutron flux change between fuel plates is not significant compared with 5% change of thermal flux.

FIG. 42
HYPERFINE THERMAL FLUX STRUCTURE IN M.T.R. TYPE FUEL ELEMENT, CONSORT CORE, USING "RIPPLE" COMPUTER CODE

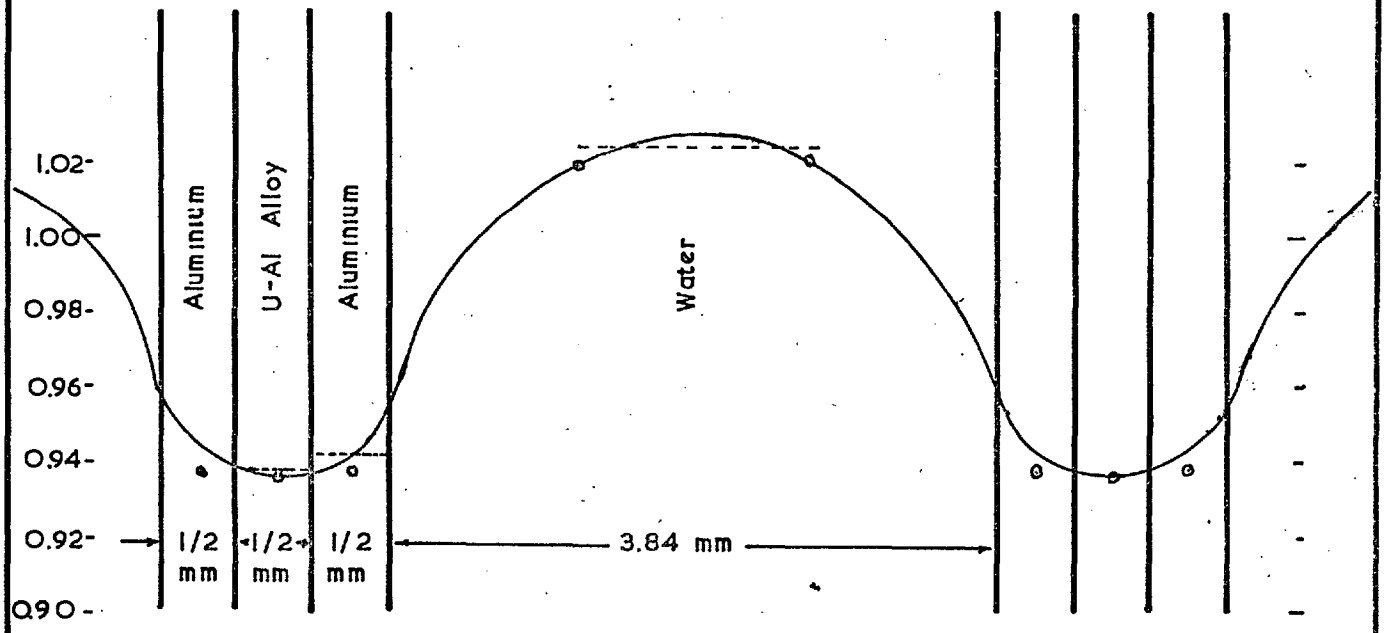

—— RESULTS FROM COMPUTER PROGRAMME " RIPPLE"

⊙ HYPERFINE STRUCTURE USING "GMS" PROGRAMME TO SOLVE TRANSPORT EQUATION BY DSN APPROXIMATION

7.4 DATA ANALYSIS AND ERRORS

A computer programme FFR-CORE was written to calculate fission ratio, U_{238} and U_{235} fission rate in the fuel elements from the gamma counts of natural and depleted foils irradiated between the fuel plates. The FFR-CORE programme is basically the same as FFRIII is discussed in Appendix 1. The programme first does all the necessary corrections such as deadtime of the counting system, pulse pileup effect, background and natural activity, weight of the foils, correction for the positions of the foils on the perspex strip during the irradiation and normalization correction. Then it calculates fission ratio, U_{238} and U_{235} fission rates using equation 3.8 and 3.10. As mentioned in section 7.2, with every batch of foils irradiated in the core one natural foil was simultaneously irradiated in the centre of the core (pneumatic system) in order to normalize all irradiations to the same flux level. The normalization correction was used in the programme is attributed to the above sentence. The FN8 and FN5 are normalized U_{238} and U_{235} fission rate to unity at 240 minutes were also obtained from each irradiation. In actual fact FN8 and FN5 are same as D8(t) and D5(t). The difference is that D8(t) and D5(t) were obtained from a series of irradiations in order to minimize the error at each point, see Appendix III for D8(t) and D5(t) table.

In order to calculate random error for F8/F5, F8 and F5 measurements at each position these values were multiplied by D5(t)/D8(t) $\frac{1}{D8(t)}$ and $\frac{1}{D5(t)}$ respectively then equation 7.1 was used

$$\sigma^2 = \frac{1}{N} \sum_{i=1}^{N} (x_i - \bar{x})^2 \qquad (7.1)$$

where σ is the standard deviation, N is the number of points (values) that is xis, x_i is the ith value and $\bar{x}$ is the averaged value of xis. The calculated random error was about one per cent for the values of fission ratio, U_{238} and U_{235} fission rates at each point.

For analyzing the results of the natural foil gamma activity irradiated acrossthe fuel element row, JIHLF, between the fuel plates and outside the core a computer programme FLUX was written, see Appendix I. In this programme a two-dimensional array was arranged to be able to normalize all natural foils count rate to a reference one (was chosen arbitrarily) and find the random error in the measurements at each irradiation position. The array was 12 by 21 where 12 is the number of positions of irradiation in each fuel element and 21 is the decay intervals from 150 to 250 minutes. In these measurements the random error was calculated by dividing decays of all the natural foils by the middle foil decay, assuming all decays in one fuel element had similar shape. The computer results showed the validity of this assumption. The standard deviation was obtained from equation 7.1. The random error was about one per cent for all the positions. The results of this measurements along with the fission ratio and fission rates are plotted in Fig. 41.

7.5 THEORETICAL CELL CALCULATIONS IN THE LONDON UNIVERSITY REACTOR CORE

In order to perform flux distribution and reaction rates

calculations in the fuel element of the London University Reactor core the Generalized Multigroup System, GMS, was used, see Section 2.3. See Fig. 40 for details of the fuel element structure. The results of the computer are shown in Fig. 43 as compared with the measured values. Since flux distribution in the fuel element is symmetrical about the midplane of the fuel element, therefore the U_{235}, U_{238} reaction rates and U_{238}/U_{235} fission ratio distributions are shown in Fig. 43, in half of the fuel element. In the calculations of reaction rates the presence of the control rods and the water gaps between the fuel elements were not taken into account in order to simplify the calculations. The results of the foil irradiations in the fuel elements J and L leading to determination of the U_{235} and U_{238} reaction rates and fission ratio are shown in Fig. 43.

In order to compare the experimental results with the theoretical predictions, the U_{235}, U_{238} and U_{238}/U_{235} fission ratio were normalized to unity at the midplane of the fuel element. In Fig 43 solid lines are the theoretical results and dashed lines are the distribution of U_{235}, U_{238} reaction ratio and U_{238}/U_{235} fission ratio in water gaps between the fuel plates. Falls and rises in the curves are due to the fuel and water structure. The fast neutron flux does not change very much in the fuel element. This is due to the low scattering cross section of hydrogen and low absorption of the fuel for fast neutrons. For true fission ratio in the fuel elements see Fig 41.

FIG. 43

U235, U238 & U238/U235

—— COMPUTE RESULTS FROM GMS-I

o, △ FUEL ELEMENT "L"

●, ▲ FUEL ELEMENT "I"

[See FIG. 41]

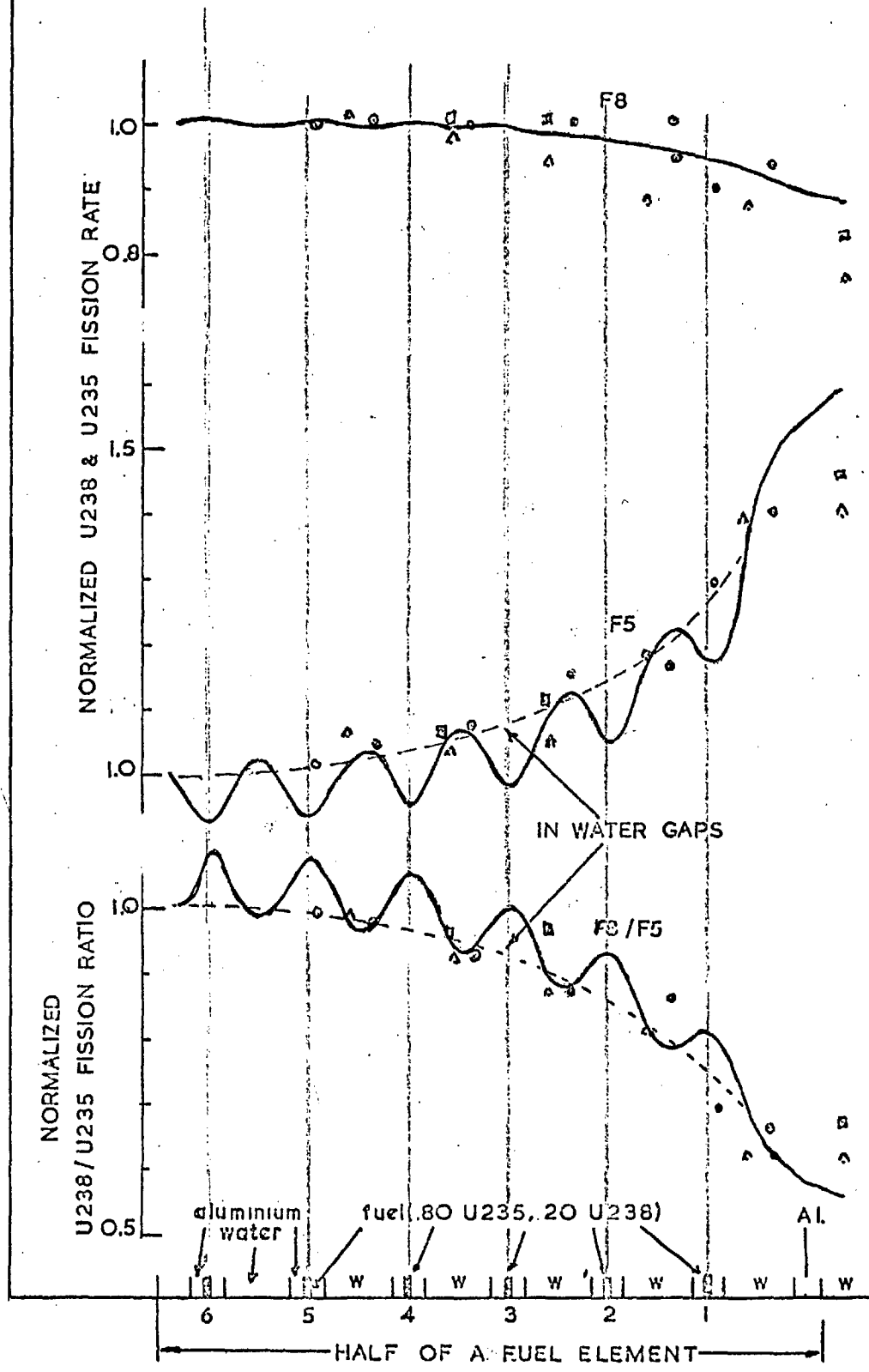

CHAPTER 8

CONCLUSIONS

The present method of fission ratios measurements, based on the fissile foils activation technique, has been shown to be capable of high accuracy. Because of the importance of fission ratios in reactor physics calculations, especially in fast reactors, accurate measurements of fission ratios have become essential for development of design and performance of reactors. Although the main effort was concentrated on U_{238}/U_{235} fission ratio measurement, the technique is universal and can be applied to other important fission ratio measurements involving other fissile isotopes. The experimental evidence shows that the foil technique is a satisfactory method being both simple and fast.

The Lanthanum-140 technique is a promising method, especially if Ge(Li) detectors are used for measuring the true fission ratio without bothering to determine the calibration factor, p(t), but at the present stage the uncertainity in the fission yields of La-140 is large and it can not therefore be used as a direct method for measuring true fission ratio. It is mainly used for monitoring the systematic errors in the fission chamber technique for measuring p(t). It should also be noted that the La-140 is a slow method.

The third method of measuring the calibration factor, p(t), involved the simultaneous irradiation of a depleted foil and deposit in a thermal and fast spectrum and as far as the experimental errors are concerned it is a good method, but it requires some limitations which make it impractical in reactor spectra especially in fast reactors.

In the process of measuring true fission ratios one of the sources of error is the neutron perturbation (flux depression, self shielding and elastic and inelastic scattering effect caused by foils). The

perturbation effect was estimated to be 1% in the calibration factor determination.

The following points were considered in order to minimize the experimental errors:

1. Using a fission chamber with the minimum amount of material, namely moderating materials.
2. Using deposits with small area of fissile coating in order to eliminate flux gradient effect.
3. Using thin deposits so that the fission product loss in the coating becomes negligible and scattering of fission product in the coating is minimized.
4. Using foils as thin as possible with the nearest area to the deposit's area, since thin foils causes low flux perturbation. The area of the foils are important in places where the flux gradient is high.
5. Using foils and deposits coating of the same fissile material in order to be able to assess the ratio of masses accurately.
6. Using deposits of the same thickness (coating) so that the fission product loss will be the same for both deposits.
7. By using Subroutine LISQFT in the Computer programme FFR3 the error due to linear interpolation between the counts was eliminated and statistical fluctuation was minimized.
8. By using a correction for pulse pileup plus deadtime the error due to individual effect was minimized.

A new technique has recently been used by Besant (8) to measure true fission ratios by Solid State Track Recorder (SSTR). The method is based on the track recording in solids proposed by Fleischer and reported in Ann. Rev. Nucl. Sci., 15, 1 (1965). Besant employed a

polycarbonate called LEXAN. The composition of LEXAN is approximately $H_{18}C_{16}O_3$. Since LEXAN has a large amount of hydrogen and carbon, both are good moderators, the perturbation effect is to be taken into account. The experimental error was given as 3% in fission ratio measurement. This method can be used as an independent method for checking the results of foil activation technique.

The method of mass determination of the fission chamber deposits is based on alpha counting. This method yields an uncertainty of 1.5% which is due to systematic errors including uncertainties in the half lives of uranium isotopes, especially U_{234}, present in deposits. In order to determine the calibration factor, p(t), to an accuracy of 1% the masses of deposits ought be be assessed with an accuracy better than 1%. By irradiating a natural and depleted deposit in thermal spectrum the mass ratio of the deposits was obtained to an accuracy of 0.8%, error being due to fission counting statistics, loss of fission products in the coating and the threshold on the counting system. The depleted and natural deposits had the same thickness (110 g/Cm^2) to within 1%. The bias curves for both halves of the double fission chamber were similar, with the slope of 0.03 C/volt-count. This was an improvement in determining the mass ratio.

Since true fission ratio measurement by foil technique is based on p(t) values it is highly important to determine p(t) accurately in different reactor spectra. The experimental results showed that p(t) varies with the neutron energy. The p(t) value in a fast reactor spectrum is by 10% lower than in thermal reactors.

The foil technique was used in measuring the fission ratio in the London University Reactor Core. The U_{235}, U_{238} reaction rates and fission ratio were measured in two fuel elements. And also the flux

variation across a fuel element row was measured by irradiating natural foils between the fuel plates and outside the core. A transport theory code, GMS-1, was used to calculate the U_{235} and U_{238} reaction rates and fission ratio in half of a fuel element. The theoretical results and experimental values are consistent within the experimental error, except the values of U_{238}, U_{235} and fission ratio near the edge of the fuel element. The calculated fission ratio is higher than measured value. This is due to the water gap between the fuel elements and in calculations a small gap of water was considered.

REFERENCES

1. Brown, W. A. V., Skillings, D. J. et al, Measurement of Fast Fission Ratio AEEW-R341 (1964).

2. Tunnicliffe, P. R. et al, A method for the accurate determination of Relative Initial Conversion Ratio, Nuclear Science and Engineering 15, 268, (1963).

3. Carter, M. D., Perks, A.J. and Saunders, L.G., The Measurement of U_{238} : U_{235} fission ratios, AERE-R 3205, 1960.

4. Besant C. B., George, C.F. and Jonstrone, I., A Review of the current W.R.P.D. technique for measuring Relative Conversion Ratio, ETM/p 70 (1966).

5. Besant, C.B., George, C.F. and Millington, R.A., Measurement of fission rate gamma activity calibration factor, p(t), ETM/p 94, 1968.

6. Stevenson, J.M. and Broomfield, A.M., Measurements and calculation of ratios of effective fission cross sections in the zero power Fast Reactor ZEBRA, AEEW-R-526 (1967).

7. Barnett, C. A., Besant, C.B., Murphy, M.F. and Taylor, W.H., Measurement of Relative Conversion Ratio and Fast Fission Ratio in low enrichment oxide, AEEW-R-648 (1969).

8. Besant, C.B. and Ipson, S.S., Progress in the application of solid state track Recorders to Reactor physics Experiments, AEEW-M.881, (1969).

9. Fast Reactor Physics Conference, 24-26 June, 1969, The British Nuclear Energy Society.

10. Meghreblian, R. V., and Holmes, D. K., Reactor Analysis, 1960.

11. Lee, C.E., The discrete Sn approximation to transport theory, LA-2595 (1961).

12. Carlson, B.G., Solution of the transport equation by Sn approximation, LA-1891 (1955).

13. Tait, J.H., An Introduction to neutron transport theory, 1964.

14. Askew, J.R and Bressenden, R.J , Some improvements in the discrete ordinate method of B.G. Carlson for solving the neutron transport equation, AEEW-R-161 (1963).

15. Gratton, C P. and Smith, P.E., GMS-I, A Generalized Multigroup System of calculation using the IBM 7030 (Stretch) Computer, AEEW-M458 (1965).

16. Francescon, S., The Winfrith DSN programme, AEEW-R273, 1963.

17. Yieftah, S., Okrent, D. and Moldauer, P.A., Fast Reactor Cross Section, 1960.

18. Kaplan I,
Nuclear Physics, 1963.

19. Broomfield, A.M. and Stevenson, J.M., Measurements of spectral indices in the zero power fast reactor ZEBRA using absolute fission chambers, Paper 19, Fast Reactor Physics Division, 1963.

20. Etherington, H. (Editor),
Nuclear Engineering Handbook, 1958.

21. Thompson, T.J., Kaplan, I., Clikeman, F.M. and Driscoll,
Heavy Water Lather Project, Sept.30., 1965., MIT-2344-4.

22. Hicks, D., Nuclear calculation methods for light water moderated reactors, AEEW-R64.

23. Wolberg, J.R., Thompson, T.J., and Kaplan, I., A study of the Fast Fission Effect in lattices of uranium rods in heavy water, NYO-9661, 1962.

24. Weinberg, A.M. and Wigner, E.P., The physical theory nuclear chain reactors, 1959.

25. Grant, P.J., Elementary Reactor Physics, 1966.

26. Lederer, C.M., Hollander, J.M. and Perlman, I., Table of Isotopes (6th edition), 1967.

27. Croall, I.F., Yields from Neutron Induced Fission, AERE-R-5086 (1967).

28. Murphy Jr., H.M., PPA, A computer program for Photo Peak Analysis, AFWL-TR-65-11 (1966).

29. Leachman, R.B., The fission process - Michanisms and data, Proc. of 2nd UN Conference, 1958, Vol. 15, p.229.

30. Hemmedinger, A, Fission cross sections at Mev excitation, Proc. of 2nd UN Conference, 1958, Vol. 15, p.663.

31. Chawla, R. Intrinsic peak efficiency of Ge(Li)detector by γ-γ coincidence with a NaI(Tl) counter, (M.Sc. thesis), 1967.

32. Olive, B., Cameron, J.F. and Clayton, C.C., A Review of High Intensity Neutron Source and their application in industry, AERE-R 3920, (1962).

33. Grant, P.J., The London University Nuclear Reactor Consort, Nature, Vol. 207, No. 5000 (August, 1965).

34. Newmarch, D.A., A method of computing the thermal neutron fine structure for thin plate assemblies, AERE-R/R 2425 (1959).

35. Fayers, F.J., Lecture notes on selected topics in numerical methods in Reactor Physics, AEEW-M677 (1966).

36. Leslie, D.C., The calculation of collision probabilities in cluster type fuel elements, Nuclear Science and Engineering 23, 272-290 (65).

37. EANDC "53" S, EANDC Round table on high precision mass spectrometry and α-counting, Nov. 29th - Dec. 2nd, 1965. Euratom, Brussels.

38. Conte, S.D., Elementary Numerical Analysis an algorithmic approach, 1965.

39. McCracken, D.D. and Dorn, W.S., Numerical Method and FORTRAN programming, with applications in Engineering and Science, 1964.

40. ANL-5800, Reactor Physics Constants, Argon National Laboratory, 1963.

41. Carlson, B.G., Solution of transport equation by Sn Approximations, Los Alamos Scientific Laboratory Report, LA-1599, October, 1953.

42. Barnett, M.R. (Miss) and Ward, J.A.,GMS3, A users manual for an improved generalized WDSN MK2 for the KDF9 computer, AEEW-M 825, 1963.

43. Wade, R.D. (edited by), Solution of the one dimensional Multi-group Stationary Neutron Transport Equations on the IBM 7030 (Stretch)Computer, AWRE O-12/63, Sept. 1963.

44. International Atomic Energy Agency, Directory of Nuclear Reactors, Volume IV, 1962, Power Reactors.

45. International Atomic Energy Agency, Fast Reactor Physics, Vol. 1, Proceedings of a symposium, Karlsruhe, 30th October - 3rd November, 1967.

46. McCracken, A.K. and Gammon, R., The measurement of epithermal neutron spectra in bulk media by the foil sandwich method. AEEW - R412, 1965.

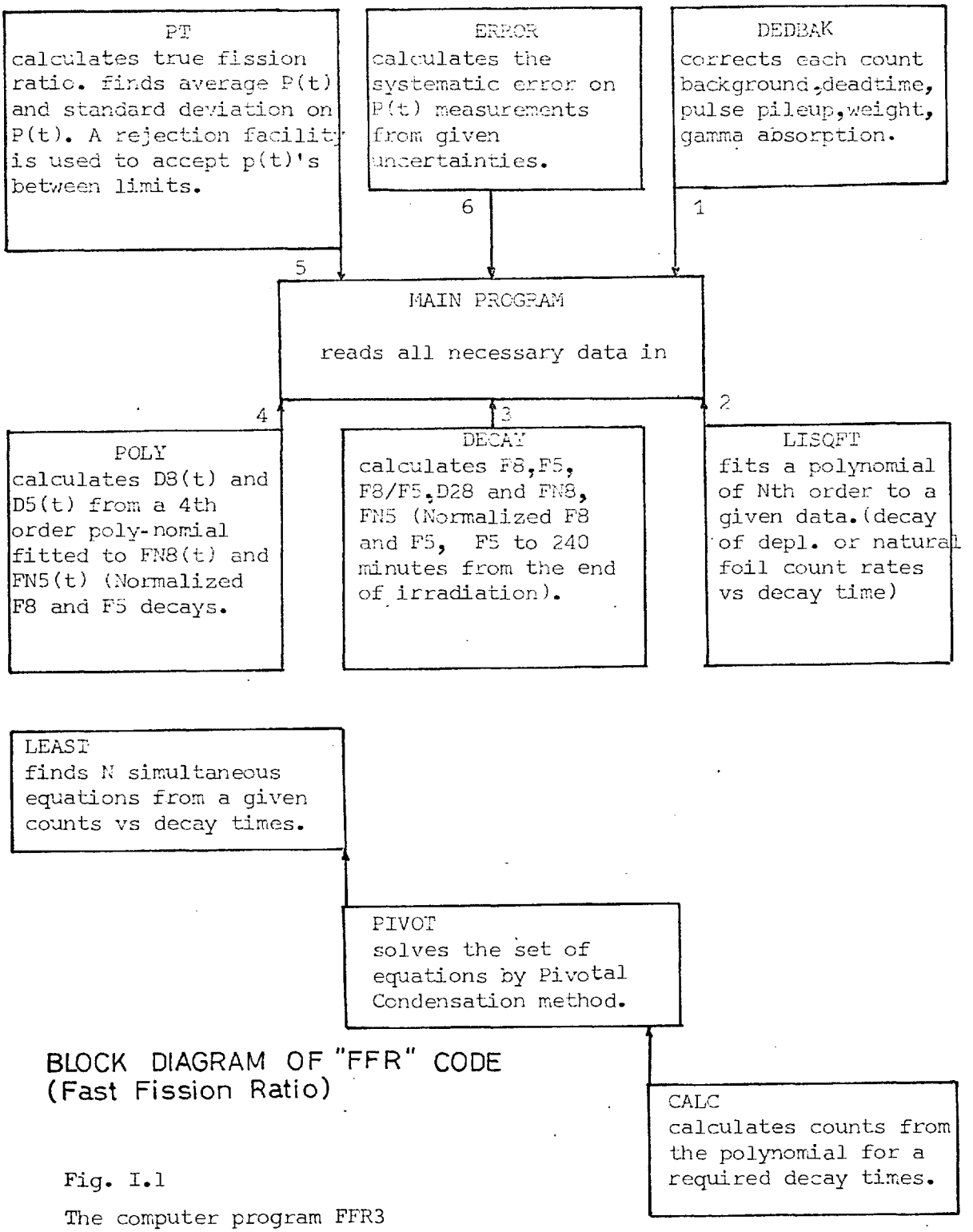

BLOCK DIAGRAM OF "FFR" CODE
(Fast Fission Ratio)

Fig. I.1
The computer program FFR3
and the subroutine LISQFT.

APPENDIX I

FFR PROGRAMS AND SISTER PROGRAMS

The Fast Fission Ratio, FFR, programme was designed to calculate fission ratio, U_{238} and U_{235} fission rates, FN8 and FN5 from observed gamma counts of depleted and natural foils. The FFR also calculates the true fission ratio from fission counts of the double fission chamber. By dividing the true fission ratio by the gamma activity fission ratio the calibration factor (p(t), is calculated. The programme finally calculates random and systematic errors involved in the measurements. The programme has three versions which are FFR1, FFR2 and FFR3. They are very similar and have common subroutines. A block diagram of FFR3 is given in Fig. I.1. The FFR1 version comprises of the following subroutines -

(1) DEDBAK

This subroutine first finds the count rate of each foil, then corrects each count rate for deadtime of the counting equipment, pulse fileup effect, weight of the foil, gamma absorption in the foil, tray calibration and for position of the foil.

(2) INTPLT

The INTPLT interpolates linearly between two successive count rates in order to find the count rates of each foil for a given decay time.

(3) DECAY

This subroutine calculates F8(t)/F5(t), δ_{28}, F8(t), F5(t), FN8 and FN5 from interpolated count rates.

(4) PT

PT calculates the true fission ratio from fission counts (obtained from the double fission chamber), mass of the deposits and the

fission product absorption rate in the coating and finally calculates the calibration factor p(t) from equation I.1

$$p(t) = (F8/F5) \;/\; (F8(t)/F5(t))_{\gamma} \qquad (I.1)$$

where F8/F5 is the true fission ratio and $(F8(t)/F5(t))_{\gamma}$ is the gamma activity fission ratio. p(t) is a time dependent quantity because the true fission ratio is a constant value and gamma activity fission ratio is a time dependent ratio, see Fig. 22. In order to calculate random error on p(t), the p(t) values were multiplied by $\frac{D8(t)}{D5(t)}$ then the average value was obtained. Using the following equation the standard deviation was calculated:

$$\sigma^2 = \frac{1}{N} \sum_{i=1}^{N} (x_i - \bar{x})^2 \qquad (I.2)$$

D8(t) and D5(t) are given in Appendix III. PT reject those p(t) values that are outside a chosen range.

(5) ERROR

ERROR calculates the systematic error involved in the measurement. The method of calculation was based on the following equation:

$$(\Delta Q)^2 = (\frac{\partial Q}{\partial Q} \Delta x)^2 + (\frac{\partial Q}{\partial y}) \Delta y)^2 + \ldots \qquad (I.3)$$

where ΔQ, Δx, Δu, . . . are absolute errors on function Q(x,y, ..), x,y,. . . respectively. Other elements are partial

derivatives of the function Q with respect to x, y, ...

The FFR2 version is a modified FFR1 programme with subroutine INPLT replaced by subroutine POLY. Subroutine POLY calculates D8(t) and D5(t) from two 4th order polynomials fitted to the D8(t) and D5(t) values using programme LISQFT (Least Squares Fit). FFR2 calculates F8(t)/F5(t), F8(t) and F5(t) from equations 3.6 and 3.10 . The rest of the programme is identical to FFR-1.

In FFR3 a subroutine LISQFT was added to FFR2 in order to fit a required polynomial to natural and depleted corrected count rates, see Fig. 6. LISQFT gives an improvement to the linear interpolation, and is discussed later in this Appendix.

FFR CORE

This programme is similar to FFR1. FFR CORE does not have the pT subroutine, but calculates fission ratio, U_{238} and U_{235} fission rates. The random error is calculated from equation I.2. The average values of F8(t)/F5(t), F8(t) and F5(t) are obtained by multiplying corresponding values by $\frac{D5(t)}{D8(t)}$, $\frac{1}{D8(t)}$ and $\frac{1}{D5(t)}$ respectively and taking algebraic average.

FLUX

FLUX is similar to FFR1 without the pT subroutine. This routine corrects the counts of each foil for flux change by applying a factor obtained from a monitor foil. Each fuel element in the core is treated separately. The programme

uses a two dimensional 12 x 21 array, where 12 is the number of positions of foil irradiations and 21 is the number of decay periods from 150 to 250 minutes, taken in 5 minutes intervals. All decay intervals are based on mid-time of the counting period. All foil decays irradiated in one fuel element are devided by the decay of the foil irradiated in the centre of the fuel element. Then the average is obtained. The random error is calculated from equation I.2.

ENRICH

This programme was written to determine the U_{235} enrichment in an unknown foil, by use of the gamma activity of a natural uranium foil as compared to the gamma activity of the unknown foil. This programme is basically similar to FFR1. The normalized U_{235} decay at 240 minutes is also obtained from the programme.

LISQFT

In this computer code the method of least squares is used in order to fit a polynomial to a set of data.

Suppose $x_1, x_2, x_3, \ldots, x_n$ are the measured values of quantity x and $y_1, y_2, y_3, \ldots, y_n$ are measured values of another quantity y. We assume there exists a relation between x and y that can be given by

$$A_0 + A_1x + A_2x^2 + A_3x^3 + \ldots + A_{nx}{}^n = y$$

On substituting experimental values of x the obtained values for

y are not in general equal to experimental values of y. To obtain the required relationship which best fits the data we chose the coefficients such that the sum of the squares of errors on y's is least. The condition is obtained by differentiating partially the polynomial with respect to its coefficients as follows:-

$$A_0 + A_1x_1 + A_2x_1^2 + \ldots + A_nx_1^n = y_1$$

$$A_0 + A_1x_2 + A_2x_2^2 + \ldots + A_nx_2^n = y_2 \qquad \text{(I.4)}$$

$$A_0 + A_1x_{np} + A_2x_{np}^2 + \ldots A_nx_{np}^n = y_{np}$$

where np is the number of experimental values.

Summing up all the coefficients of equation (I.4) one equation is obtained in terms of A_0, A_1, . . . A_n. Then by multiplying each equation of (I.4) by the coefficient of the second column (i.e. x_1) and adding as above a second equation is obtained. By performing the same procedure for all x's a set of N equation is obtained as follows:-

$$A_0 \sum_{1}^{NP} (1)_i + A_1 \sum_{1}^{NP} x_i + \ldots + A_n \sum_{1}^{NP} x_i^n = \sum_{1}^{NP} y_i$$

$$A_0 \sum_{1}^{NP} x_i + A_1 \sum_{1}^{NP} x_i^2 + \ldots + A_n \sum_{1}^{NP} n_i^{n+1} = \sum_{1}^{NP} x_i y_i$$

(I.5)

$$A_0 \sum_{1}^{NP} x_i^{n+1} + A_1 \sum_{1}^{NP} x_i^{n+2} + \ldots + A_n \sum_{1}^{NP} x_i^{n+n} = \sum_{1}^{NP} x_i^n y_i$$

The solution of equations I.5 leads to determination of coefficients A's.

The programme LISQFT consists of three subroutines, COEF, PIVOT and CALC. Subroutine COEF finds N equations shown in I.4. PIVOT solves the set of equations given in I.5 by pivotal condensation method, and CALC calculates the values of y for a given set of values of x. The subroutine CALC. finds average residual per point and standard deviation.

APPENDIX II

THE COMPUTER PROGRAMME RIPPLE

In a reactor core which consists of closely spaced thin fuel-plates with moderator in-between fuel-plates (such as the London University Reactor, see Fig. 40), the neutron flux can be measured by foil techniques.

We want to find the flux distribution between fuel plates and the effect of the hyperfine neutron distribution for use in reactivity calculation. These calculation may show a variation of up to four per cent reactivity depending on the accuracy of determining the flux fine structure. There is no practical means of measuring reaction rates in the fuel meat or cladding so the alternative is to tackle the problem by calculational methods. Several methods may be used to estimate the flux depression in the fuel plates. Diffusion theory, for example, underestimates the effect and it is not suitable for this kind of boundary conditions. The spherical-harmonics method may be used, but it requires a high order approximation. A third approach is to solve the problem using transport theory, which gives accurate results. A fourth method appears easier and simpler than the later, and is based on collision probability. The disadvantage with this method is that the conception is based upon isotropic scattering. For cases of non-isotropic scattering it has been suggested by Newmarch (34) that the transport mean free path be used instead of total mean free path to improve accuracy.

Briefly, the concept of collision probability is as follows, however for more detail consult Refs. (34), (35), (36).

In an isotropic scattering medium the total reaction rate is a

volume element dr at r and in energy interval dE about E, is given by Peierl's equation

$$\Sigma(r,E)\phi(r,E)drdE = \Big[\int_{r'}\int_{E'} p(r'\to r)p(E'\to E)\ \Sigma_s(r',E')\phi(r',E')dr'dE'$$

$$+ \int_{r'} s(r',E)p(r'\to r)dr'\Big]\ drdE \qquad \text{(AI.1)}$$

The two terms on the right hand side of the equation represent the contribution in reaction rate. The first term calculates the number of neutrons at r after having had the last collision at r' with the change in energy from group dE' about E' to dE about E. The second term gives the number of fission neutrons and extraneous source (if any) at r in the energy interval dE at E.

$p(r'\to r)dr'dr$ represents the probability that a neutron in volume dr' at r' suffers the next collision in volume dr at r.

$p(E'\to E)dE'dE$ is the similar probability function for transferring from energy interval dE' at E' to dE about E.

According to the centre of mass system the scattered neutrons is given by

$$p(E'\to E)\ dE'dE = \frac{dE}{(1-\alpha)E'},\ dE' \qquad \text{(AI.2)}$$

if $\alpha E' < E < E'$, and otherwise zero

and $$\alpha = \left(\frac{A-1}{A+1}\right)^2 \qquad \text{(AI.3)}$$

where A is atomic mass number.

At thermal energies because of upscattering the form of the function, $p(E' \rightarrow E)$ will be different.

The function $p(r' \rightarrow r)\, \underline{dr}\, \underline{dr'}$ is given by

$$p(r' \rightarrow r)\underline{dr}\, dr' = \frac{\Sigma\, \underline{dr}}{4\pi(r'-r)2}\, e^{-\Sigma(r-r')}\, \underline{dr'} \qquad \text{(AI.4)}$$

where Σ is the total cross section of the medium. By substituting AI.2 and AI.4 into AI.1 and considering the volume of the cell V divided into a number of regions each with volume V_i and cross section Σ_i we obtain,

$$V_j \Sigma_j \bar{\phi}_j(E)dE = [\int_{E'} \sum_i \Sigma_i \bar{\phi}_i(E') \int_{r'} \int_{V_j} p(r' \rightarrow r)dr'dr$$

$$p_i(E' \rightarrow E)dEdE' + \sum_i \bar{s}_i(E) \int_{V_i} \int_{V_j} p(r' \rightarrow r)drdr']dE \qquad \text{(AI.5)}$$

when; $\bar{\phi}_i$ is the average flux in region i, $\bar{s}_i$ is the average source in region i, symbol $\sum_i$ is for the summation, $V_j \equiv \underline{dr}$, and $v_i \equiv \underline{dr'}$.

The quantity $\frac{1}{V_i} \int_{V_i} \int_{V_j} p(r' \rightarrow r)\, drdr'$ is defined as the first collision probability p_{ij} for neutrons uniformly born or scattered in

region i suffering their next collision in region j. p_{ij} is a function of energy,

$$p_{ij} = \frac{1}{V_i} \int_{V_i} \int_{V_j} \frac{1}{4\pi(r_i - r_j)^2} e^{-\Sigma(r_i - r_j)} \Sigma_j dr_j dr_i \qquad \text{(AI.6)}$$

Finally, the collision probability form of the integral transport equation becomes:

$$V_j \Sigma_j \bar{\phi}_j(E) = \sum_i V_i p_{ij}(E) \int_{E'} \Sigma_{si}(E') \bar{\phi}_i(E') p_i(E' \rightarrow E) dE'$$

$$+ \sum_i V_i p_{ij}(E) \bar{s}_i(E) \qquad \text{(AI.7)}$$

The subscript i on $p_i(E' \rightarrow E)$ indicates that the moderating property can vary with the region index.

Equation AI.7 can be expressed in the form of the group structure:

$$V_j \Sigma_j^g \bar{\phi}_j^g = \sum_i V_i p_{ij}^g \sum_k \Sigma_i(k \rightarrow g) \bar{\phi}_i^k + \sum_i V_i p_{ij}^g s_i^g \qquad \text{(AI.8)}$$

Newmarck (34) has developed a computer program, RIPPLE, to calculate the ripple structure of thermal neutrons between fuel plates using collision probability concept.

TABLE 9 $D^8(t)$ and $D^5(t)$

U235 AND U238 DECAY (NORMALIZED TO 240 MINUTES)

I	TN	D5	D8	D8/D5
1	65.00	.40952E+01	.45359E+01	.11076E+01
2	67.50	.39763E+01	.43924E+01	.11046E+01
3	70.00	.38619E+01	.42545E+01	.11017E+01
4	72.50	.37520E+01	.41222E+01	.10987E+01
5	75.00	.36463E+01	.39952E+01	.10957E+01
6	77.50	.35445E+01	.38733E+01	.10927E+01
7	80.00	.34472E+01	.37564E+01	.10897E+01
8	82.50	.33534E+01	.36442E+01	.10867E+01
9	85.00	.32633E+01	.35366E+01	.10837E+01
10	87.50	.31768E+01	.34334E+01	.10808E+01
11	90.00	.30937E+01	.33345E+01	.10778E+01
12	92.50	.30138E+01	.32396E+01	.10749E+01
13	95.00	.29371E+01	.31487E+01	.10721E+01
14	97.50	.28633E+01	.30616E+01	.10692E+01
15	100.00	.27925E+01	.29781E+01	.10665E+01
16	102.50	.27245E+01	.28981E+01	.10637E+01
17	105.00	.26591E+01	.28214E+01	.10610E+01
18	107.50	.25962E+01	.27479E+01	.10584E+01
19	110.00	.25357E+01	.26774E+01	.10559E+01
20	112.50	.24776E+01	.26099E+01	.10534E+01
21	115.00	.24217E+01	.25451E+01	.10509E+01
22	117.50	.23679E+01	.24832E+01	.10485E+01
23	120.00	.23161E+01	.24238E+01	.10463E+01
24	122.50	.22662E+01	.23668E+01	.10441E+01
25	125.00	.22181E+01	.23113E+01	.10420E+01
26	127.50	.21717E+01	.22579E+01	.10400E+01
27	130.00	.21270E+01	.22067E+01	.10380E+01
28	132.50	.20839E+01	.21574E+01	.10352E+01
29	135.00	.20422E+01	.21124E+01	.10344E+01
30	137.50	.20019E+01	.20692E+01	.10327E+01
31	140.00	.19629E+01	.20240E+01	.10311E+01
32	142.50	.19252E+01	.19821E+01	.10295E+01
33	145.00	.18887E+01	.19416E+01	.10277E+01
34	147.50	.18533E+01	.19029E+01	.10265E+01
35	150.00	.18189E+01	.18653E+01	.10259E+01
36	152.50	.17855E+01	.18289E+01	.10243E+01
37	155.00	.17530E+01	.17937E+01	.10232E+01
38	157.50	.17215E+01	.17596E+01	.10222E+01
39	160.00	.16907E+01	.17266E+01	.10212E+01
40	162.50	.16608E+01	.16947E+01	.10203E+01
41	165.00	.16315E+01	.16633E+01	.10194E+01
42	167.50	.16030E+01	.16329E+01	.10187E+01
43	170.00	.15751E+01	.16034E+01	.10179E+01
44	172.50	.15479E+01	.15749E+01	.10173E+01
45	175.00	.15212E+01	.15470E+01	.10166E+01
46	177.50	.14951E+01	.15197E+01	.10160E+01
47	180.00	.14695E+01	.14932E+01	.10153E+01
48	182.50	.14445E+01	.14671E+01	.10150E+01
49	185.00	.14199E+01	.14419E+01	.10145E+01
50	187.50	.13958E+01	.14153E+01	.10140E+01

U235 AND U238 DECAY (NORMALIZED TO 240 MINUTES)

I	TN	D5	D8	D8/D5
50	187.50	.13958E+01	.14153E+01	.10140E+01
51	190.00	.13721E+01	.13907E+01	.10136E+01
52	192.50	.13489E+01	.13666E+01	.10131E+01
53	195.00	.13261E+01	.13430E+01	.10127E+01
54	197.50	.13038E+01	.13198E+01	.10123E+01
55	200.00	.12819E+01	.12971E+01	.10118E+01
56	202.50	.12604E+01	.12748E+01	.10114E+01
57	205.00	.12394E+01	.12529E+01	.10109E+01
58	207.50	.12188E+01	.12315E+01	.10104E+01
59	210.00	.11985E+01	.12105E+01	.10099E+01
60	212.50	.11787E+01	.11900E+01	.10094E+01
61	215.00	.11593E+01	.11699E+01	.10088E+01
62	217.50	.11403E+01	.11503E+01	.10081E+01
63	220.00	.11218E+01	.11313E+01	.10075E+01
64	222.50	.11052E+01	.11127E+01	.10067E+01
65	225.00	.10862E+01	.10947E+01	.10060E+01
66	227.50	.10717E+01	.10772E+01	.10051E+01
67	230.00	.10569E+01	.10604E+01	.10042E+01
68	232.50	.10408E+01	.10442E+01	.10033E+01
69	235.00	.10258E+01	.10287E+01	.10022E+01
70	237.50	.10128E+01	.10140E+01	.10012E+01
71	240.00	.10000E+01	.10000E+01	.10000E+01
72	242.50	.98367E+00	.98657E+00	.10050E+01
73	245.00	.97268E+00	.97624E+00	.10037E+01
74	247.50	.96266E+00	.96493E+00	.10024E+01
75	250.00	.95366E+00	.95458E+00	.10010E+01

$$D5(t) = A0 + A1*t + A2*t^2 + A3*t^3 + A4*t^4$$

$$D8(t) = A0 + A1*t + A2*t^2 + A3*t^3 + A4*t^4$$

Coefficients for D5(t): and D8(t):

A0	$+9.3415889400$	$+10.99655780$
A1	-0.1227382499	-0.150875921
A2	$+0.795173013\,46*10^{-3}$	$+0.979259615\,8*10^{-3}$
A3	$-0.2563067728\,7*10^{-5}$	$-0.3099934835*10^{-5}$
A4	$+0.3237445635\,7*10^{-8}$	$+0.3816899206*10^{-8}$

TABLE 19 Natural FOIL COUNTS AND FITTED POLYNOMIAL RESULTS

DECAY TIME MINUTES	OBSERVED COUNTS	CALCULATED COUNTS	C(CAL)-C(OB)	PERCENTAGE DIFFERENCE
.8425E+02	.1242E+06	.1238E+06	-.3241E+03	-.2610E+00
.9425E+02	.1112E+06	.1116E+06	.4238E+03	.3812E+00
.1042E+03	.1011E+06	.1010E+06	-.6648E+02	-.6577E-01
.1142E+03	.9226E+05	.9181E+05	-.4432E+03	-.4804E+00
.1242E+03	.8332E+05	.8383E+05	.5094E+03	.6114E+00
.1342E+03	.7661E+05	.7688E+05	.2670E+03	.3486E+00
.1442E+03	.7058E+05	.7081E+05	.3086E+03	.4377E+00
.1542E+03	.6565E+05	.6550E+05	-.1557E+03	-.2371E+00
.1642E+03	.6098E+05	.6082E+05	-.1580E+03	-.2591E+00
.1742E+03	.5704E+05	.5668E+05	-.3585E+03	-.6285E+00
.1842E+03	.5314E+05	.5299E+05	-.1458E+03	-.2744E+00
.1942E+03	.5006E+05	.4968E+05	-.3148E+03	-.6296E+00
.2042E+03	.4688E+05	.4669E+05	-.1845E+03	-.3937E+00
.2142E+03	.4382E+05	.4397E+05	.1550E+03	.3537E+00
.2242E+03	.4143E+05	.4148E+05	.5481E+02	.1323E+00
.2342E+03	.3921E+05	.3919E+05	-.1523E+02	-.3885E-01
.2442E+03	.3699E+05	.3707E+05	.7538E+02	.2038E+00
.2542E+03	.3493E+05	.3509E+05	.1108E+03	.3168E+00
.2642E+03	.3286E+05	.3325E+05	.3880E+03	.1181E+01
.2742E+03	.3131E+05	.3153E+05	.2237E+03	.7144E+00
.2842E+03	.3007E+05	.2992E+05	-.1535E+03	-.5103E+00
.2942E+03	.2824E+05	.2841E+05	.1708E+03	.6046E+00
.3042E+03	.2674E+05	.2701E+05	.2650E+03	.9911E+00
.3142E+03	.2572E+05	.2570E+05	-.2476E+02	-.9626E-01
.3242E+03	.2453E+05	.2448E+05	-.5223E+02	-.2129E+00
.3342E+03	.2344E+05	.2334E+05	-.9277E+02	-.3959E+00
.3442E+03	.2261E+05	.2230E+05	-.3120E+03	-.1380E+01
.3542E+03	.2144E+05	.2133E+05	-.1108E+03	-.5169E+00
.3642E+03	.2069E+05	.2043E+05	-.2580E+03	-.1247E+01
.3742E+03	.1963E+05	.1961E+05	-.1601E+02	-.8154E-01
.3842E+03	.1912E+05	.1885E+05	-.2690E+03	-.1407E+01
.3942E+03	.1811E+05	.1815E+05	.3896E+02	.2150E+00
.4042E+03	.1736E+05	.1750E+05	.2022E+03	.1169E+01
.4142E+03	.1704E+05	.1689E+05	-.1454E+03	-.8535E+00
.4242E+03	.1622E+05	.1631E+05	.9273E+02	.5717E+00
.4342E+03	.1568E+05	.1576E+05	.1143E+03	.7308E+00
.4442E+03	.1510E+05	.1522E+05	.1257E+03	.8323E+00
.4542E+03	.1455E+05	.1470E+05	.1440E+03	.9892E+00
.4642E+03	.1410E+05	.1418E+05	.7606E+02	.5395E+00
.4742E+03	.1354E+05	.1365E+05	.1170E+03	.8642E+00
.4842E+03	.1302E+05	.1314E+05	.1127E+03	.8655E+00
.4942E+03	.1273E+05	.1262E+05	-.1091E+03	-.8569E+00
.5042E+03	.1219E+05	.1212E+05	-.6925E+02	-.5679E+00
.5142E+03	.1171E+05	.1165E+05	-.5295E+02	-.4523E+00
.5242E+03	.1140E+05	.1123E+05	-.1679E+03	-.1474E+01
.5342E+03	.1108E+05	.1088E+05	-.1983E+03	-.1790E+01
.5442E+03	.1063E+05	.1064E+05	.1264E+02	.1189E+00
.5542E+03	.1036E+05	.1057E+05	.2096E+03	.2024E+01

AVERAGED RESIDUAL= -.68666E-07 STANDARD DEV.= .30606E+02

TABLE 10 Depleted FOIL COUNTS AND FITTED POLYNOMIAL RESULTS

DECAY TIME MINUTES	OBSERVED COUNTS	CALCULATED COUNTS	C(CAL)-C(OB)	PERCENTAGE DIFFERENCE
.7925E+02	.5194E+05	.5169E+05	-.2680E+03	-.5158E+00
.8925E+02	.4616E+05	.4627E+05	.1128E+03	.2444E+00
.9925E+02	.4147E+05	.4161E+05	.1368E+03	.3299E+00
.1092E+03	.3730E+05	.3760E+05	.2697E+03	.5608E+00
.1192E+03	.3391E+05	.3416E+05	.2512E+03	.7409E+00
.1292E+03	.3145E+05	.3119E+05	-.2536E+03	-.8066E+00
.1392E+03	.2869E+05	.2863E+05	-.5876E+02	-.2048E+00
.1492E+03	.2629E+05	.2641E+05	.1205E+03	.4582E+00
.1592E+03	.2439E+05	.2448E+05	.9112E+02	.3737E+00
.1692E+03	.2320E+05	.2278E+05	-.4189E+03	-.1806E+01
.1792E+03	.2171E+05	.2128E+05	-.4306E+03	-.1983E+01
.1892E+03	.1977E+05	.1995E+05	.1840E+03	.9306E+00
.1992E+03	.1880E+05	.1876E+05	-.4220E+02	-.2244E+00
.2092E+03	.1765E+05	.1768E+05	.2653E+02	.1503E+00
.2192E+03	.1661E+05	.1670E+05	.8725E+02	.5253E+00
.2292E+03	.1582E+05	.1579E+05	-.3118E+02	-.1970E+00
.2392E+03	.1491E+05	.1496E+05	.5031E+02	.3375E+00
.2492E+03	.1394E+05	.1416E+05	.2336E+03	.1675E+01
.2592E+03	.1325E+05	.1345E+05	.2036E+03	.1537E+01
.2692E+03	.1278E+05	.1277E+05	-.2512E+01	-.1966E-01
.2792E+03	.1191E+05	.1214E+05	.2235E+03	.1876E+01
.2892E+03	.1150E+05	.1154E+05	.4115E+02	.3578E+00
.2992E+03	.1104E+05	.1099E+05	-.7628E+02	-.6896E+00
.3092E+03	.1049E+05	.1047E+05	-.2403E+02	-.2291E+00
.3192E+03	.1008E+05	.9985E+04	-.9207E+02	-.9137E+00
.3292E+03	.9709E+04	.9539E+04	-.1703E+03	-.1754E+01
.3392E+03	.9244E+04	.9127E+04	-.1168E+03	-.1263E+01
.3492E+03	.8869E+04	.8749E+04	-.1198E+03	-.1351E+01
.3592E+03	.8515E+04	.8403E+04	-.1120E+03	-.1316E+01
.3692E+03	.8094E+04	.8087E+04	-.7463E+01	-.9220E-01
.3792E+03	.7859E+04	.7797E+04	-.6063E+02	-.7715E+00
.3892E+03	.7593E+04	.7533E+04	-.6043E+02	-.7958E+00
.3992E+03	.7221E+04	.7289E+04	.6785E+02	.9396E+00
.4092E+03	.6874E+04	.7063E+04	.1886E+03	.2744E+01
.4192E+03	.6761E+04	.6850E+04	.8918E+02	.1319E+01
.4292E+03	.6564E+04	.6648E+04	.8375E+02	.1276E+01
.4392E+03	.6395E+04	.6452E+04	.5679E+02	.8881E+00
.4492E+03	.6222E+04	.6259E+04	.3717E+02	.5974E+00
.4592E+03	.6161E+04	.6067E+04	-.9355E+02	-.1518E+01
.4692E+03	.5792E+04	.5875E+04	.8319E+02	.1436E+01
.4792E+03	.5722E+04	.5682E+04	-.3972E+02	-.6941E+00
.4892E+03	.5441E+04	.5490E+04	.4935E+02	.9070E+00
.4992E+03	.5353E+04	.5303E+04	-.4986E+02	-.9314E+00
.5092E+03	.5220E+04	.5127E+04	-.9300E+02	-.1782E+01
.5192E+03	.5040E+04	.4971E+04	-.6867E+02	-.1363E+01
.5292E+03	.4900E+04	.4849E+04	-.5085E+02	-.1038E+01
.5392E+03	.4723E+04	.4778E+04	.5465E+02	.1157E+01
.5492E+03	.4720E+04	.4779E+04	.5876E+02	.1245E+01

AVERAGED RESIDUAL= .54651E-07 STANDARD DEV.= .21379E+02

POLYNOMIAL FITTED IS Y=A0+A1.X+A2.X**2+...+A6.X**6